Final Report on the Project "Infrared Thermal Imaging for Use in Restoration of Defaced Serial Numbers"

Award Number: 2013-R2-CX-K012
Author(s): Rene Rodriguez, Lisa Lau, Ikwulono Unobe, John Kalivas, Andrew Sorensen

Abstract

The problem under investigation was the recovery of serial numbers from metallic objects such as firearms or automobile engines using non-destructive techniques based on the localized changes in the thermal conductivity of a substance known as thermal infrared imaging or infrared thermography coupled with sophisticated multivariate image analysis (MIA) techniques. The construction and implementation of three types of instruments that utilize an infrared camera to image the residual traces of defaced serial numbers was accomplished for this purpose, transient infrared thermography (TIT), pulsed infrared thermography (PIT), and lock-in infrared thermography (LIT). TIT, PIT, and LIT techniques have been successfully used to image defects in materials like airplane wings, circuit boards, and solar cells, and with regard to serial number recovery, these techniques rely on the fact that plastic strain regions and/or melted regions exist below stamped or laser engraved serial numbers. Best practices for use of infrared thermography coupled with sophisticated MIA processing were investigated using a FLIR Inc. SC6700 infrared camera to detect differences in the temperature and thermal wave phase due to heat flow of material in the plastic strain region below the filed away serial numbers compared with the surrounding largely undisturbed areas.

Our studies required the production of a reproducible temperature change induced about some starting temperature, the suppression of background thermal noise, and the ability to collect IR camera images for a particular amount of time and after a given amount of delay.
To induce reproducible starting temperatures and cyclical temperature changes in the stamped and defaced metal surrogates the materials had to be preheated to some initial temperature and then absorb a cyclical heating pulse. Both a Peltier cooler and a digital hot plate proved useful for our investigations of the effect of the initial temperature, and pulsed heating cycles were achieved by one of the following types of heating/cooling methods: a pulsed heat gun, a chopped high-wattage stage lamp, a chopped laser beam, and a Peltier cooler. The emissivity of the defaced surface due to the absorption and a reduction in the reflectivity of the sample also played a significant role in the ability of the camera to resolve sample emissions from reflected background noise, and black paint, graphite, and colored dye were used for this purpose. Several trials with each coating were part of the investigations. A special variable timing circuit was constructed to provide for evaluation of the effect of the timing of the heating pulse relative to the camera shutter opening. This was essential for implementation and our investigations using the PIT and LIT techniques. Furthermore in the case of the LIT, the timing circuit allowed the camera to take images several times at set intervals over the course of one heating pulse.

The MIA procedures proved to be an essential part of recovering the defaced serial numbers. Processing of the IR camera images using Principal Component Analysis (PCA) and Zernicke Moment Analysis proved to provide processed plots that reconstructed the defaced numbers even when there was no number present in the raw image or phase image. Employment of multiple similarity merit measurements to the processed plots, along with combination fusion rules, shows great promise in accurately determining the identities of defaced serial numbers.

Table of Contents

List of Figures

List of Tables

Executive Summary

The purpose of this research was to determine if thermal imaging methods coupled with multivariate image analysis could be adapted for the purpose of recovering serial numbers that have been defaced on metal samples. The technique requires only a slight polishing and painting of the surface of the sample making the technique a non-destructive technique in stark contrast to the chemical methods often currently used for this purpose. Since the thermal imaging technique is non-destructive, samples could be reanalyzed at a later date.

Three thermal imaging methods were constructed and implemented for this purpose. The three techniques, Transient Infrared Thermography (TIT), Pulsed Infrared Thermography (PIT) and Lock-in Thermography (LIT) use an infrared camera to take advantage of the differences in the thermal characteristics of objects to study those objects for the presence of defects or hot spots. Toward the application of these techniques to serial number recovery, the techniques take advantage of the differences in thermal conductivities and densities between the metals removed from the serial numbers, and the metals beneath the serial numbers which have altered physical constants. Implementation of these experiments for serial number recovery require some preliminary sample treatment, a heating source, a pulsing circuit, and a sensitive, high resolution infrared camera. The camera captures images of the defaced sample during the heating or cooling process. The captured images do not normally reveal the identity of the serial number without further processing. Principal component analysis (PCA), Zernike moment analysis (ZMA), and similarity merit measures are the multivariate image analysis techniques which can take the camera images or phase images derived from the camera images, and use these to identify the serial number or VIN number that was defaced.

Test samples consisting of 2 cm x 6 cm x 0.6 cm were used to test the ability of each of the experimental and multivariate image analysis techniques to recover the serial numbers. The test samples were aluminum or steel samples, and several numbers were stamped into the metal. The numbers were defaced in a variety of ways including manual sanding with a rasp and sand paper, use of a Dremel tool with a sanding wheel, or more precisely by a machinist. The samples prepared by the machinist had the serial number metal removed to specified depths below the point where the serial number disappeared. Preparation of these so called "graded samples" for infrared thermography required polishing of the surface with a fine grit sandpaper (600 grit) followed by painting the surface with black BBQ paint or India Ink using a doctor blade method to provide constant emissivity.

The TIT experiments consisted of heating the samples to a high temperature ~250^{o}C followed by taking images as the samples cooled. A hot plate or a tubular furnace was used to heat the test samples. Alternatively the samples were cooled to a low temperature and allowed to heat while taking IR images. Dry ice or a Peltier cooler was used to cool the samples. The images were analyzed for traces of the defaced serial number. The TIT method showed very limited positive results for recovery of the defaced serial numbers.

The PIT experiments consisted of taking images while the heating source was pulsed off and on at regular intervals. Three different heating sources were used to heat the test samples,

one or two heat guns, one or two theatre lamps, or the 1-3 Watt laser light from a Ar-ion laser. A special pulsing circuit was constructed to pulse the heat guns and theatre lamps by pulsing the AC current. The laser light was pulsed by inserting a chopper in the beam path. The temperature swing associated with the heat pulses varied with the pulse rate. The pulse rate was varied between 0.25 Hz and 10 Hz. Typical temperature swings ranged from 0.1 to 2 ^{o}C. The IR images collected during the pulses were subjected to analysis and only limited success was obtained with this method. Larger temperature swings tended to yield better results, but the analysis did not always reveal the identity of the defaced serial number.

The LIT experiments required taking multiple images at equally spaced intervals after a given heating source pulse and before the next pulse began. Mathematical processing of the multiple images provide for both magnitude and phase images of the defaced area on the metal. The phase images are images where background reflectance and noise are minimized. The phase images were then processed with Principal Component Analysis (PCA) to yield score images of the defaced test samples. The score image, PC1, resulting from the image containing the most information of the original image, rarely contained any hint of the defaced serial number, but the score image of higher numbered principal components, like PC7 or PC10, appeared to contain a significant amount of this information. Usually one of the principal component score images looked very much like a number, while the others did not, although in many cases there appeared to be hints of that number present in some of the other higher numbered principal components. The coupling of the LIT method with the PCA treatment appeared to give good results in many cases and use of the chopped laser as the heating source appeared to give the best results. Using this combined method, several of the experimental parameters were systematically altered in the LIT experiment to determine the best conditions for serial number recovery. These comparisons were largely based on a visual analysis of how closely the best looking score image resembled the original serial number before it was defaced. The parameters varied were the coating material used on the polished surface, the intensity of the laser, the initial temperature of the sample, and the pulse rate of the heating source. Good results were obtained for several different combinations using the defaced number 2 on the steel "graded sample" prepared by a machinist.

Attempts to take "human judgement" out of the comparison of score images to the number library were made through implementing similarity merit measurements. In order to use the similarity measurement, the score images had to be further processed using the Zernike moment analysis (ZMA). This provided an image vector that was the same size for any score image or number library image. The PCA-ZMA analysis combination then was used to calculate up to ten similarity merit measures; which are various mathematical ways to compare the similarity of a particular score image, or the whole set of score images, to a set of library images. The library images should reflect the original undefaced serial number, perhaps altered slightly to account for the broadening of the number in deformation zone. The PCA-ZMA analysis combination with the similarity merit evaluation applied to the defaced numbers 6, 2, and 5, for the graded sample, resulted in the highest merit values assigned between the 6 in the undefaced

sample and the 6 in the library, and likewise for the 2 and the 5. Thus this technique shows good promise in recovering defaced serial numbers.

The LIT method with PCA-ZMA processing and similarity merit measurements was applied to a real world sample obtained from the Bannock County Sheriff's Office. This sample was a 12 gauge shotgun barrel with the text "*12 Gauge*" stamped into the barrel. The italics numbers *1* and *2* were defaced and re-polished using two types of sandpaper with fine and very fine grit. The sanded area was then painted with India ink. The barrel was placed into the LIT experimental setup and phase images were computed and then analyzed with the PCA-ZMA method followed by comparison with numbers in a library using the similarity merit measurements. The results from this showed that the defaced number 2 was identified as the number 2 through a comparison of score images, using all of them, with the library. The computer based this on the fact that the match to a library "2" had the highest sum of merit values from 10 different similarity merits. For the number 1, the library number 1 had the second highest sum of merit values, with a number 4 having the highest. However the number library used for the comparison did not have an italics number 1 in it. Subsequent studies with the shotgun barrel data, showed that if a set of fusion rules was defined, which, rather than simply adding the similarity merits as was done previously, combined them to optimize the use of several similarity measures by obtaining a consensus among them, thus minimizing the possible effects of some incorrectly ranked values, then the number 1 was correctly identified as being the best match. This involved determining the similarity merits for each score image in comparison to the digital number images across four libraries. Thus this method showed good promise in the recovery of serial numbers from even a curved sample like a gun barrel.

The recoveries of serial numbers from three other defaced samples, provided a reasonable test of the general applicability of the method which uses the LIT, PCA-ZMA, and similarity merit fusion rules. One was a set of stainless steel forceps with a **laser engraved** serial number that was defaced and all numbers were recovered. Two others samples provided by the Power County Sheriff's office, were from a stolen motorcycle with a defaced VIN number and motor ID number. The defacing was done by the burglar. The VIN number on the neck of the steel body was almost completely removed, but the serial number on the aluminum motor was largely still visible with only two incomprehensible numbers. The LIT technique provided both a VIN number and a motor serial number. Chief Deputy Sprague from the Power Co. Sheriff's office found the VIN number matches that of a motorcycle reported stolen in Pocatello. The motor and VIN numbers also match, which is consistent with the ID stamping used on this motorcycle type.

The overall goal of the study was to determine if infrared thermography techniques coupled with multivariate analysis methods could be used as a non-destructive method to recover defaced serial numbers from materials that are typically involved in criminal activities. Based upon these studies the use of lock-in thermography combined with PCA and ZMA processing followed by a fusion of similarity merit measures, provides a non-destructive method that can be used to recover defaced serial numbers that were originally, stamped or laser engraved on aluminum, steel, or stainless steel, on a rounded or flat surfaces.

I. INTRODUCTION

The overall purpose of the research projected titled "Infrared Thermal Imaging for Use in Restoration of Defaced Serial Numbers" was to determine if an Infrared Imaging techniques complimented with Multivariate Image Processing could be used to recover defaced serial numbers. The physical basis of this number recovery method relies on the ability of the infrared (IR) camera to discern differences in the heat flow, i.e. thermal conductivities, of the metal in areas where the metal is relatively pristine as compared to areas where the metal was deformed by stamping or engraving a serial number into the metal. As addressed in the research proposal, the following research questions and hypotheses were to be addressed by this research.

1) Does thermal imaging represent a non-destructive, relatively quick, and cost effective method for restoring defaced serial numbers which have been **mechanically stamped** or engraved into a metal material such as an automobile engine or firearm surface?

2) Does thermal imaging represent a non-destructive, relatively quick, and cost effective method for restoring defaced serial numbers which have been **laser engraved** into a metal material such as an automobile engine or firearm surface?

3) Can one validate the hypothesis that there will be a large enough difference in the thermal conductivities of the pristine metal and the plastic strained or melted metal below the serial number to create a temperature difference between the two regions allowing Transient Infrared Thermography (TIT) and Pulsed Infrared Thermography (PIT) techniques to be used to recover the serial number.

4) Can one validate the hypothesis that there will be a large enough difference in the thermal conductivities between the deformed and pristine regions of the metal to provide a significant difference in the thermal gradient and change the thermal velocities enough to observe a difference in the velocity and phase of the thermal wave which will be observable with Lock-In Thermography (LIT).

A possible pitfall was that the difference in thermal conductivities between the deformed area below the serial number and the surrounding metal might prove to be insufficiently substantial to be measured with the temperature resolution provided by the camera, but the hypotheses were based on studies where the techniques were used for imaging defects in semiconductors.[1-3] Another potential problem was mentioned related to the emissivity of a significantly scratched surface as compared to one that is more finely filed. Preparation of the defaced metal surfaces, in terms of the amount of both polishing and painting of the surface, was expected to reduce effects of emissivity differences, and determination of the correct polishing and painting techniques proved to be an essential part of the project.

Since the ordering and delivery of the camera required several months, it was decided that the research studies should be modified slightly by modeling the serial recovery methods using a Finite Element Analysis Program. The Ph.D. candidate working on the project, Ikwulono Unobe modeled both the plastic deformation that occurs with the serial number stamping and also the changes in the thermal conductivity and density of the metals that can result in the plastic deformation zone. He also adjusted the program to model temperature

movement through a sample with a particular bulk density and thermal conductivity, where the sample also contains localized areas near the surface where the thermal conductivity and density differ from the bulk, such as in a plastic deformation zone below a serial number. The program allows modeling of experimental conditions similar to those that would be used in our different types of thermographic analysis, and the results were used to help dictate the initial metal temperatures needed to produce an effect that can be monitored with the infrared camera.

The infrared camera chosen for this research was the FLIR SC6700 IR camera. This camera has the following features which made it a good choice for these research studies: data capture directly into MATLAB software for custom image analysis, a built-in cryo cooler for the high sensitivity InSb detector, excellent image quality, image size of 640 x 512 pixels, Sync In and Sync Out for triggered applications, sub-microsecond integration times, Frame Rate (Full Window) Programmable 0.0015Hz to 125Hz, and capture rates for smaller window sizes up to 4000 Hz. The ability to trigger the camera was essential both for the PIT and LIT imaging techniques. The MATLAB compatibility for image data was advantageous and essential since the image processing programs were either written in MATLAB or available in the Imaging Toolbox available for MATLAB users.

The other essential part of the project was to determine the best data handling practices and image processing techniques. Multivariate analysis techniques like Principal Component Analysis (PCA) and Zernike Moment Analysis (ZMA) methods were employed to transform the data from the various thermal imaging methods (TIT, PIT, and LIT) into sets of orthogonal eigenvectors with the idea that score plots from specific eigenvector components of the larger set of eigenvectors would contain the data necessary to reconstruct the serial number. Determining which eigenvector components contribute and determining the identity of the defaced number required further computer processing using various similarity measurements (comparison) programs including Euclidean distance, Procrustes analysis, Mahalanobis distance, and others.

The ultimate test of any firearm serial recovery technique is how well it is able to identify serial numbers on a real firearm that have been defaced by filing them off the surface. Over the course of the investigations, a relationship was established with Lt. Toni Vollmer, an officer in the Bannock County Sheriff's Office, and with Chief Deputy Sheriff Max Sprauge from Power County. Lt. Vollmer indicated that she had a few gun pieces in their gun vault that we could use for this purpose and she was kind enough to provide this to us for our research studies. Although no formal serial number was stamped into this particular firearm, there were some letters and numbers stamped into the barrel which could be defaced and analyzed. Deputy Sheriff Sprague provided us with a motorcycle with a defaced VIN number. He was seeking help in recovering the number so that the owner of the motorcycle could be identified and contacted.

This final report will provide detailed information on the various studies we performed to test each of the three thermal imaging techniques: TIT, PIT and LIT. Success with the TIT and PIT techniques was limited, and the best results at serial number recovery were accomplished using the LIT, lock-in thermography, technique. It will also detail the various multivariate image analysis and similarity measurement programs that were used to process the data acquired with

the imaging techniques. The best success resulted from a combination of the LIT imaging, coupled with the Zernike Moment Analysis of the phase images derived from the LIT technique and a fusion of all of the similarity measurements. Using all of these methods together and comparing the recovered images to a library of non-defaced numbers, one can reliably identify the identity of the serial number that was defaced in a certain area. The degree of reliability is related to the quality of the original stamping, and whether the numbers were completely or only partially stamped in the material, this limits the capability of the technique.

Several important aspects of the studies are covered here. The final report will provide details on the methods used to perform the Finite Element Analysis modeling. Results from the modeling will be provided with an interpretation of how the results guided the initial conditions used in the various imaging techniques. Finite Element Analysis modeling is well known and has a history of being useful for studying the effects of the physical property of substances on the movement of heat in that system.

Other sections of the report will define the various multivariate imaging analysis techniques used. As noted above these included Principal Component Analysis (PCA) and Zernike Moment Analysis (ZMA). During most of the grant period, PCA was used and ZMA was implemented after the research group attended a research meeting in Toronto Canada. Descriptions of the various similarity measurements employed for this project will also be provided in this section.

A detailed description of the equipment used for each of the three imaging techniques will also be presented. The ability of the specific technique to recover defaced serial numbers will be discussed by providing some examples of its use on some surrogate metal samples. Specifics regarding test samples and the preparation of the defaced surface by first polishing it with progressively finer grits of sand paper followed by coating the surface with black paint, India ink, graphite, or various dyes, will be provided here as well.

In the final sections of the report the findings from the experimental studies carried out with each of the three thermal imaging methods coupled with the multivariate imaging processing techniques will be summarized. Studies carried out with metal surrogates, with a barrel from a firearm, with a laser engraved serial number on set of forceps, and with the motorcycle VIN # will be presented and analyzed. Conclusions regarding the best thermal imaging process and multivariate image analysis techniques will be provided. The overall suitability and future of thermal imaging for the recovery of defaced serial numbers will be discussed.

II. METHODS

Modeling with Finite Element Analysis

Although this modeling was an addition to the original activities given in the research proposal, it provided some additional evidence that the experimental research proposed for the project would yield significant results. Again the idea was to ***model*** the plastic deformation that occurs with the serial number stamping and changes in the thermal conductivity and density of the metals that can result in the plastic deformation zone. With this information the program can

then also model the temperature movement through a sample with a particular bulk density and thermal conductivity, where the sample also contains localized areas at the surface with different thermal conductivity and density than the bulk, such as in a plastic deformation zone below a serial number. The program allows the experimental conditions to be similar to those used in TIT analysis. That is the initial temperature and the cooling or heating rates can be input as initial parameters in the model. By varying these initial parameters the results can be used to help dictate to what temperature the metal should be heated to produce an effect that can be measured through the use of infrared thermography. An example of the type of information that was gained from Finite Element Analysis is described here.

These are the results for an example carried out on a plate of Aluminum 7075-T6 with the number 9 stamped on it. First the model requires the input of the parameters corresponding to the unstamped pristine aluminum sample. This is shown below in Figure 1. The model basically consists of a meshed 3-dimensional array or mesh model.

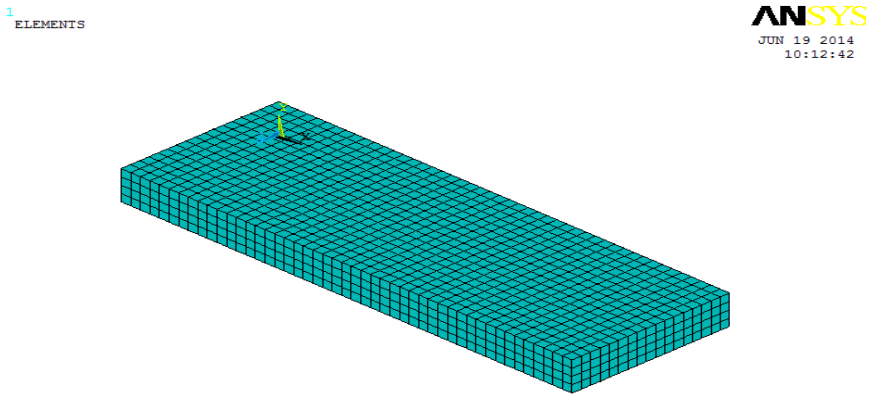

Figure 1: Meshed model of Aluminum plate

Changes in the physical parameters (i.e. density) can result in each cell of the array by modifying the forces present in each cell. The force changes realistically result from the serial number being stamped or engraved in the metal. The increased forces in the cell lead to a plastic deformation zone where the thermal conductivity and density of the metal change. Changed forces due to stamping the serial number "9" into the metal are shown in Figure 2.

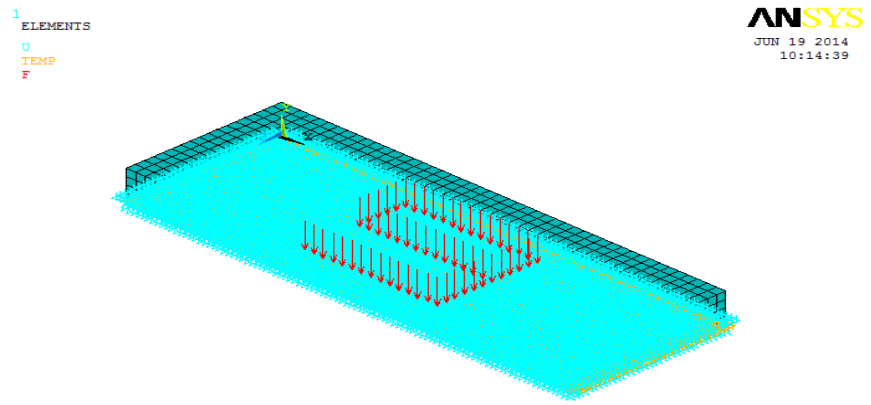

Figure 2: Model loaded with force used to engrave number

This resource was prepared by the author(s) using Federal funds provided by the U.S. Department of Justice. Opinions or points of view expressed are those of the author(s) and do not necessarily reflect the official position or policies of the U.S. Department of Justice

At a high enough force the physical patterning of the 9 becomes part of the metal. This is shown in Figure 3.

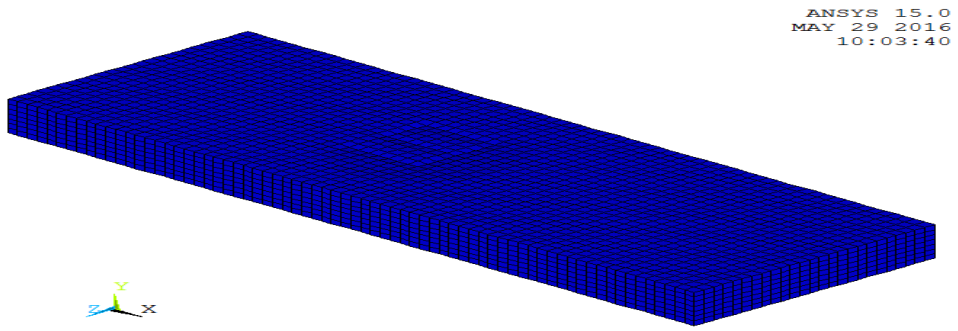

Figure 3: Model of plate engraved with a number 9

Presumably the physical properties of the metal are permanently altered below the imprint of the serial number. Figure 4 shows the elastomeric strain on the aluminum sample from the forces associated with stamping the 9 into the metal. This strain means that a plastic deformation zone would form below the stamped or engraved surface due to a heating or cooling of the material. Additionally the magnitude of the elastomeric strain allows for a calculation of the maximum depth at which the plastic deformation is operative. For this Aluminum 7075-T6 sample, the maximum depth of the plastic deformation for forces typically associated with firearm stamping is 5.9 mm.

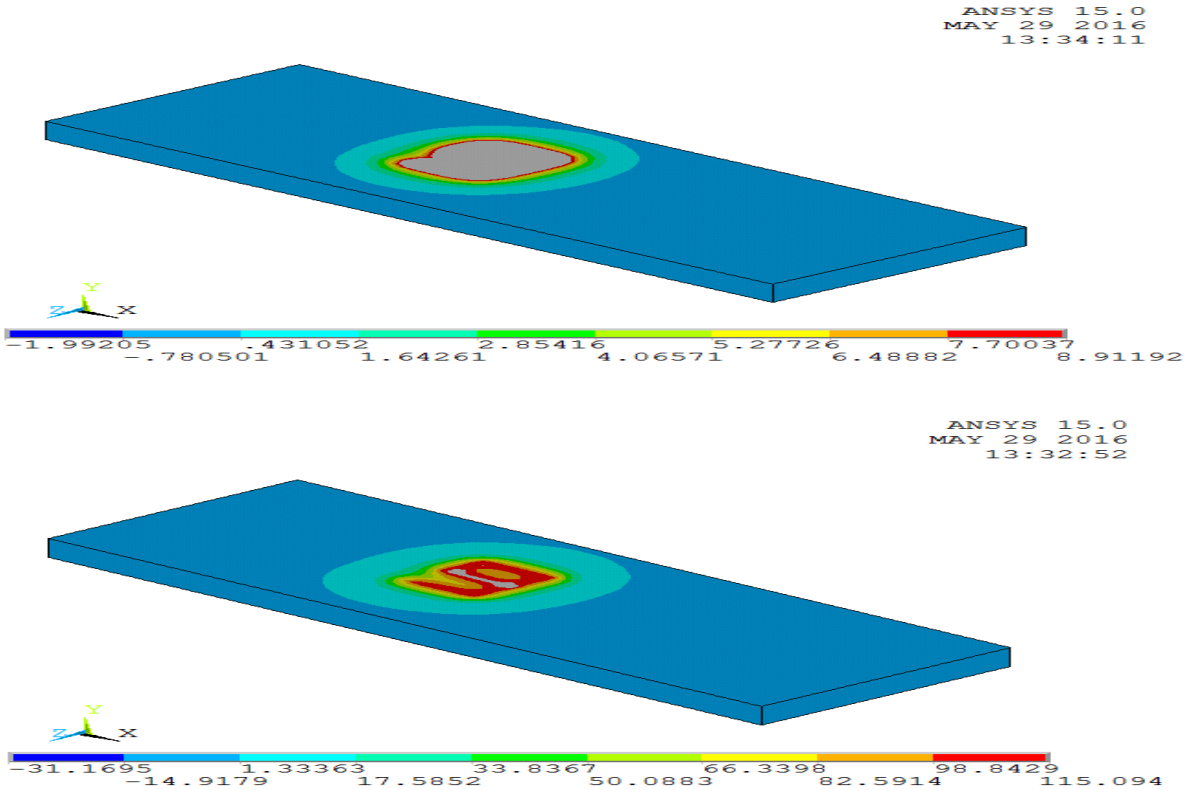

Figure 4: Isometric view of Elastic thermal strain showing plastic deformation on an engraved surface before and after applying the thermal load.

This resource was prepared by the author(s) using Federal funds provided by the U.S. Department of Justice. Opinions or points of view expressed are those of the author(s) and do not necessarily reflect the official position or policies of the U.S. Department of Justice

The results from this finite element study suggest that the use of a thermal wave over an indented surface can be used to reveal the existing plastic deformation zone beneath the indentation and help restore defaced markings. The thermal wave could be either introduced by controlled heating or cooling of the sample as is done in Transient Infrared Thermometry (TIT), or in a repetitively heated or cooled samples as in Pulsed Infrared Thermometry (PIT) or Lock-in Thermometry (LIT).

As mentioned, the Finite Element Analysis method can be applied to the stamping or engraving of other metals and the maximum depth of plastic strain deformation can be determined. The results of these calculations are reported in Table 1 for various metal sample types. It is reported plastic strain depths can extend to 2-3 (or more) times the indentation depth.[4]

Table 1. Max. Depth of Plastic Deformation for Several Metal Types from Finite Element

Metal Sample Type	Maximum Depth of Plastic Deformation (mm)
Hot rolled Steel	4.3
Stainless Steel	3.9
Heat Treated Alloy (4140)	4.0
Aluminum (7075)	5.9

The plastic deformation will likely fan out and diminish with increasing depth for the defaced serial number sample, and so the region of highest plastic strain and deformation should be at or just below the defaced surface. Presumably, if these samples were filed to more than the maximum plastic deformation depth, then IR thermometry methods would not be suitable for recovering the serial numbers. Since the plastic deformation fans out with depth, it is best to minimize the amount of sample polishing used in order to remove a minimal amount of material.

Based on the Finite Element Analysis models, one can also determine the initial temperature required to induce a thermal wave of sufficient intensity to induce a thermal gradient that would be observable with an IR camera. For the aluminum samples, the initial temperature required was calculated to be approximately 250^{o}C.

Multivariate Imaging Techniques

The infrared experimental methods chosen provide a significant tool for taking a set of infrared images and focusing on the temperature changes due to differences in thermal conductivity and density below the serial number in neighboring areas. However, in the case of a real experiment, often the relevant data need to be extracted from all the rest of the information present in that data set. In the case of serial number recovery, the information in the imaging data collected contains the desired image information related to the altering of the temperature flow through the serial number region in the defaced samples, but it also contains a plethora of other information such as information about the samples reflectivity. The desired information is likely a small subset of all the other information contained in the imaging data. Experimental

tools such as chopping the source and filtering the light reaching the detector help narrow in on the desired information, but may fall short of providing sufficient fidelity to separate the needed information from the rest. Computer based multivariate image analysis techniques like Principle Component Analysis (PCA) and Zernike Moment Analysis (ZMA) can be used to further separate the important information from the "background" information. Here background means all of the information that is not related to the alteration of the temperature flow and the recovery of the serial number image including white noise. Data preprocessing techniques can be applied to the data before or after the PCA or ZMA analyses, in an effort to minimize the noise. Ones that are commonly available with data analysis packages include: Savitsky Golay (SG), a convolution process that fits neighboring sets of adjacent data points with a low-degree polynomial by the method of linear least squares, thereby providing smoothed data set; Moving Average Filter (MAV) which averages an array of pixels surrounding a central pixel and assigns the value to the central pixel; Multiplicative Signal Correction where changes in the signal for each sample is estimated relative to that of a sample that lacks the sample alteration (here the plastic deformation zone); Generalized Least Squares Weighting (GLSW) is a multivariate filter calculated from the differences between samples that should be identical and the differences are considered to be white noise and the filter reduces the importance those interferences, External Parameter Orthogonalization (EPO) which is similar to GLSW but performs a complete subtraction of some of the orthogonal vectors identified as noise, and the Extended Multiple Mixture Model subtracts all of the orthogonal vectors identified as noise.

The goal then of the multivariate image analysis techniques is to re-express the image data set information in terms of a linear combination of a new orthogonal basis set, one that helps filter out the background and reveals the hidden structure related to the difference in the temperature flow in the plastic deformation region as compared with the rest of the sample. One restriction of PCA and ZMA is that the original data must be expressed as a linear combination of the new basis vectors. To find the new set of orthogonal basis vectors, PCA relies on the well-known method of SVD, singular value decomposition, to provide the basis vectors in PCA. Zernike Moment Analysis is like PCA in that the Zernike moments are orthogonal but the magnitude of the Zernike moments are also rotationally invariant. The Zernike moments are found by projecting the image of interest onto the complex set of orthogonal Zernike basis functions or polynomials.

Once transformation to a more relevant orthogonal basis set is accomplished, then each of these score vectors must be examined to determine if it contains information that is related to the information of interest. The score vectors are basically a projection of the original object onto a particular principal component direction. If the information of interest with a small amount of noise is well represented in the original image then the score vectors associated with PC1, and perhaps the secondary vector, PC2, would be largely associated with that original image, however if the information of interest is not a significant feature in the original data, then a higher score vector would represent that information. In the case of defaced serial number recovery, the difference in the thermal flow in the plastic deformation region is likely not a

significant feature and therefore is likely to be associated with a higher numbered score vector. A score vector then can be folded to yield a 2d score image corresponding to that vector.

If a particular score vector is largely associated with the defaced number then the score image will likely contain that information. Other types of plots can be helpful in determining the relevance of a score vector to the image information that is desired. One is called a score plot which is a two dimensional plot of the projection of the original object (image) onto the two dimensional space defined by the designated score vectors. Most often the x axis is the score vector corresponding to PC1 and the y axis can be PC2, PC3, or a higher order score vector, and the score plots are named simply by the y axis score vector. Thus the PC4 score plot would be the projection of the original image on a two dimensional space with score vector 1 as the x axis and score vector 4 as the y axis. The PC4 score plot then could be thought of as the footprint left by the original image in the space defined by PC1 and PC4.

The other type of plot that can be helpful is called a score loading plot. This is a 2 dimensional plot that shows how much each of the original unit vectors contributes to each of the principal components. The loadings themselves are the coefficients in the linear combination that defines each of the PCs. Since each variable can contribute to more than one PC, this helps determine the amount of overlap present between the PCs. For instance in the loading plot of PC1 and PC2 (P1,P2) the x-axis contains the coefficients for the original unit vectors making up PC1 and the y axis denotes the coefficients for the original unit vectors that make up PC2.

Post processing image filtering techniques are also often used for image enhancement. These included binary filtering, morphological filtering, and segmentation processing. In binary filtering a threshold level is set where pixels containing an image value higher than the set level are colored white and pixels containing an image value lower are colored black. For morphological filtering, instead of just black and white, three colors are used with two threshold values. For segmentation processing some knowledge of both the position of the serial number and the possible values of the number are required. Basically, pixels in the region of an image, where a serial number is believed to be, are selected in a score image that best represents a reproduction of the number. All other pixels are then excluded and PC analysis is carried out with only the selected pixels. Score images are then reconstructed using both the included as well as the excluded pixels. A score plot, which shows the overlap of the intensity values of pixels from different score images, can also be used to select regions of greatest density (regions where more pixels overlap) as areas of interest to be further investigated. In principle, this should leave out any noise that does not fall within the overlap and yield a better image of the number.

The other component of the Multivariate Analysis has to do with comparing the information from the multivariate analysis and post processing, with library information that corresponds to a number that could be part of the original serial number. For instance if the score image of one principal component, say PC6, largely contained an image of the plastic deformation zone beneath the serial number, then a comparison of the score image to a set of images of the digits, 0-9 in a library should allow a positive identification of the defaced serial number. The degree of confidence associated with that number assignment should also be

addressed. These comparison tools are often known as similarity merits, and they define a relative merit value in the comparison of images or the vectors corresponding to those images.

Several "similarity merit" measures are available for this purpose. These are also commonly available with the image analysis software that is available for MATLAB. The following methods were some of those used in these studies to measure the similarities between our recovered serial numbers and library sets of pristine undefaced numbers between 0 and 9: cosine θ, Euclidean Distance, Determinant, Unconstrained Procrustes Analysis, Constrained Procrustes, Mahalanobis Distance. Pooled Mahalanobis Distance, Bartlett Stats and Correlation coefficient. These similarity measures utilize different characteristics of vectors to make comparisons between them, eventually resulting in a similarity value that defines how similar or dissimilar the vectors are within the characteristic captured by the measure. As such, employing several of these measures to compare the score images to the library ensures that different defining characteristics including angle between the vectors, the distance between vectors and the transformation necessary to make one vector similar to another, are captured and used to give a holistic comparison between the recovered numbers and the library. The mathematical equations associated with these similarity measures are given in Appendix 1.

Infrared Thermometric Methods, TIT, PIT, and LIT

Sample Considerations

Most of our studies employed surrogate test samples obtained from Precision Forensic Testing from Dayton, OH. They consisted of aluminum, stainless steel, and some rolled steel plate samples stamped with several numbers. The samples were 6.35 mm thick and roughly 2 cm wide by 6 cm long. The company indicated that the force applied to stamp the serial numbers was approximately 500 N. The metals were generally shiny with some darkening due presumably to oxidation.

Several methods were used to deface the test samples. In early studies a simple qualitative method using a rough metal rasp to file down the surface, until the numbers were no longer readily observable, was employed. In a second method, a Dremel tool with a sanding roller was used to grind away the number until it was no longer observable. This was followed by polishing with a finer grit to remove the rough grooves and ridges left by this procedure. This method was also fairly qualitative as the amount of material removed was not exactly known. The majority of the studies were done with test samples with the metal material removed to a specific depth. In this method, called the successive milling method, or graded samples method, each number of the test sample was progressively shaved off with the area around each successive number removed 0.02 mm depth beyond the previous. The first number on the plate is left visible to serve as control. Figure 5 and Figure 6 show a visible photograph of a test sample before and after it was defaced by the successive milling method. After the defacing, it is quite impossible to identify the numbers that were present before the material was removed.

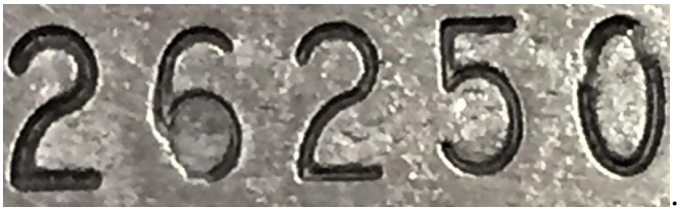

Figure 5 Photograph of the serial number area on stainless steel test sample before defacing it with the successive milling method.

Figure 6 - Photograph of the serial number area on the same stainless sample after it was defaced with the successive milling method.

Since these samples are metal samples, initial studies included the development of surface preparation methodology to correct for emissivity differences. Polishing the defaced surface is important. Roughened areas may warm and emit heat differently than less roughened areas making it difficult to observe the plastic zone serial number image that is left after the number is obliterated. To try to minimize emissivity differences across the polished surfaces a number of thin coatings were attempted and as well as the tilt of the surface relative to the camera face. In **Figure 7** and Figure 8 below it is apparent that a small tilt in the angle of the sample relative to the camera face can provide lower noise and better temperature uniformity.

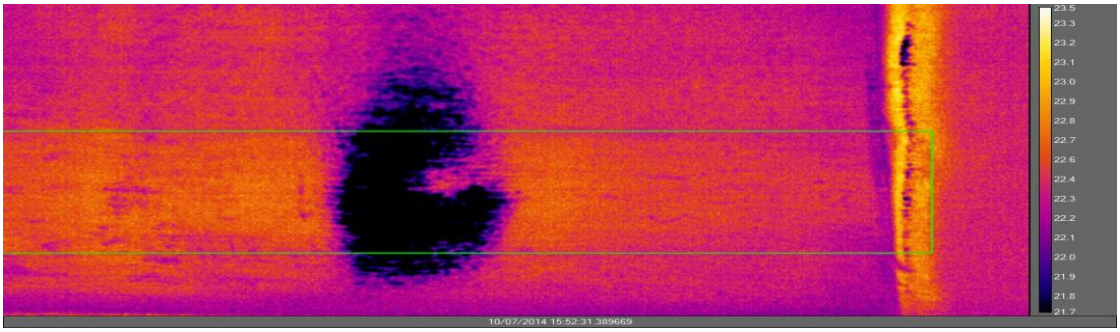

Figure 7 - Infrared image of test sample without any tilting of the sample relative to the camera. Temperatures range from 21.7°C(dark purple) to 23.3°C (light yellow).

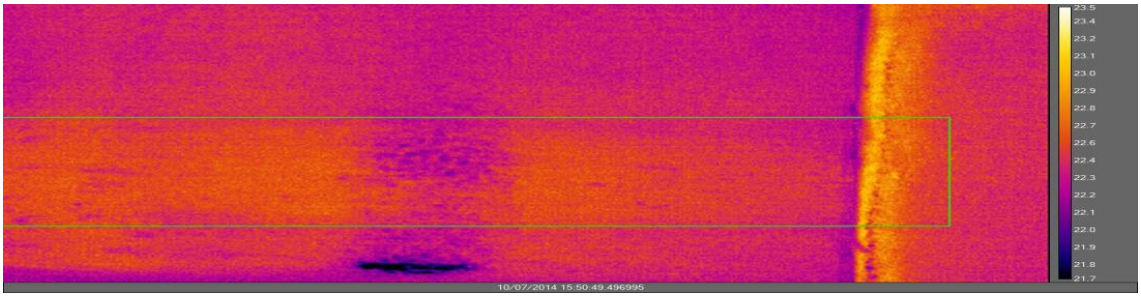

Figure 8 - Image of the same test sample with some small tilting relative to the camera. Temperatures range from 21.7°C(dark purple) to 23.3°C (light yellow).

Further emissivity differences were minimized by applying a thin layer of a low emissivity material as a thin film. A variety of materials were tried including thin layers of graphite, black watercolor paint, red dye, India ink, and high temperature flat black spray paint. These coatings provide for a surface which has a more uniform emissivity and this reduces the noise in the infrared emission due to differences in surface polish or other preparation, and allows differences in thermal conductivity to be more pronounced. As an example, the three upper panels of Figure 9 are regular pictures of the metal samples coated with a thin layer of graphite, watercolor, and high-temp paint. The bottom panel is an IR image of the surface and it contains an area in the center which is coated with a thin layer of the paint and the surrounding areas which are not. It is apparent that the surface emission from the painted spot at a constant low temperature is much more uniform than from unpainted regions.

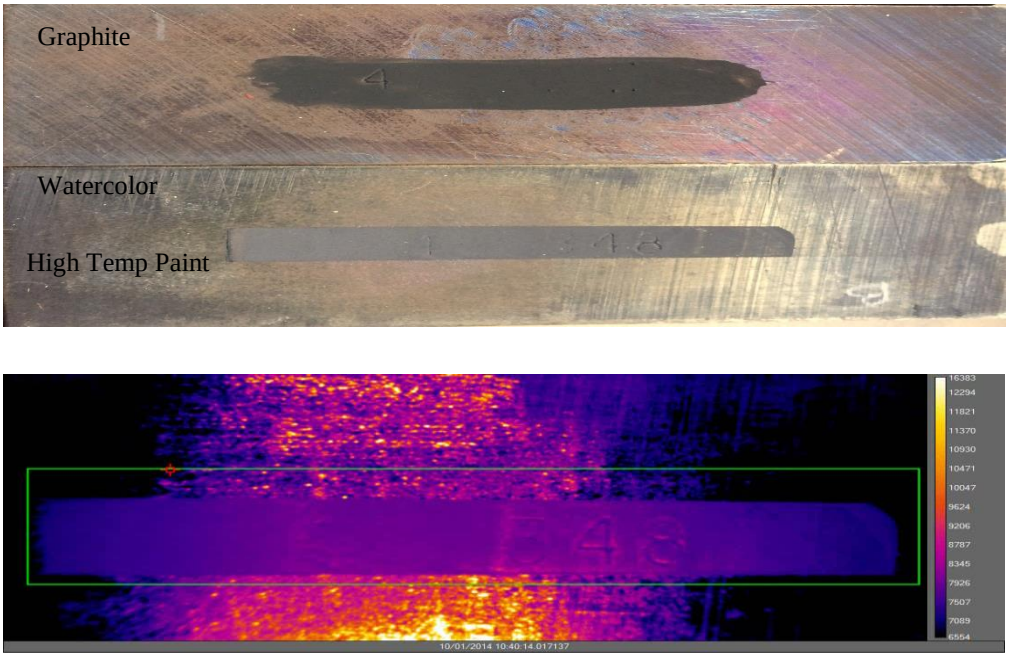

Figure 9 - Surfaces prepared with various films; bottom is an infrared image of a coated sample. Note that temperature scale units are counts. Lower temperatures are dark purple, lighter temperatures are light yellow.

The thin coating was applied using the following procedure:

1. Form a tray around the area of interest using scotch tape strips to form the walls of the tray.
2. Take the black heat resistant paint or any of the other coatings and pour the coating on tape at the edge of the well.
3. Next, use the edge of a microscope slide to smooth the coating material into the tray such that the material is spread evenly in the tray and leveled at the height of the scotch tape. This process is commonly known as "Doctor Blading" .
4. Depending on the coating material, some shrinkage may occur and this process may have to be repeated once or twice. The best coating to use to reduce emissivity-related problems was evaluated throughout many of the experimental studies performed.

In summary, it appears that the black high-temperature paint and the India ink coatings provided the best coating for emissivity uniformity.

Transient Infrared Thermometry (TIT)

The first technique used for the thermographic studies was the one that required the least amount of supporting electronic equipment. Both the PIT and LIT experiments required that the camera image acquisitions be timed to the pulsing of the heat source. In TIT one simply heats the sample to a higher temperature and then starts collecting images as it cools, or one can cool it to a low temperature and collect images as it heats up. The serial images then provide information about how the heat flow varies across the sample of interest by looking at the temperature differences in the serial images, or by averaging the images over the cooling time or over some portion of the cooling time.

The finite element theoretical studies mentioned previously were used to guide the initial studies that were performed in terms of the initial conditions that should be employed. From the theory, it appeared that bringing the defaced samples to the highest temperature possible followed by cooling in a controlled environment at room temperature or lower would provide the best conditions for the serial number recovery. Cooling them to a very low temperature with, for instance, dry ice initially and then equilibration back to room temperature also merited some study.

In our heating experiments a tube furnace or a hot plate was used to heat the sample to a high, but manageable temperature followed by cooling either in an insulated container to slow the cooling rate or by placing it on a heat sink material to try to draw the heat away from the sample and provide a higher cooling rate. The camera and the insulated sample containment apparatus are shown below in Figure 10.

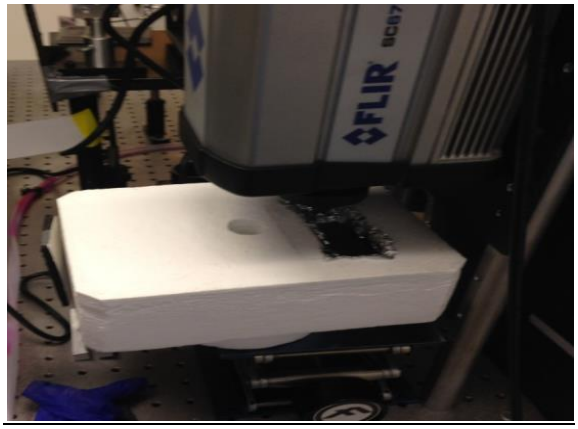

Figure 10 - Picture of Insulated Sample holder below the infrared camera.

Most of the samples were heated to between 100 and 300^{o}C as a starting point. In practice, two different experimental designs were employed. One design used a temperature controlled hot plate to heat primarily just the surface with the defaced serial number. In the second type of experiments, the test sample was heated by placing the entire sample in a tubular furnace. Here the entire metal piece reaches 100-300^{o}C, rather than just the surface. In both types of heating experiments the metal is allowed to cool in a constant lower temperature environment such as at room temperature or in a controlled temperature environment at 40^{o}C, losing heat to the environment by radiation and convection processes as the surface cools. In the first case, heat flows both from the surface to the lower temperature inside of the bar stock and also to the surroundings, whereas in the 2nd type of experiment, it flows primarily from the inside to the surface and then out to the surroundings. The data collected in this type of experiment are the surface temperatures as a function of time, once the material is placed in the new temperature-controlled environment. These time snapshots may provide partial images of the destroyed serial numbers that will have to be reconstructed from several images collected over time.

In the cooling experiments the entire sample was initially cooled, rather than heated, using a Peltier cooler or a block of dry ice. Then the Peltier cooler or dry ice is removed and then the sample is allowed to warm to room temperature by placing it on a metal surface at room temperature or on a hot plate set to control at a slightly warmer temperature, such as 40^{o}C. Images were taken every 5 to 10 seconds during the warming of the sample.

Pulsed Infrared Thermometry (PIT)

In PIT, the thermal equilibrium of the test sample surface is disturbed for a brief period of time, with a heat energy impulse. The heat then diffuses into the rest of the test sample. The IR camera then takes image sequences after the pulse and the behavior of the temperature fluctuation decay is analyzed at each pixel as the material returns to thermal equilibrium. The jump in temperature must be large enough to allow the decay to be followed, and thus the temperature loading of the surface must be reasonably substantial more than several tenths of a degree temperature change at the surface. The depth of thermal diffusion as a function of

frequency for a material can be calculated from theory and the results are given for carbon steel here in Table 2.

Table 2. Thermal diffusion length for Carbon Steel with Diffusivity of 18.8 x 10-5 m/s

Pulse Frequency (Hz)	Thermal Diffusion Length (mm)
0.10	7.7
0.50	3.5
1.00	2.4
1.85	1.8
2.00	1.7
2.33	1.6
6.00	1.0
10.0	0.8

The stamped metal samples from Precision Forensics we are using are about 6 mm thick. For the carbon steel samples a frequency of 0.5 Hz will penetrate more than half way into the sample and a frequency of 10 Hz will penetrate less than 1 mm into the sample. The plastic strain will likely fan out and diminish the deeper one probes into the defaced serial number sample, and so the region of highest plastic strain should be at or just below the defaced surface. In terms of the experiments, this means that higher heating pulse frequencies should be more sensitive to the region of plastic strain deformation and therefore areas where the temperature differences may be largest. Based on these experimental considerations, it was deemed necessary to have a pulsing circuit that could have both a variable heating pulse rate and a variable delay pulse out to trigger the image acquisitions by the camera.

Test were made with three different pulse heating sources, commercially available heat guns from Milwaukee (model 8975-6, 1400w 120V), 1000 watt theatre lamps(American DJ Model 64 Black Combo), and a chopped or pulsed laser source either an Coherent Innova Model 70 Argon-ion or a Continuum YAG laser Model YG 610. The all-lines setting of the Coherent laser gave a turquoise colored light with up to 5 watts of continuous wave (cw) lighting that was chopper with a mechanical chopper and the Continuum YAG has a 6 ns pulsewidth of 1064 nm light at 100 mJ of energy. In practice, the high power ~ 100 kW power realized in the 6 ns pulses was too powerful for the coated test samples. In some preliminary samples, it ablated the surface, and the laser heating studies almost exclusively employed the Coherent turquoise colored cw laser. The mechanical chopper was a Uniblitz Shutter (Model S25 and Uniblitz Model T132 Shutter Driver Timer) available from Vincent Associates Inc.

A pulsing circuit interface was constructed by the university electronics specialist. The interface was designed to be versatile enough to handle up to two heat guns or two 1000 Watt theatre lamps and was triggered by an external trigger source. The external trigger source used

for the experiments was a Stanford Systems Synthesized Function Generator (Model DS340). The Stanford function generator drives the pulsing circuit interface which uses power amplifiers to pulse the power. The pulsed power output is available at two regular 120V outlets mounted on the pulser circuit box. In this way either two heat guns or two 1000 Watt lamps can be plugged into these outlets and pulsed off and on at a frequency selectable on the Stanford function generator. An overall system schematic and a picture of the pulsing circuit interface box are given in Figure 11.

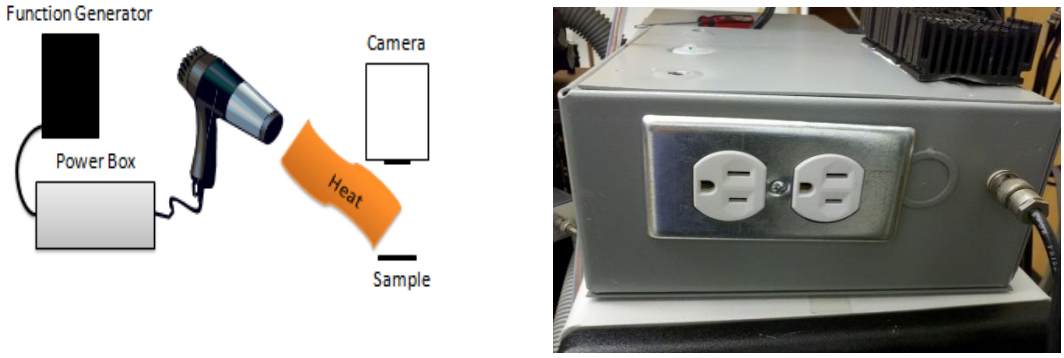

Figure 11 - Overall pulse system schematic and pulsing circuit interface box.

The Coherent Innova laser was also used to heat the samples for the PIT experiment. A schematic diagram of the laser heating experiments is given in Figure 12. The 5 watt laser was placed on a table next to the camera. Initially, the all-lines output of the laser beam entered a beam expanding telescope and then into the shutter. After a few experiments the laser beam was first put through a top hat optic from Eksma Optics Inc. The purpose of the top-hat optic was to take the normally Gaussian intensity profile of the laser beam and convert it to square-wave or "top-hat" profile such that the intensity profile was more constant across the beam. The telescope increased the spot size of the beam. Next the sample was steered to the table containing the camera and sample. A second and third prism moved the beam around the table to a high-power laser mirror. The laser mirror was used to put the laser beam onto the surface of the test sample. The size of the laser beam at the sample was about 2 cm by 3 cm at the sample.

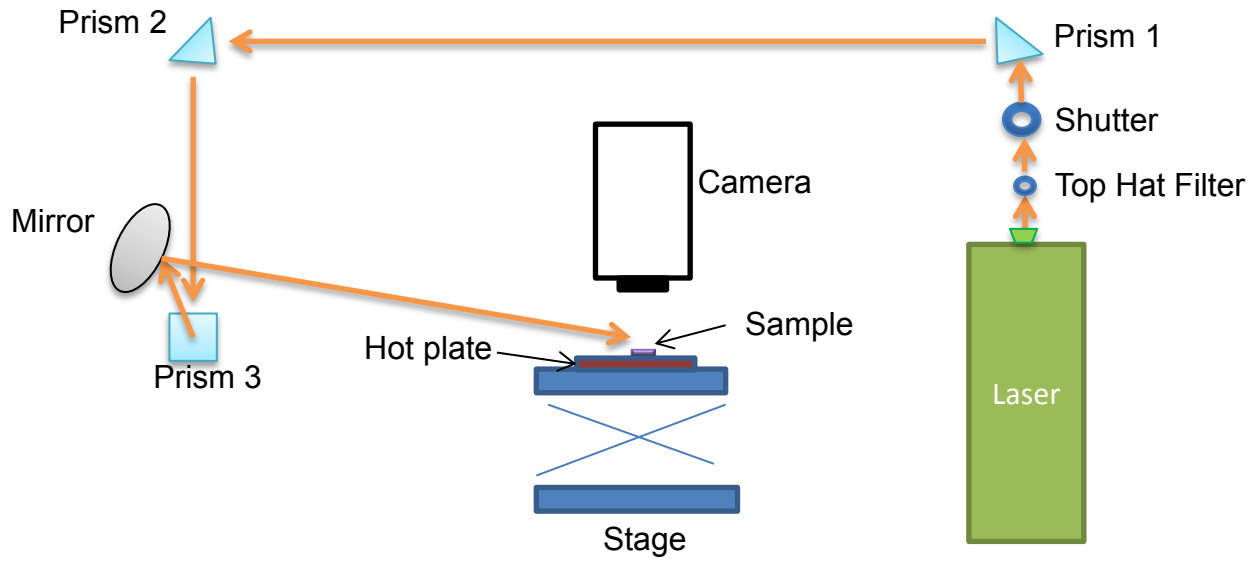

Figure 12 -Schematic diagram of the laser heating experiments.

Lock-In Thermography (LIT)

The pulsing circuitry used for the PIT studies had to be upgraded for the LIT experiment. In the LIT experiment the camera shutter has to be opened several times during the sinusoidal heating pulse, and number of times that the camera opens as well as the amount of time the shutter is open must be controllable as well. Thus a more complicated heating pulse synchronization scheme is required for lock-in thermography (LIT). In particular for lock-in thermography, the camera must take images at various evenly-spaced delays during one heating pulse. A minimum of four images must be taken during one pulse, and the more evenly spaced images acquired over the heating pulse, the higher the signal to noise. Additionally, the length of the heating pulse cycle time must also be tunable, since in general the deformation depth may be different and the thermal diffusion distance varies with the heating pulse frequency.

Thus one must be able to vary the pulse cycle time anywhere from a very slow pulse cycle time of 100 seconds/pulse to a rapid pulse cycle time of 0.01 seconds/pulse, and the camera must also be able to capture anywhere from 4 to 64 evenly spaced camera frames per pulse. Additionally, the starting point of the evenly spaced frames must also be controllable. These three variables: the pulse cycle time, the frames per pulse, and the starting point delay are important variables that have to be investigated to maximize the thermal phase image of the deformed serial number. These variables are shown in Figure 13 for the case where the camera takes a total of 8 frames (images) per pulse cycle. In Figure 14 the starting point is delayed to a different starting point, and in Figure 15 there are only 4 frames per cycle.

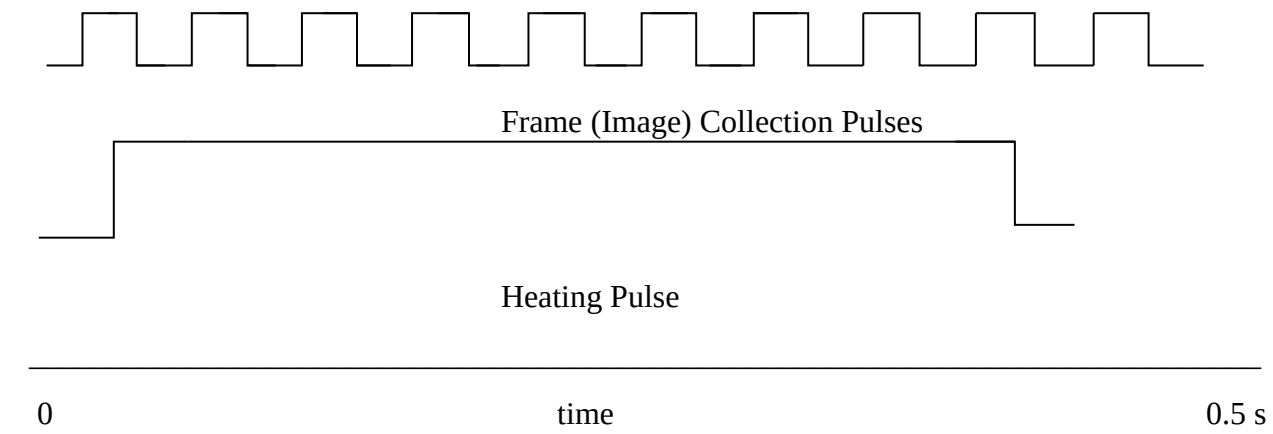

Figure 13 Pulse scheme for one pulse/sec with 16 frames/pulse.

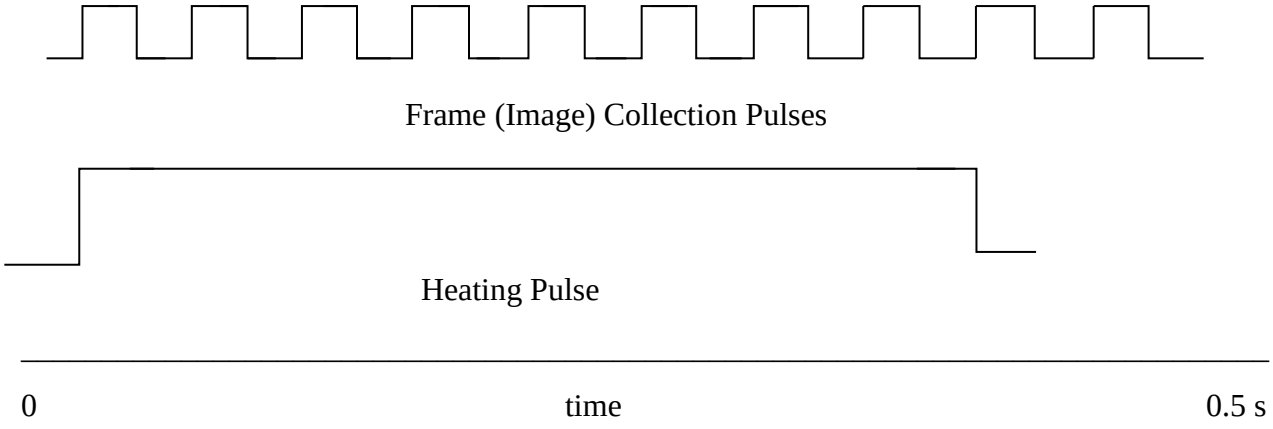

Figure 14 Pulse scheme for one pulse/second with 16 frames/pulse at a new start time delay.

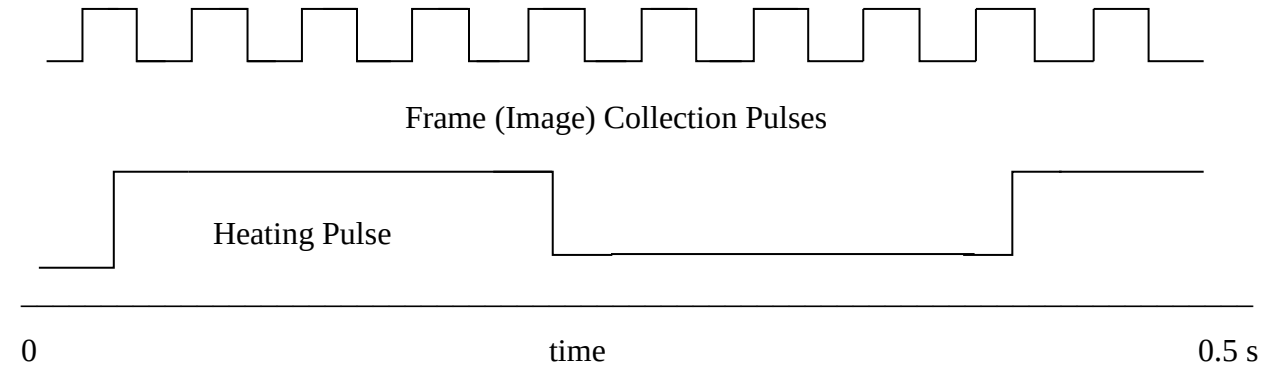

Figure 15 Pulse scheme for two pulse/sec. with 8 frames/pulse at original start time delay.

The pulsing circuit constructed to allow this variability in heating pulses/sec, image frames/sec, and start time was accomplished using a standard variable pulse source (Stanford Instruments) connected to a counting circuit with a variable delay. Essentially the variable pulse source set the image acquisition time-width and the rate at which the frames (images) are collected, then a counter could be set which relayed the number of frames pulses that are counted

until the next heating pulse occurs. A variable delay circuit between the Stanford Instruments pulser and the rate at which the frames are collected allowed the position start time delay to be varied.

The enhancement in lock-in thermography is that it looks at the oscillating part of the detected signal. Since the statistical noise is not correlated with the oscillation it can be removed. In LIT, essentially the lock-in signal treatment involves multiplication of the detected signal (say F(t)) by a correlation function K(t) which is related to the modulation of the heating and would be the symmetric longer square wave function shown above in Fig 11. The resulting Signal S is calculated by

$$S = \frac{1}{(nN)} * \sum_{i=1}^{N} \sum_{j=1}^{n} K_j F_{ij}$$

for N lock in periods and n frames per period. [5]

In practice two different types of signals, S^{0^o} & S^{90^o} are calculated from the data using their corresponding correlation values

$$K_j^{0^o} = 2Sin\left(\frac{2\pi(j-1)}{n}\right)$$

$$K_j^{90^o} = 2Cos\left(\frac{2\pi(j-1)}{n}\right)$$

From these two types of signals, one can calculate the phase-independent Amplitude "A" and the value of the signal phase "φ". These are given by:

$A = \left(\left(S^{0^o}\right)^2 + \left(S^{90^o}\right)^2\right)^{1/2}$ and $\varphi = arctan\left(\frac{S^{90^o}}{S^{0^o}}\right)$ (- 180° if S^{0^o} is a negative value)

Often the – cos function is used instead of the + cos function to get a positive value. The component of the signal modulation in any phase position φ' can be found from

$$S^{\varphi'} = ACos(\varphi' - \varphi)^4$$

To keep the correlation function symmetric, n has to be an even integer and to get both the amplitude and phase information this has to be done at least twice in each period. This makes 4 the minimum number of samples (frames) per period. If only 4, then this is called a 4-point correlation. Note the frame integration rate must be kept small compared to the lock-in frequency if more samples (frames) are collected per lock-in (heating) period. The higher the number of samples collected per lock-in period, the more the sum approximates the true signal. The heat introduction should be done in as harmonic a fashion as possible, but in practice this is difficult and non-harmonic heat introduction often results. As long as the number of frames per lock-in period is large and the sin/-cos correlation is used, the effective error associated with a non-sinusoidal heating pulse is minimized.

Faster heating and sampling rates may be necessary to increase the spatial resolution of the measurements. The thermal diffusion length goes at 1/((lock-in (heating) frequency))$^{1/2}$. So, if the image of interest is related to a difference in the rate of diffusion, then the difference in the amplitude signal or the phase signal may be important. Thus the LIT technique allows one to construct a phase image in addition to a direct image. The phase image theoretically subtracts out the local optical and thermographic background features and has more depth range than the direct signal magnitude.

III. RESULTS

TIT Results

Several heating TIT studies were attempted with the FLIR camera. The 300°C samples were troublesome and many of the studies were performed where the surface of the metal was heated to 200°C, followed by cooling in a room temperature environment. Our best results to date, where an aluminum test sample was qualitatively defaced using only a rough rasp are presented here as thermal images of the defaced metal before and after heating the surface to 200°C. Figure 16 is basically a visible photographic image of the defaced aluminum sample taken at room temperature. Note that the ridges and valleys have not been polished out in this sample. This image is similar to what you see if you take the sample and examine it thoroughly with just your eyes looking straight down on the surface. Figure 17 is just the same image but with a green filter inserted to determine if the filter enhanced the imaging of the defaced serial number. Finally, Figure 18 is a snapshot of the aluminum sample as its surface cooled from ~200°C to room temperature. Note that several digits of the serial number, or partial digits, become visible in this picture.

Figure 16 Photographic image of a defaced unfiltered aluminum test sample of the defaced serial number 22789043.

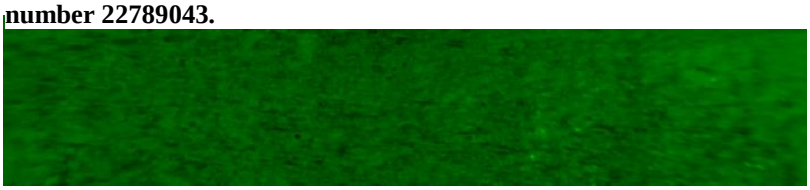

Figure 17 Photographic image of defaced aluminum test sample with the addition of a green palette filter.

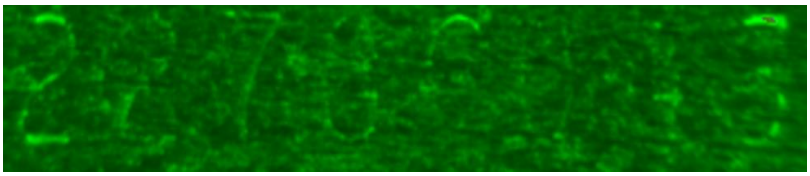

Figure 18 Infrared image of a defaced serial number during cooling to room temperature after first heating the sample to 200°C.

It should be noted that removal of some of the ridges and valleys seen in the photographic images, made some of the serial number observable again. Apparently defacing where the sample is only roughened with a rasp may render visible observation of the serial number difficult, but if not much of the serial number is removed, then it can be observed with an infrared camera. However, it is likely that most often when a sample is defaced, a more significant amount of material is removed and serial number recovery will be much more challenging.

This proved to be the case when the TIT method was employed for serial number recovery for test samples defaced with a Dremel tool or test samples defaced with the successive milling method. Several TIT experiments performed both with the heating method and the cooling method gave negative results for recovery of the serial numbers when the serial numbers were removed more completely with these methods. Several well-known preprocessing and filtering methods were applied to the images collected with the TIT methods. In particular, Standard Normal Variant (SNV), Savitsky Golay (SG), Generalized Least Squares Weighting (GLSW), External Parameter Orthogonalization (EPO), the Extended Mixture Model (EMM), Moving Average Filter (MAF), and Multiplicative Signal Correction (MSC) preprocessing were applied to the TIT data to see if each method might improve the serial number recovery. There was no significant visual change in the front face images of the defaced sample when most of these image preprocessing methods were employed.

Some improvement in the background was noted when a Moving Average Filter (MAF) was added to filter the images. The MAF averages an array of pixels surrounding a central pixel and assigns the value to the central pixel. In this case a 3 by 3 pixel array was found to be best. From all of the preprocessing and filter methods attempted, the Moving Average Filter (MAF) model showed the most promise in reducing some the background noise.

PIT Results

Investigations with the PIT system employed 1 or 2 heat guns or employed 1 or 2 theatre lamps, and these were put in close proximity to the camera and the sample holder. The camera was mounted above a laser table using two aluminum posts with a mounting plate attached. Several holes were drilled into the mounting plate, and the aluminum posts were drilled and tapped to allow the height of the camera above the table to be adjusted. The lamps and the heat guns were mounted on either side of the camera so that the heating was more uniform across the surface of the test sample. Several attempts were made to focus the light from the heating lamps to increase the heating. However this proved difficult due to the size of the lamps and also the glass absorbed the infrared light from the lamps.

The samples were placed on either a temperature programmable heat plate or on a Peltier cooler. Preliminary experiments indicated that the serial number recovery was better when the sample temperature was different than the temperature of the surrounding material. Two possible reasons for this is that when the IR camera images the higher sample temperatures, the background noise is less since much of the background appears at room temperature, and the

other reason relates to the fact that when the temperature is in fact controlled at a higher temperature, the fluctuations about that controlled higher temperature are less than the random fluctuations about a test sample not under active temperature control at room temperature. The function generator and the pulsing circuit interface box were placed in close proximity to the lamps, heaters, and camera to facilitate connections between the different parts of the system. A picture showing the relative mounting of the theatre lamps, programmable hot plate, and IR camera are given here in Figure 19**.** The function generator and connections from it to the camera are shown in the background of this picture. The graph presented next to the picture gives the sinusoidal wave input pulse in red and the resulting temperature profile of the test sample's surface as a function of time in blue. In this particular experiment the temperature profile followed the input pulse well, surface temperature only fluctuated by only a few tenths of a degree.

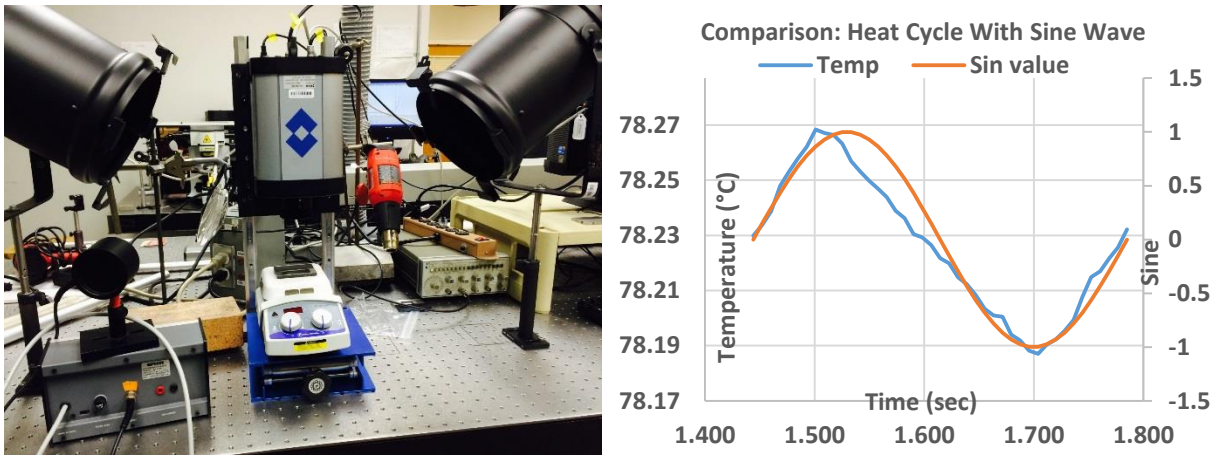

Figure 19 Heating arrangement used for PIT and LIT Experiments. The temperature profile is the blue curve and the sinusoidal pulse used to trigger the lights is the red curve.

The small temperature swing likely limits the sensitivity of the PIT technique, and a larger controlled temperature swing is desirable. The pulsing was synchronized with the camera to allow the possibility of averaging over several pulses.

This setup used for the PIT experiments yielded positive results in some cases, and in other cases the results were less consistent. An example of one of our more promising results is given in Figure 20. Here a number "2" that was not defaced and a "2" that was defaced to a total depth of about 0.6 mm, 0.3 mm below the surface where the number was just removed, were analyzed using the PIT technique with the pulsed lamps. The far left is the temperature profile resulting from the pulsed light for the middle movie. The three images correspond to different pulse rates. From left to right, the pulse rates were 0.73 Hz, 2.3 Hz, and 2.9 Hz. According to theory these correspond to thermal diffusion lengths 2.4 mm, 1.6 mm, and 1.4 mm.

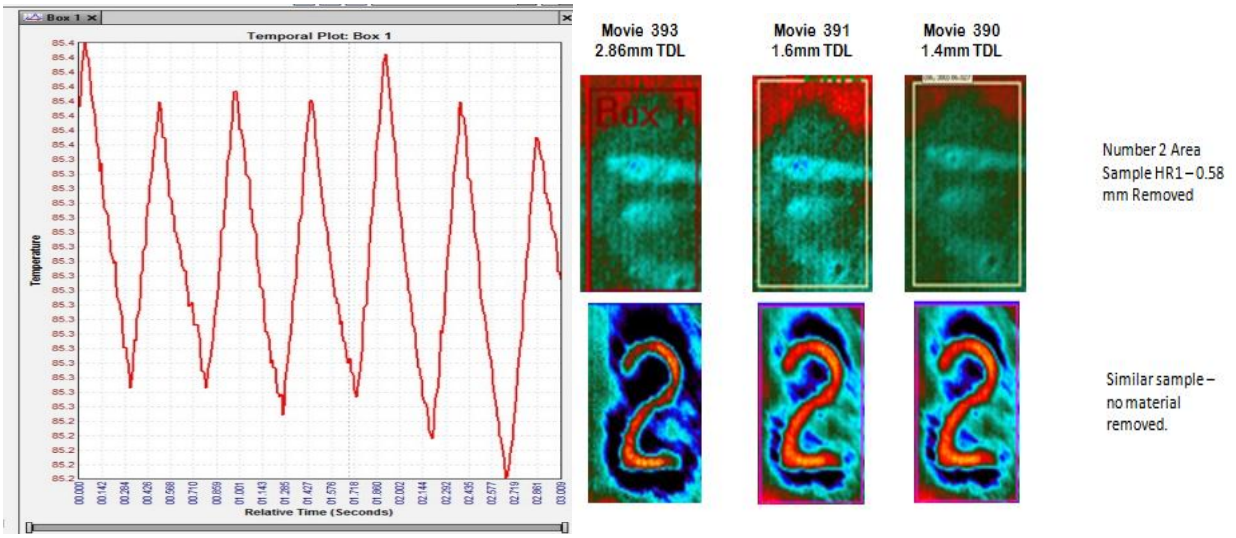

Figure 20 Temperature profile and PIT generated thermal images of a defaced "2", ~ 0.6 mm below the surface (0.3 below point where number is just shaved off) and a non-defaced "2" taken at different pulse rates corresponding to different thermal diffusion distances. The thermal profile corresponds to the middle "2" image. Y-axis shows temperature and X-axis shows relative time in seconds during the data acquisition.

Unfortunately, the results for other numbers prepared in a similar manner were not as promising. Some physical limitations were encountered during the set up. The distance of the sample from the camera at the focus, was about 4 inches, making it difficult to get the heat from the heat gun or the light from the theatre lamps onto the sample, and limits the heating that can be accomplished. The focal length of the camera lens was only 25 mm. The lens was exchanged for a 50 mm lens, the focal length stated in the original bid. Additionally, the heat gun was found to be electrically noisy; likely because the fan in the gun also pulsed with the pulsing circuit. To minimize the noise, the heat guns were modified to keep the fan on throughout the experiments and the pulsing circuit now only turns the resistive element in the heat gun off and on.

The experiments using the chopped Ar-ion laser to heat the sample were also attempted at this point, but the results were not any better than the results obtained by pulsing the theatre lamps. Several different wattages were tried from 1.0 watts up to about 3.0 watts of all lines laser emission.

LIT Results

The LIT system was tested by attempting an experiment from the literature that used the LIT method.[6] In this experiment, LIT is essentially used to detect, from the front surface of the metal, three holes that were drilled in the back side of a metal sample such that one hole was 2 mm below the front side metal, the second was 4 mm below the front side surface, and the third was 6 mm below the front side. Samples were prepared with two different hole diameters. The larger diameter holes were 10 mm in diameter and the smaller holes were only 4 mm in diameter. The larger diameter hole that was 2 mm below the surface was visible in the phase image using the lock-in system with theatre lights as the heating source. Typical results are shown in Figure 21 for several different frame rates on a heating pulse cycle that was 8 seconds in length (a

frequency of 1 pulse/8 seconds = 0.125 Hz). The upper four images labeled 1, 4, 5, 6, for each different number of frames, indicate the delay point at which the calculation given above was started for the raw data, and the lower four images are from the primary principal component score image from the PCA treated data.

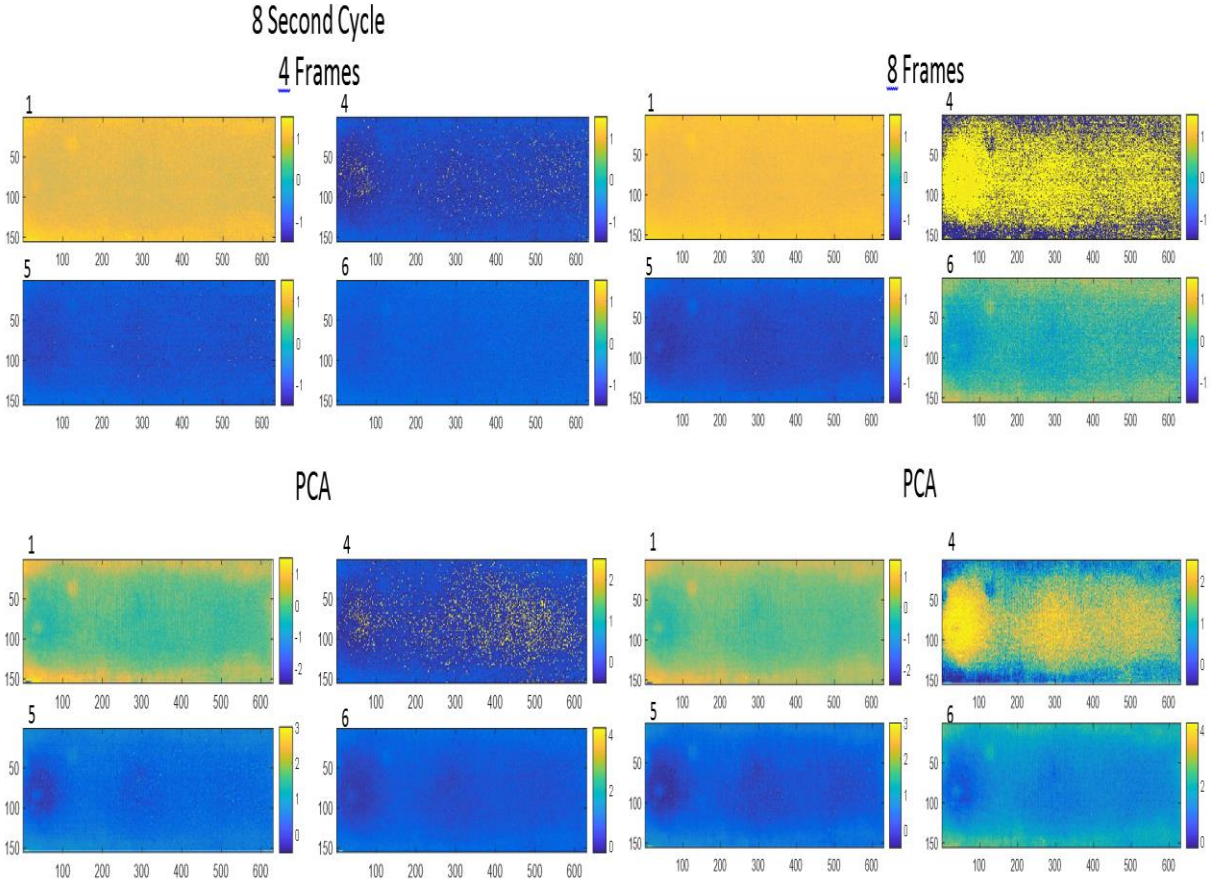

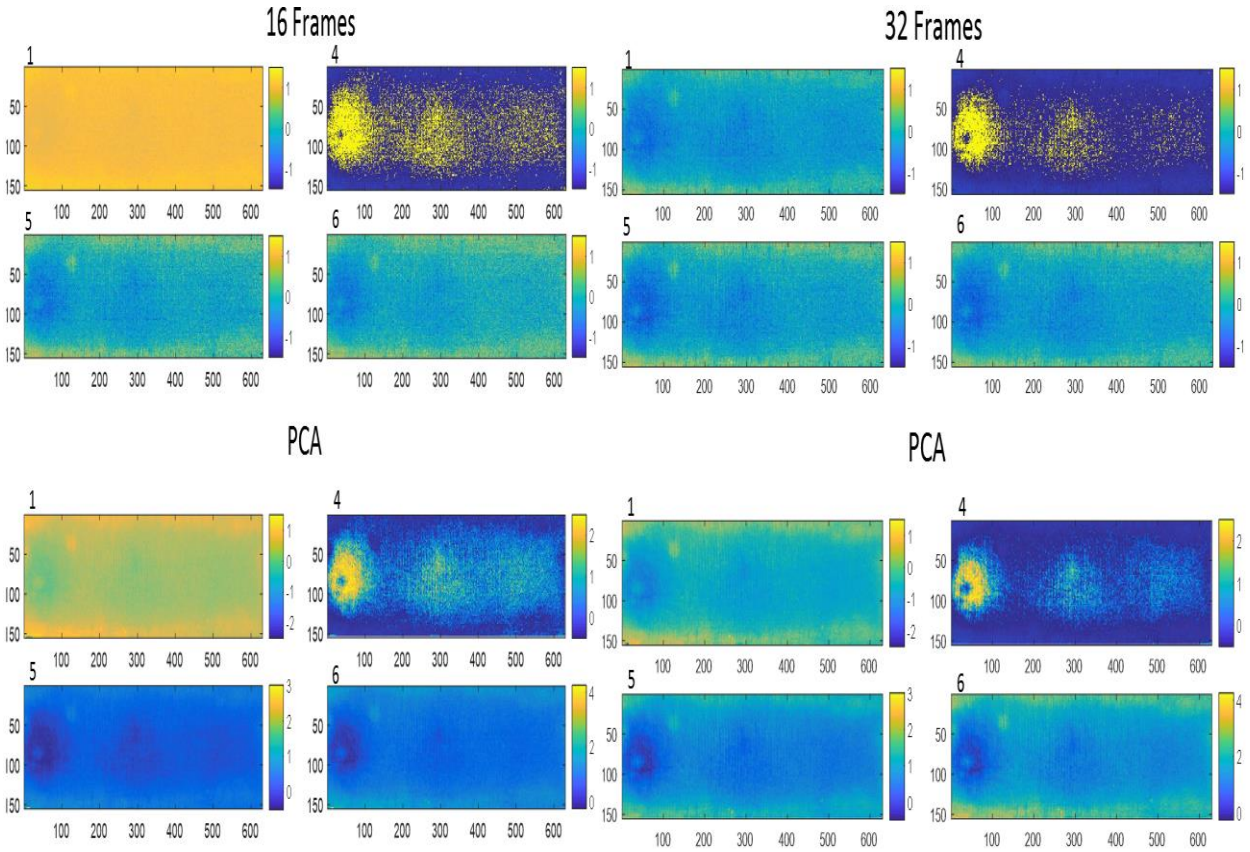

Figure 21 Front-side Phase Image Pixel maps of three 10 mm Diameter Holes, drilled from the back-side. Depths from the surface are 2 mm, 4mm, 6mm from left to right. Colors indicate degrees of phase shift.

Note that the hole drilled to around 2 mm from the front-side surface was visible in almost all cases. The other holes were less well defined except at the higher number of frames collected per pulse. If a Moving Average Filter (MAF) is applied to the data it appears that the hole boundaries become more well defined especially for the 16 and 32 frames/pulse collection rate. (See Figure 22)

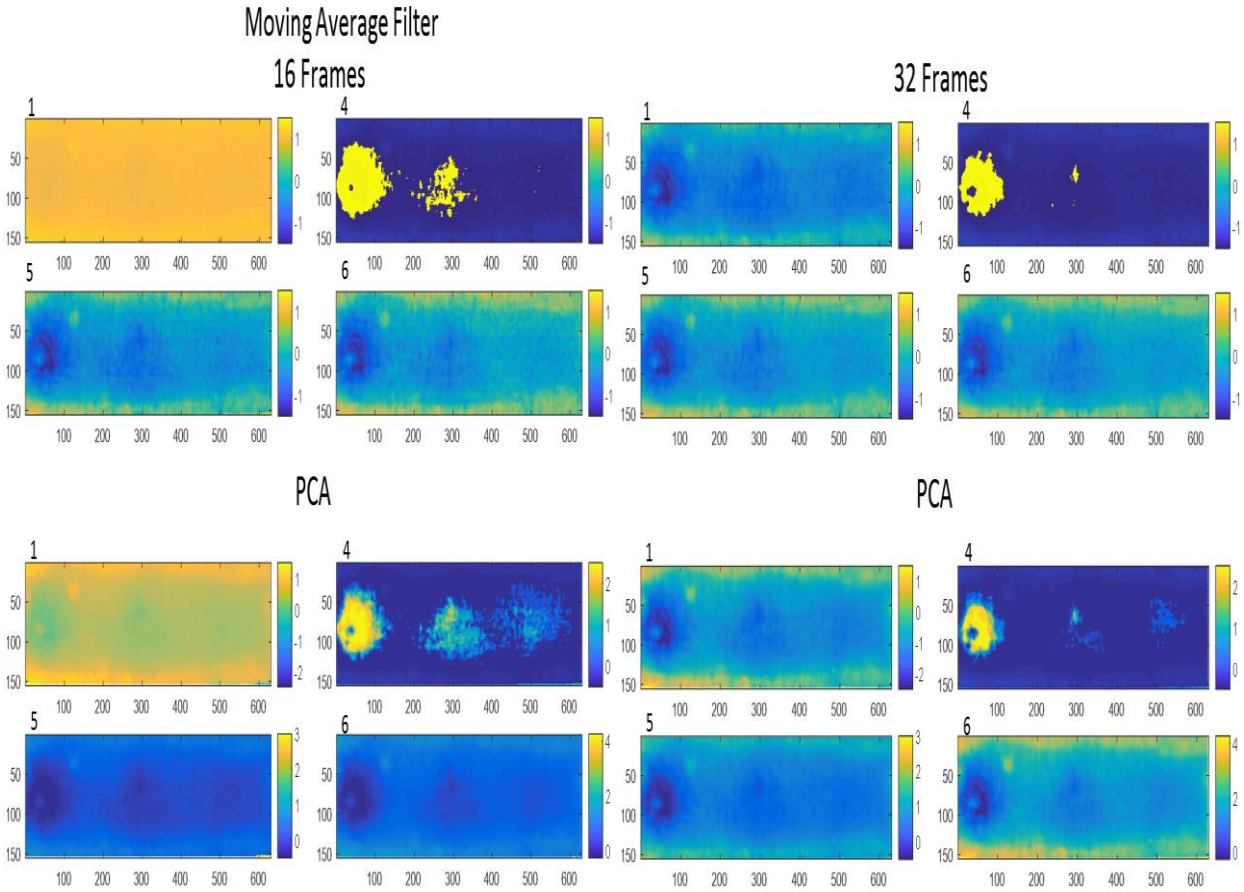

Figure 22 Front-side Phase pixel map Images of the same holes in Figure 15, but with a Moving Average Filter. Colors indicate degrees of phase shift.

The smaller holes proved more difficult to image from the front surface. In Figure 22, only one complete hole and a half of another hole are visible. The magnification in this image was higher than in the previous figures. The holes were machined from the back side of one of our samples with a serial number on the front. The serial numbers on the front are visible in the image and the holes that drilled through the back surface were at depths of 4 mm and 2mm from the front surface for the full hole and for the half hole respectively. The full and half hole can best be viewed in the bottom image of Figure 23. The holes are the lighter features in that figure. This is a score plot corresponding to PCA 6.

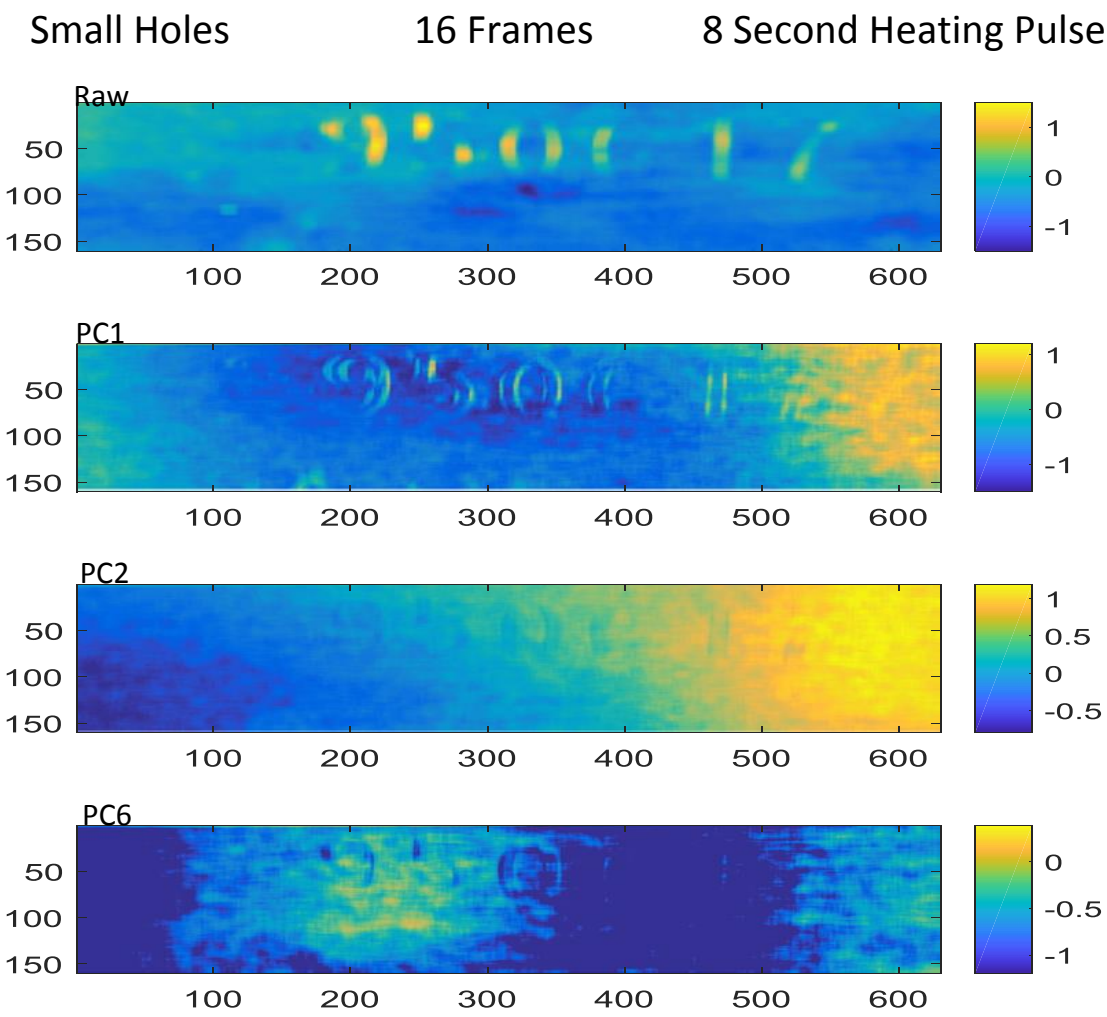

Figure 23 Front-side Phase Images of two smaller 4 m/m Diameter Holes, drilled from the back-side. Depths from the surface are 2 mm and 4mm from left to right. Colors indicate degree of phase shift.

The choice for the length of the heating cycle must include a consideration of the depth of the feature and the thermal diffusion distance corresponding to a particular metal. A characteristic Phase Difference Plot (Background Area – Defaced Number Area) for a particular sample type can be constructed to help determine the optimal heating cycle time. The phase difference can be positive and negative or zero. The zero represents a crossover point where the phase difference switches from negative to positive or positive to negative, and represents a "blind" cycling time where there is minimal difference between the thermal signal from the defaced number area, and the background area. This type of plot can be used to help determine the best cycle time since the maximal difference between the background area and the defaced number area should give the best results. An example of a phase difference plot is given in Figure 24.

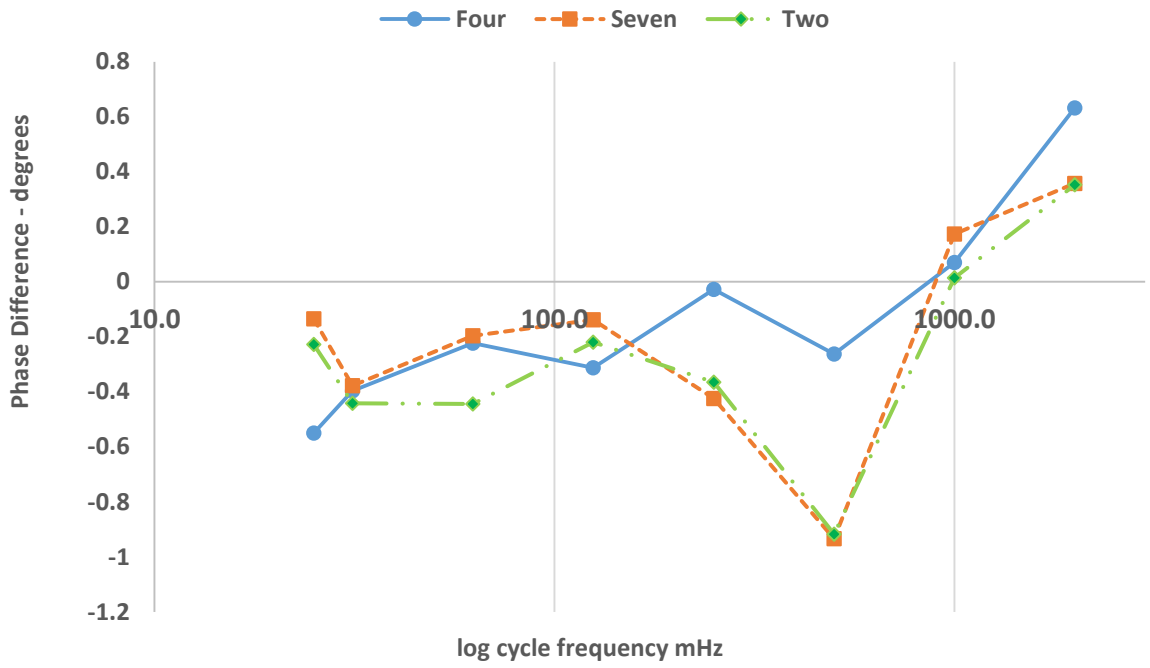

Figure 24 Plot of Phase Difference versus the log10 of the cycle frequency for steel sample starting the phase difference computation at different points in the cycle.

For this particular sample the "blind" frequency occurs at about 1000 mHz which corresponds to a pulsed heating cycle time of 1 second/pulse. This type of plot requires much information to be collected and processed and requires a significant amount of time to construct. However, this type of plot should prove useful in determining the best heating cycle time to be used for a particular experiment, and the fact that the plot has the correct overall character suggests that the LIT setup is working properly.

All three heating sources were investigated for their potential to heat the surface and also their inherent noise. Each was used to try to image the holes drilled in the backside of the metal and attention was paid to the temperature swing and the noise. The theatre lamps and the Ar-ion laser had lower noise and experiments with the Ar-ion laser operating at 4 Watts indicate that the temperature swing can be increased to more than 1 ^{o}C, and the heat gun also had a large temperature swing but the noise was larger than the noise from the laser. The theatre lamps had a low noise factor associated with them, but the temperature swing during the heating pulse was also much lower. For these reasons most of the later studies on serial recovery from the test samples was done with the laser as a heating source.

The LIT studies on the imaging of the holes, especially the small holes drilled in the back of the test samples provided evidence that the LIT experiment was setup correctly and that it might be applicable for serial number recovery. The next step was to use it on the defaced serial numbers from the test samples. As mentioned previously, the surface preparation including polishing and the thin coating of the sample, along with the depth to which sample has been

defaced, are important experimental parameters. The effect of insufficient polishing can be seen in the series of images that follow.

The LIT experimental setup was applied to the recovery of the numbers on the steel test sample, mentioned previously in the sample considerations section, where the numbers were progressively machined away to lower and lower depths going from left to right in the figure. The number 2 is the first number and it is still visible in left side of the figure. The next number is the number 6, and part of the number 6 is still visible in the picture as well. Other numbers which have been shaved off completely to lower and lower depths from the surface are another number 2, a number 5, a number 0 and a number 3. Striations left over from the machining process are also readily evident in this thermal image. Figure 25 is just the raw image and has had no additional processing.

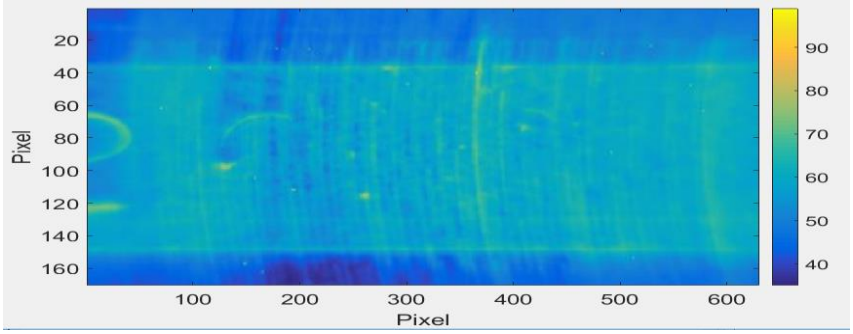

Figure 25 Raw thermal image of defaced serial number sample with metal shaved off to progressively greater depths from left to right. The numbers defaced are a 2 (visible), 6 (partly visible), 2 and 5 in that order. The 0 and 3 are not part of the area imaged. Temperature is indicated by colors scale (dark = 40°, light yellow = 90°C)

The thermal images in Figure 26 below were gathered using a pulsed laser as the heating source. The pulse cycle was 40 seconds. The laser used was an argon-ion laser operating in all-lines mode at about 3 watts. The images are from the area on the metal where the number 6 has been defaced. One can see the striations from the machining in the raw image and in the Score Image from PC 1 and the Score Image from PC 5. The machining grooves are readily visible in the 1st Score Image and also disrupt the score image for the best recovery of the number 6, the Score Image from PC5. These score images were pre-filtered with a moving average filter, MAF, as described previously.

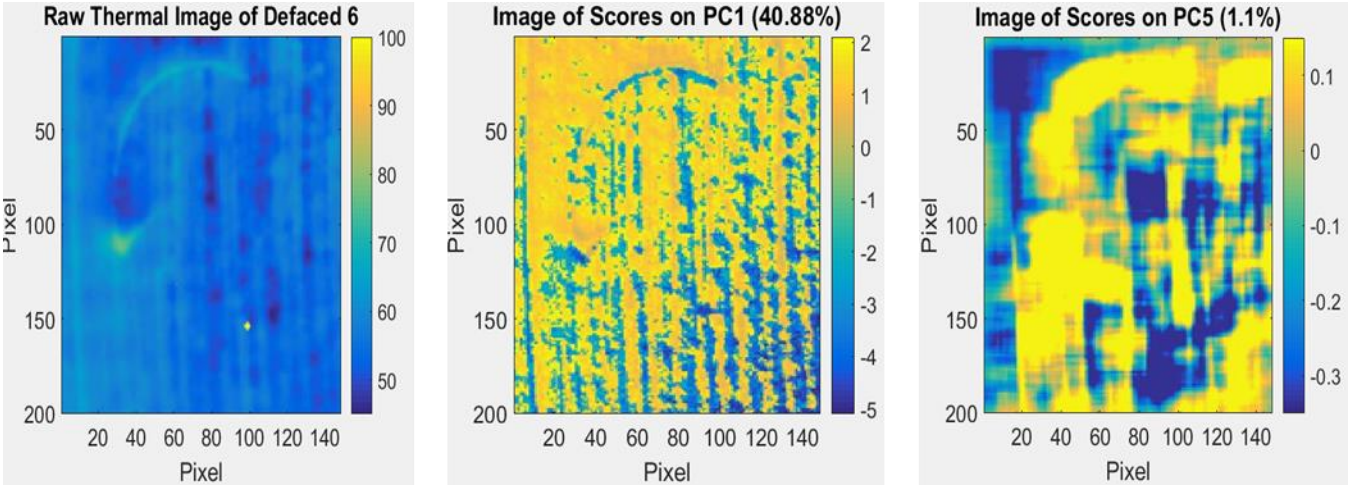

Figure 26 Raw thermal image of number 6, and two score plots from the same region.

Light sanding with progressively finer grit sand paper was applied to the defaced samples as a preparation step for the thermal imaging. This greatly reduced noise and improved the image quality of the recovered number. As mentioned, the serial number originally stamped into this steel sample was 2, 6, 2, 5, 0, 3. The last number, the 3, was removed by machining with a mill to a depth of 5 mm below the surface. Thermal images of the graded sample were taken at several different pulse frequencies. These raw images were then processed with the lock-in thermography equations to generate both magnitude and phase images. The phase images were further processed with a moving average filter and then principal component analysis (PCA). The score images corresponding to the various eigenvectors determined by the PCA analysis were then examined for evidence of the defaced serial number. In Figure 27, three score images are given for the area where second number 2 were defaced respectively.

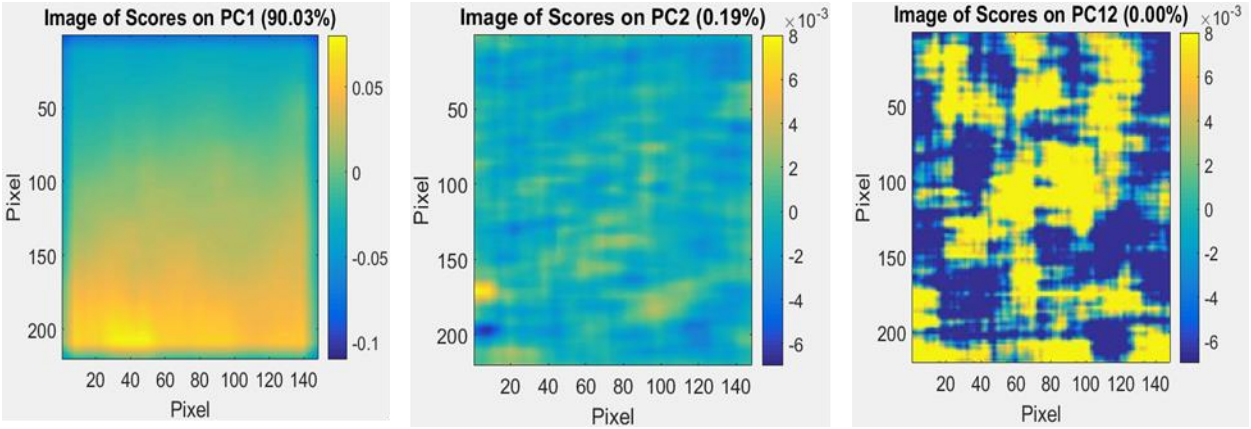

Figure 27 Three score Images corresponding to the area with the number 2, data taken at 2.4 Watts and 40 seconds/pulse.

It is apparent that the score images for PC 1 and PC 2 are not significantly associated with the defaced serial number, however in these cases PC 5 (for number 6) and PC 12 (for

number 2) seem to be very much associated with this information. It should be noted that although the other score images with smaller PCs contained some information, it appears to be less associated with the number's image. This same procedure was used to process the thermal image information for the region associated with the next number on the graded sample, the 5.

As the laser beam impinges on a significant portion of the graded sample, images for the area with the number 5 are collected at the same time as for the number 2. However, as mentioned previously, since the laser beam intensity is not completely uniform across the surface, the actual heating of the area with the 5 is different than the area with the 2. This is expected to change the processed results as well. The moving average filter (MAF) and PCA analysis for the region with the defaced 5 resulted in the score images presented in **Figure 28**.

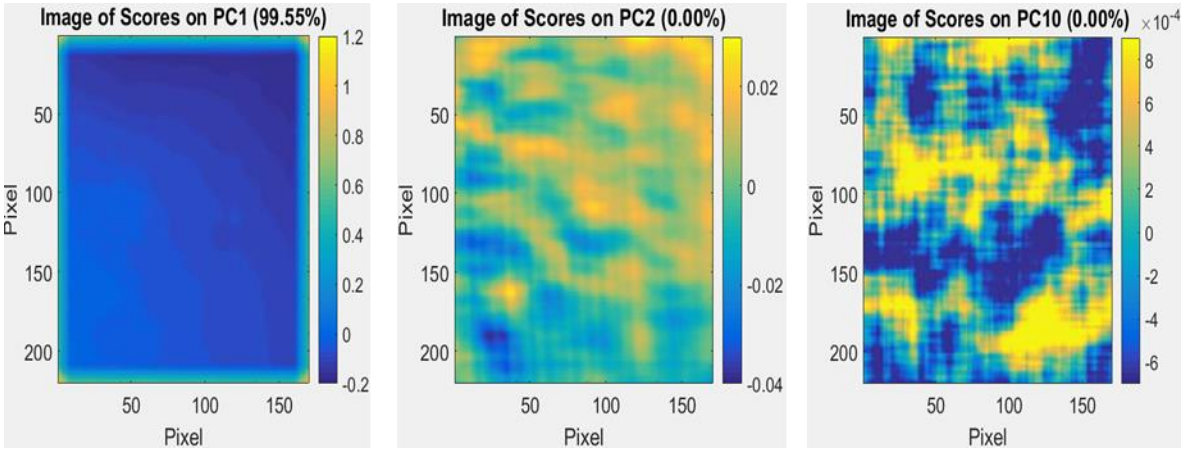

Figure 28 Score images in the region containing the number 5 on the graded sample, data taken at 2.4 Watts and 40 seconds/pulse.

Here again the 1st and 2nd score images are apparently not significantly associated with the defaced number, but score image PC 10 does appear to contain significant information on the image of the number of interest. These images were actually collected with the LIT system before the 25 mm lens was replaced with a 50 mm one. The pulse rate used was 40 seconds/pulse. Although these images do seem to contain information that would lead to recovery of the defaced 2 and the defaced 5 respectively, the question of reproducibility must be addressed. A good test of this was to replace the 25 mm lens with the 50 mm lens thereby changing the setup somewhat, and retest the graded sample in the same area. This was accomplished and Figure 29 and Figure 30 display the score images that result.

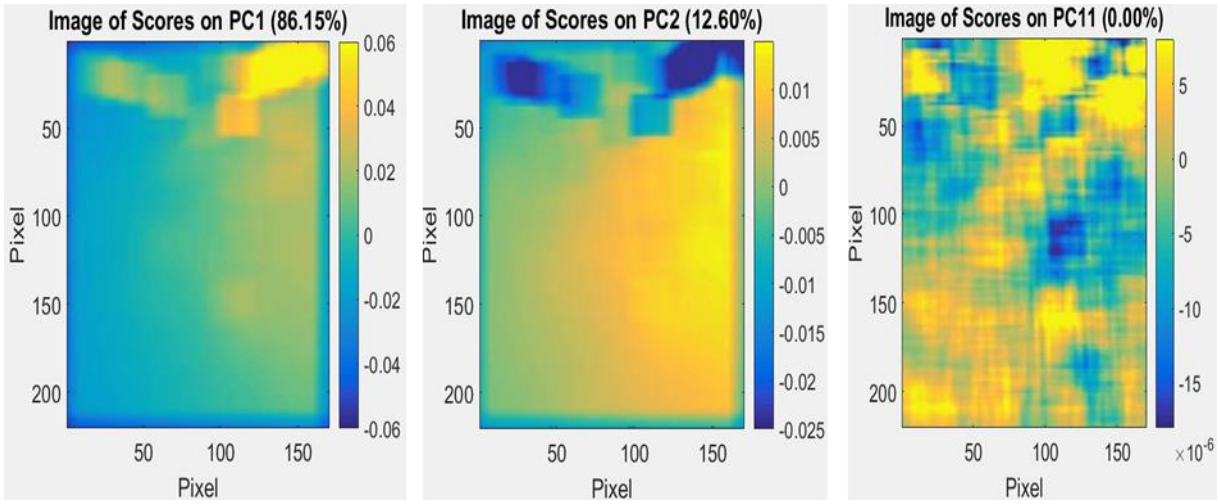

Figure 29 Score images in the region containing the number 2 after replacing the lens, 24 seconds per pulse, and 4 watt laser heating.

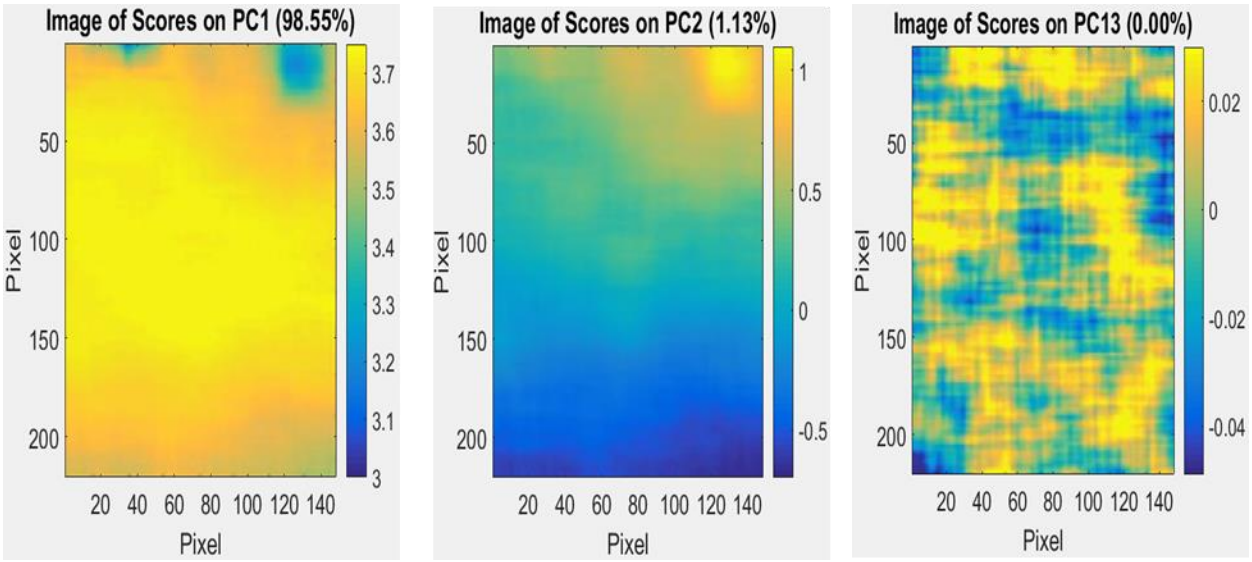

Figure 30 Score images in the region containing the number 5 after replacing the lens, 24 Seconds/pulse, 4 watt laser heating.

The defaced serial numbers also appear to be visible in the higher PC score images after replacing the 25 mm lens with the 50 mm lens. The exact numbers of the score images differ before and after the lens replacement, going from PC 12 to PC 11 in the case of the number 2 and from PC 10 to PC 13 in the case of the number 5. Also the shapes of the numbers in the images appear to be different. It is encouraging that the score images here also appear to contain the defaced numbers, but the fact that the image does not always appear in one particular numbered score image, may be troublesome for use as a routine investigation tool. Application of some of the measures of similarity mentioned in the Multivariate Image Analysis section proved useful for this. This will be discussed later in the report.

One should note in Figure 29 and Figure 30, the laser power was higher at 4 watts and the pulse rate was different as well. Experiments to investigate the effect of changing the pulse rates and altering the laser powers were started with the intent of finding some optimal operational parameters for the laser power and pulse rate. One of the results is shown here in Figure 31and Figure 32. Here the laser power was maintained at 4 watts, but the pulse rate was changed from 24 to 20 seconds/pulse.

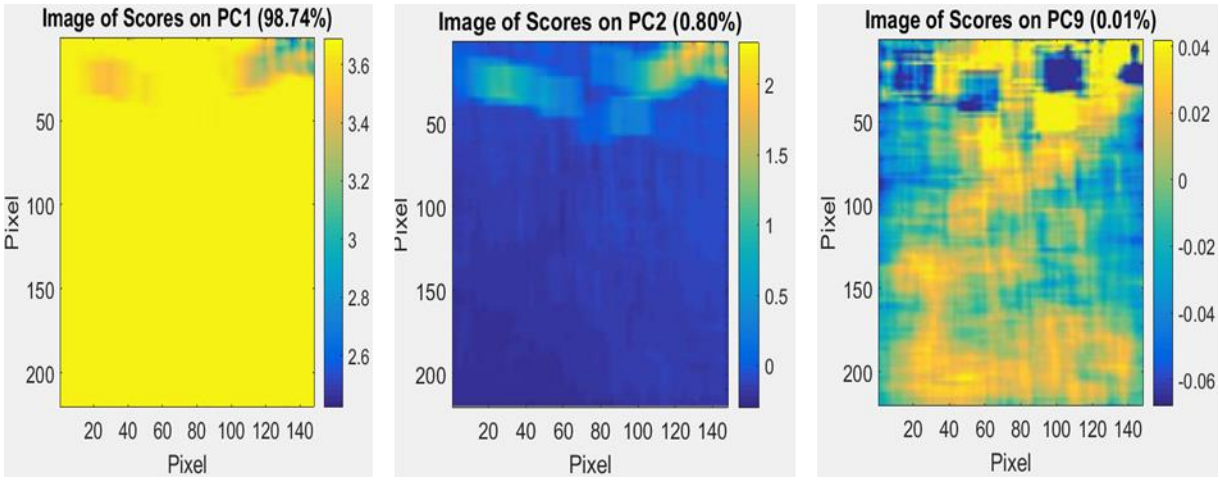

Figure 31 Score images in the region containing the number 2 after replacing the lens, 20 sec/pulse and 4 watt laser heating.

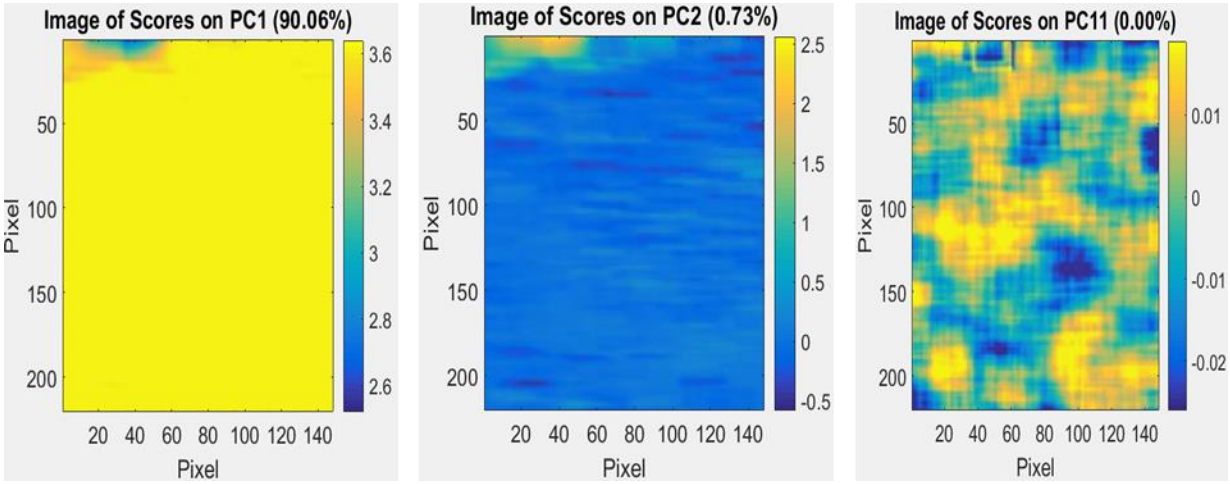

Figure 32 Score images in the region containing the number 5 after replacing the lens, 20 seconds/pulse and 4.0 watt laser heating.

The PC score image value where the score image gives the best picture of the defaced number changes from score image 11 to 9 for the defaced 2 and from 13 to 11 for the defaced number 5.

One additional way to address the efficacy of this method for recovering the defaced serial numbers is to apply LIT to look for other numbers on the graded sample. Using the same LIT experiment, the portions of the image containing the regions with the numbers 0 and 3 were

analyzed using the same conditions as those used above. Figure 33contains the score images from these analyses.

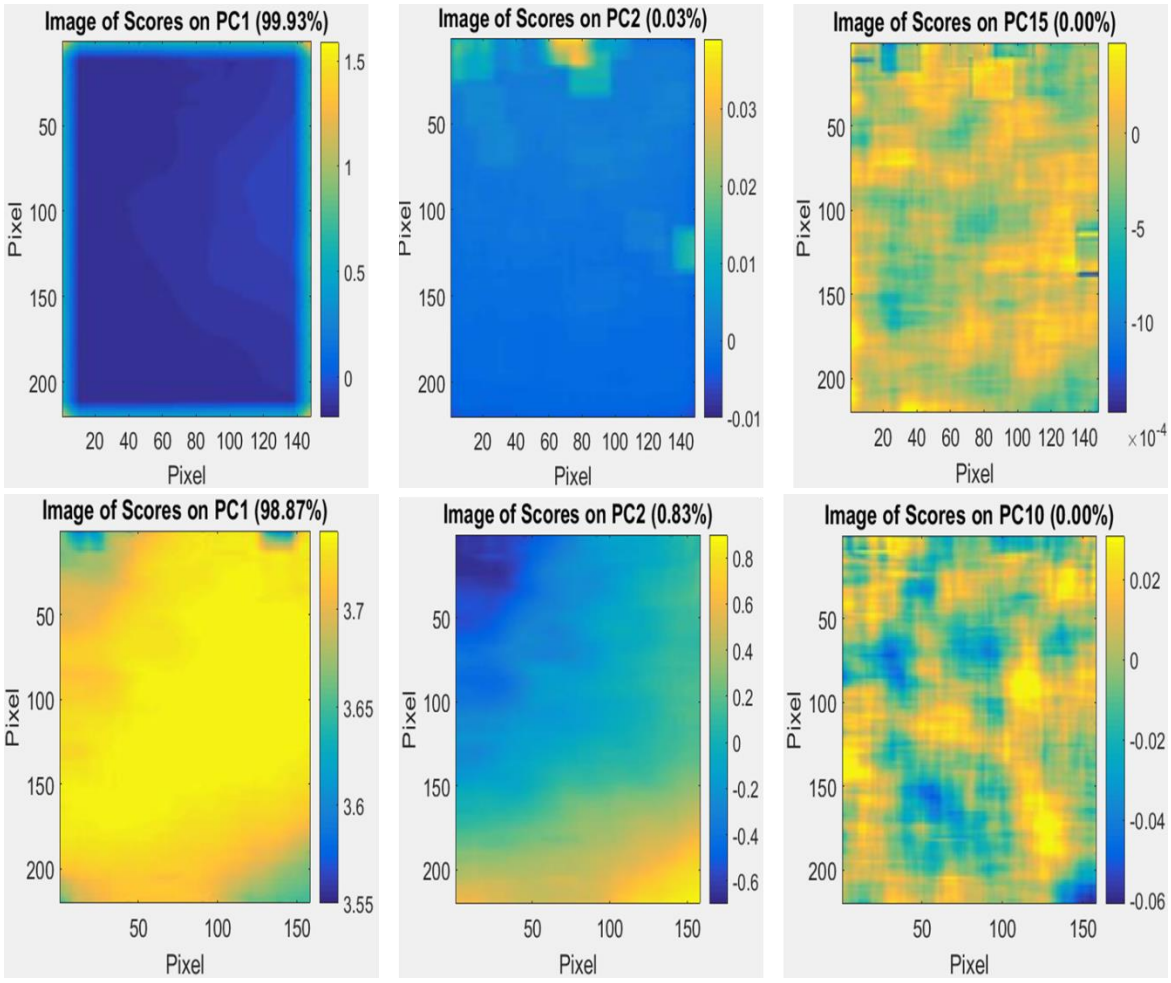

Figure 33 Score images from the region containing the number 0 (upper set) and the number 3 (lower set)

The area where these numbers originated had more metal removed, and these score images are much more difficult to interpret as containing an image of the defaced number. That being said, if the conditions can be optimized this might lead to improved results.

A top hat beam-shaping optic from Eksma Optics was incorporated into the laser path to change the Gaussian beam intensity profile into a top hat profile. A comparison of the LIT experiments on the graded sample without the top hat optic and with the top hat optic was performed. Score images from some of these experiments are presented in Figure 34.

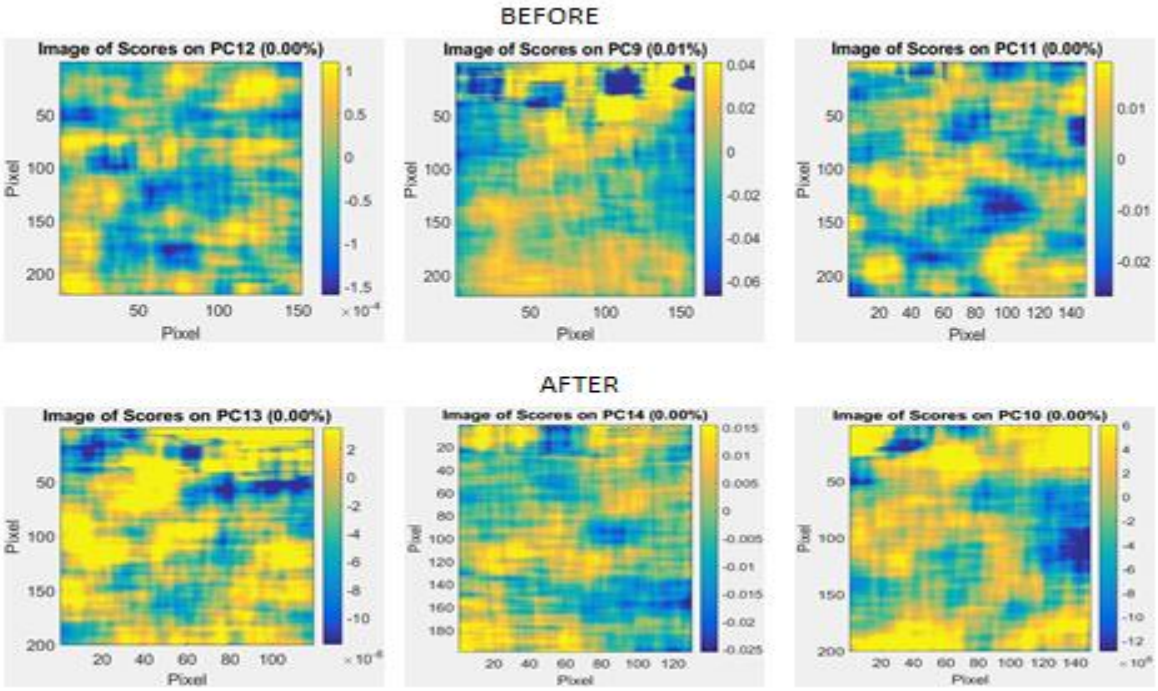

Figure 34 LIT Analysis of Regions with defaced 6, 2, and 5 before and after insertion of the Top Hat optic into the laser beam path.

It appears that in the case of the region with the numbers 6 and 5, there may be some improvement in the number recovery, but the recovery of the number 2 does not seem to be significantly improved.

A few nagging question regarding the use of the coupling of LIT experiments and PCA analysis persist. One is what do the score images for an area without serial number stamped into it look like? A second set of questions is why does the image show up best at some high numbered PC score plot, and if that is so, do images that could be identified as a different number show up at other numbered PC score plots? Also, do the other score images contain information that might help identify the identity of the defaced serial number?

Experiments were performed to try to answer these questions. All but the last question will be addressed in the information presented here. The last question regarding whether or not the other score images can help identify the number, will be addressed in a later section of the report. In Figure 35 below, a region of the graded defaced sample that had no number stamped into it was analyzed with the LIT method and then PCA analysis of the phase image was performed. The score images of PC1 vs the higher numbered PC score vectors are shown in Figure 35.

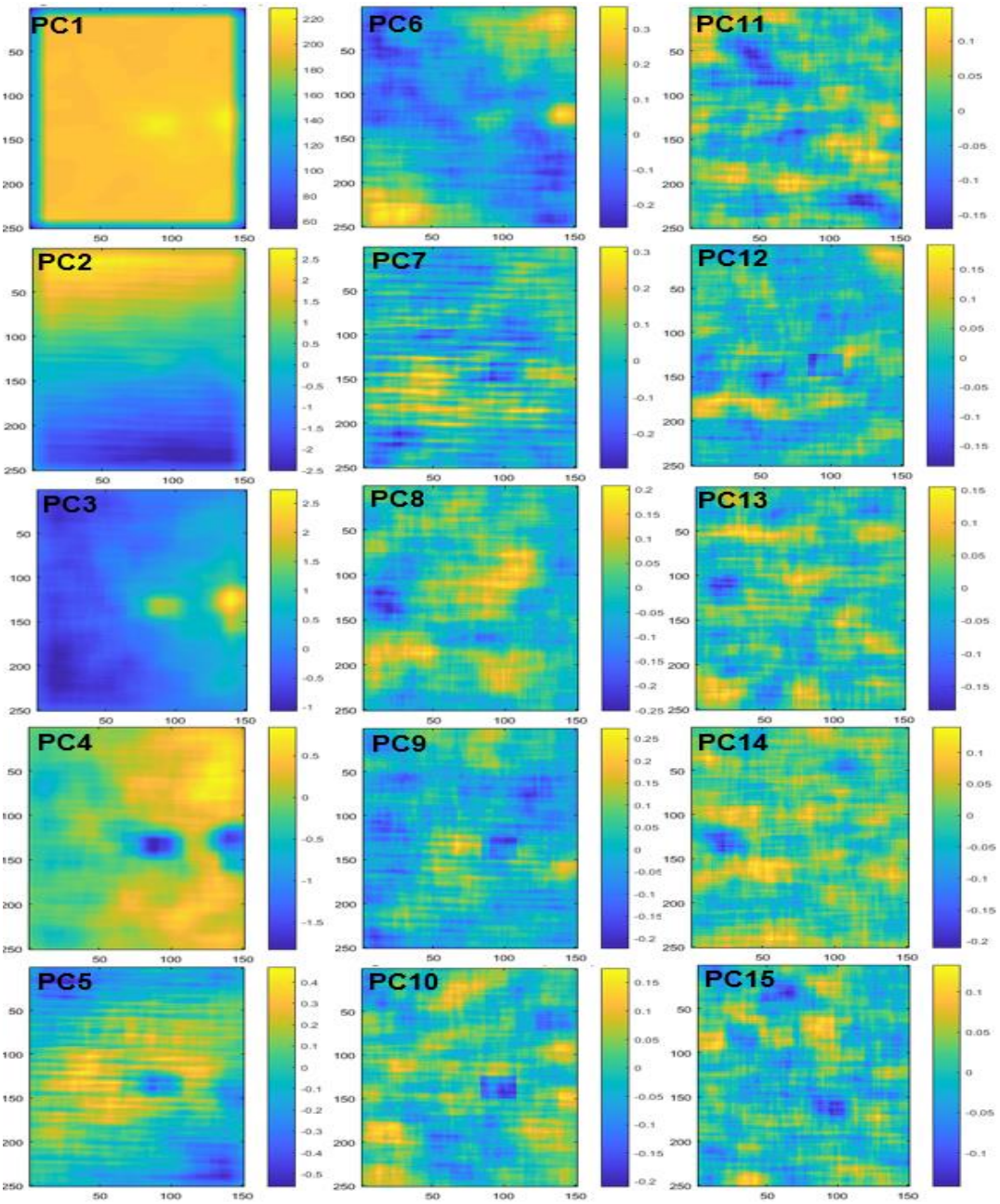

Figure 35 Score images 1-15 for the graded sample in the area without a serial number. X and Y Axes unit is relative pixel number.

One might be able to argue that the score plot PC9 might be a zero, but it appears that the area without a serial number is has primarily random score plots. What do the PC1 through PC15 score plots look like when there is a serial number present in the original sample that has been defaced? This is shown in Fig. 36. Figure 36 gives score images from the phase images of the region where the second number 2 was defaced.

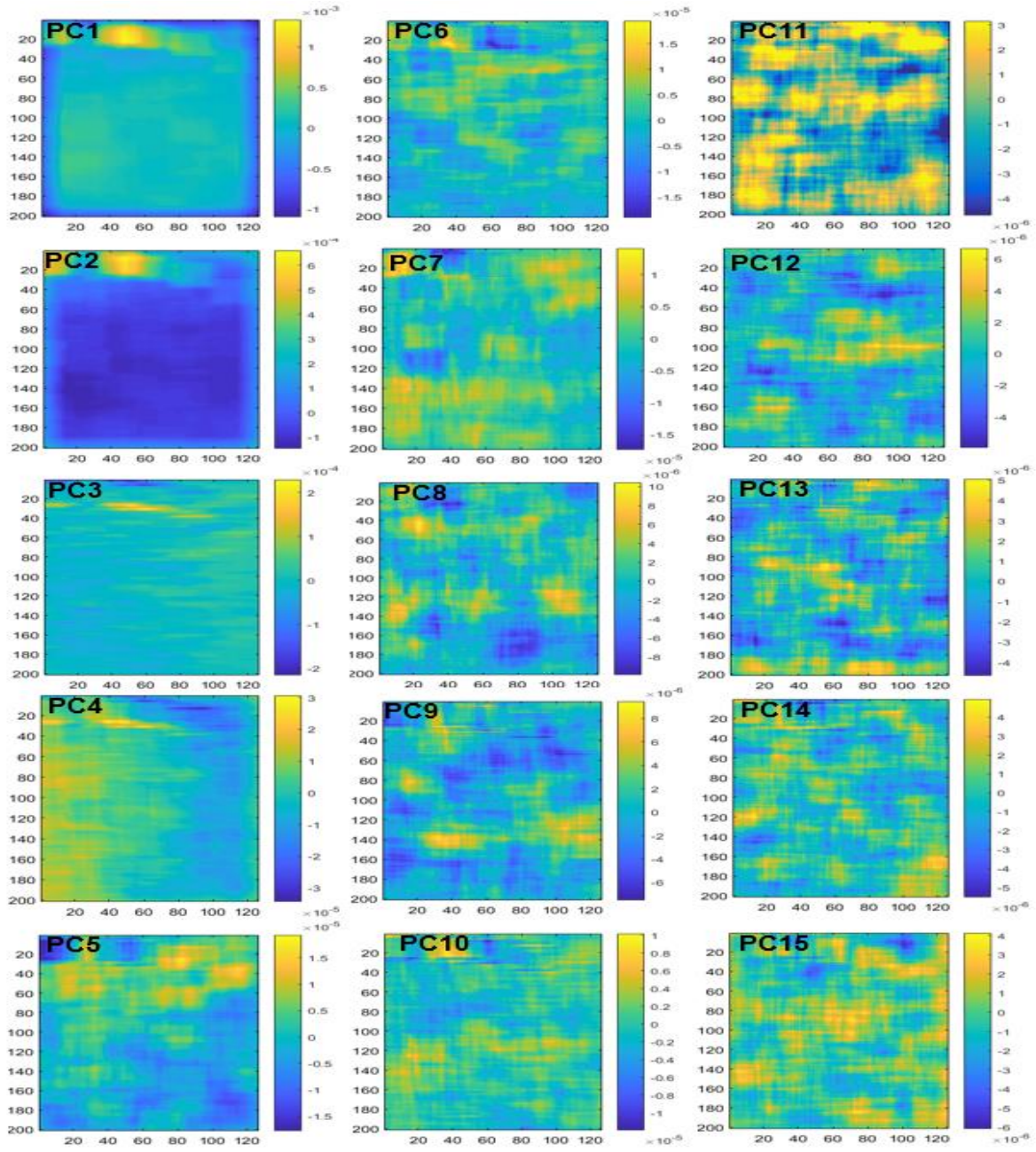

Figure 36 Score plots 1-15 for the graded sample in the area where the second number 2 has been defaced. X and Y Axes unit is relative pixel number

In Figure 36, it is apparent that score plot PC 11 stands out from the rest of the score plots. One could argue that the PC 10 and PC 12 score plots do appear to contain part of the image associated with the number two, and inclusion of these score plots in the Similarity Measurement Analysis may provide for a positive identification of this image.

Image Filtering Studies

Post processing image filtering techniques were attempted. These included binary filtering and segmentation processing. In binary filtering a threshold level is set where pixels

containing an image value higher than the set level are colored white and pixels containing an image value lower are colored black. The binary filters were applied after the LIT data had been previously subjected to MFA filtering and PCA analysis. This type of filtering often helps with visualization. If one has an idea of what the defaced serial number might be and where it was located, then segmentation processing may provide help in pulling the number out of the background.

As an example, binary filtering was applied to first row of score images given in Figure 37. Results are shown in row 2. The threshold level was adjusted visually to provide the most effective contrast between the number images and the background.

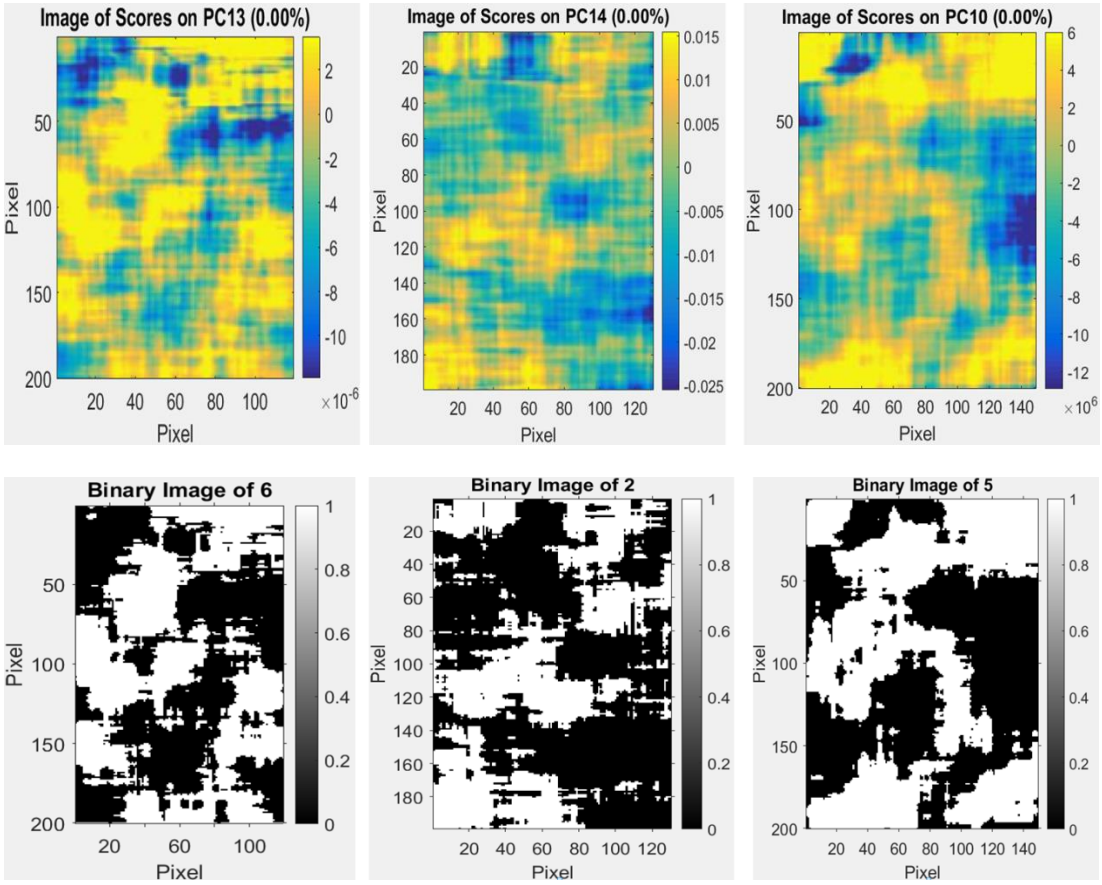

Figure 37 Lower set of images are the binary filtered images corresponding to the upper set of score images.

The binary filtering does not appreciably improve the visualization of the score images of the defaced numbers. Morphological filtering was also attempted. Here instead of just black and white colors, three colors are used with two threshold values. The results with morphological filtering were similar to the binary data results and did not improve the serial number images significantly. If the contrast between the noise and image was slightly better, then these filtering techniques might prove to be more useful.

As mentioned, segmentation processing requires some knowledge of both the position of the serial number and the possible values of the number. Basically, pixels in the region of an

image, where a serial number is believed to be, are selected in a score image that best represents a reproduction of the number. All other pixels are then excluded and PC analysis carried out with only the selected pixels. Score images are then reconstructed using both the included as well as the excluded pixels. A score plot, which shows the overlap of the intensity values of pixels from different score images, can also be used to select regions of greatest density (regions where more pixels overlap) as areas of interest to be further investigated. In principle, this should leave out any noise that does not fall within the overlap and yield a better image of the number. The score image corresponding to the best thermal image for the defaced 2 from PC 11 is displayed in the leftmost image in Figure 38. Pixels in the region identified to be part of the defaced number 2 were selected in the score image (PC11) as shown in the middle image of Figure 12, and a score plot showing the overlap of score image pixel intensity values from PC 1 with those from PC11 is given in the right figure. The pink dots correspond to the selected pixels and the blue dots correspond to the background pixels not selected in the score image. Note that there is a significant region of overlap but also regions where the overlap is minimal.

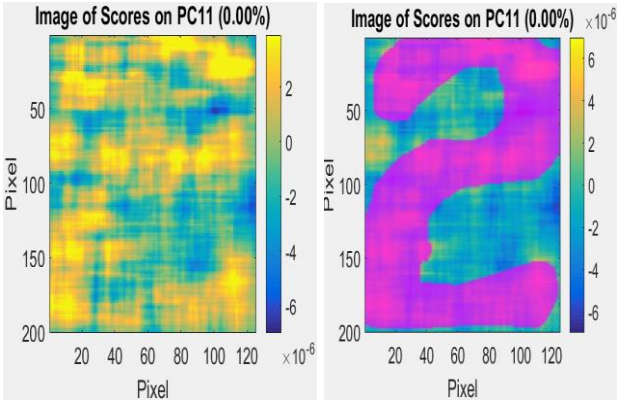

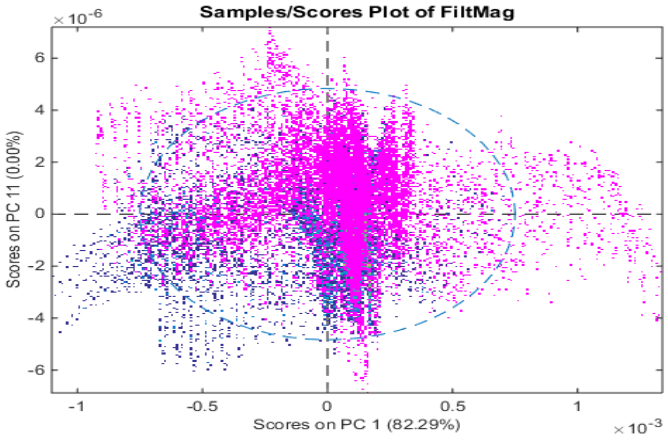

Figure 38 Segmentation processing images corresponding to the defaced number 2.

In principle, PC analysis of only the selected region in the score image leaving out the background pixels should provide a better score image of the number 2. Initial attempts at the reconstruction do not provide a score image with significant improvement, but this type of processing may warrant further investigation. If segmentation processing worked well, and the

region where the number should appear is known, then one could try selecting pixels on the images for all the numbers, and then applying the segmentation process, pick the score images that provide the best match.

Much of the research involved construction and testing of the Lock-in Thermography technique coupled with processing of data with several image analysis techniques. Detailed systematic investigations were started with the goal of finding sets of parameters that would provide good recovery of the serial numbers. There are a number of variables involved in the LIT experiments. The parameters that can be varied systematically include the power of the heating source, the frequency and duty cycle of the heating pulses, the number of images collected during a particular heating cycle, the depth of the defacing, the polishing characteristics use on the defaced area, the coating used to lower the emissivity and promote heating of the defaced area, and the starting temperature of the defaced sample before the pulsed heating begins. These systematic investigations were performed where only the depth of the number was held constant. We decided to use the same test sample, the second number 2 on the graded sample for these systematic studies. The second number 2 was machined down to a depth of about 1 mm below the depth where the number was barely still visible. The other parameters were varied as follows. Three sample coatings were used, high temperature black paint, India Ink, and red dye. The black BBQ paint and India Ink were not diluted. The concentration of the red ink, Rhodamine 110, was 1.85g/L. The solvent used was ethanol. The starting temperatures used were 5, 60, 75, 85, and 95 ^{o}C. The heating source used was the Ar-ion laser operating in all lines mode under constant power control. The laser power, as measured after the top hat optic, were 1.6, 1.8, 2.2, and 2.4 Watts power. The periods/frequencies of the pulses attempted were 1 second/1Hz, 8 seconds/ 0.125 Hz, 20 seconds/ 0.05 Hz, and 32 seconds/ 0.03125 Hz. The number of images collected during each period was also held constant at 32. Collecting 32 images over the period seemed to provide the best tradeoff between reduction of noise and processing time. Table 3 is labeled with the parameters that were varied. The representative values presented in the table are the maximum temperature fluctuations due to the laser heating pulse. One expects that a larger temperature fluctuation should result from a longer pulse time and this is evident in the data presented in the table.

Table 3. Data table for systematic investigation of the effect of each parameter on the quality of the serial number recovery. The values given in the table above are the maximum temperature fluctuations.

Paint type	BBQ					India Ink				
Base Temp.	peltier	60°C	75°C	85°C	95°C	peltier	60°C	75°C	85°C	95°C
Laser Power - after top hat										
1.6 watts - 01 sec				0.25						
1.6 watts - 08 sec				0.274						
1.6 watts - 20 sec				0.43						
1.6 watts - 32 sec				0.73						
1.8 watts - 01 sec				0.196						
1.8 watts - 08 sec				0.312						
1.8 watts - 20 sec				0.536						
1.8 watts - 32 sec				0.961						
2.2 watts - 01 sec				0.197						
2.2 watts - 08 sec				0.645						
2.2 watts - 20 sec				0.541						
2.2 watts - 32 sec				1.097						
2.4 watts - 01 sec				0.349						
2.4 watts - 08 sec				0.747						
2.4 watts - 20 sec				0.892						
2.4 watts - 32 sec				1.16						

Since the overall goal was to find parameters that gave the best serial number recovery, methodologies that could be used to determine the quality of the recovery were needed. The quality is best defined in terms of how well the image of the recovered number matches an image of the original number, or perhaps how well does the image of the defaced number predict the identity of the original serial number. For the latter, similarity merit measurements like cos θ or Euclidian distance could be applied to compare the score images to a library of possible numbers. These types of comparisons are given later in the report. For the former comparison, a methodology was developed that relied on the idea that each number between zero and nine could be divided into three pieces, and these three pieces together represent a unique set that significantly differs from any other set, see Figure 39. If the three areas of the recovered image, match well with the three areas of the standard images derived from undefaced numbers, then the recovery was judged to be excellent. If none of the areas matched, it was judged as poor. The scale is more fully described below.

Figure 39 Numbers 1-9 and 0 separated up into 3 sections.

The following rules were used to rank the LIT recovered images between 1 and 4, with 1 being the best and 4 being the worst:

Rank 1 – has at least 2 sections that can only be the number, number could be in every section

Rank 2 – has at least 1 section that can only be the number, number could be in every section

Rank 3 - possibility of the number in every section

Rank 4 - number is not in every section

Examples of each rank are given here in Figures 40-43.

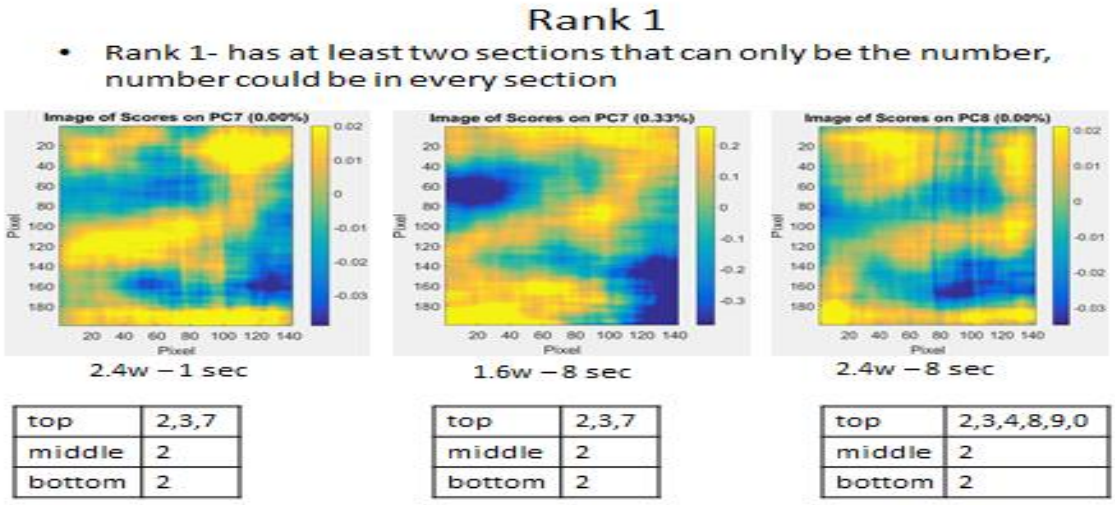

Figure 40 Images of the number 2 assigned best rank.

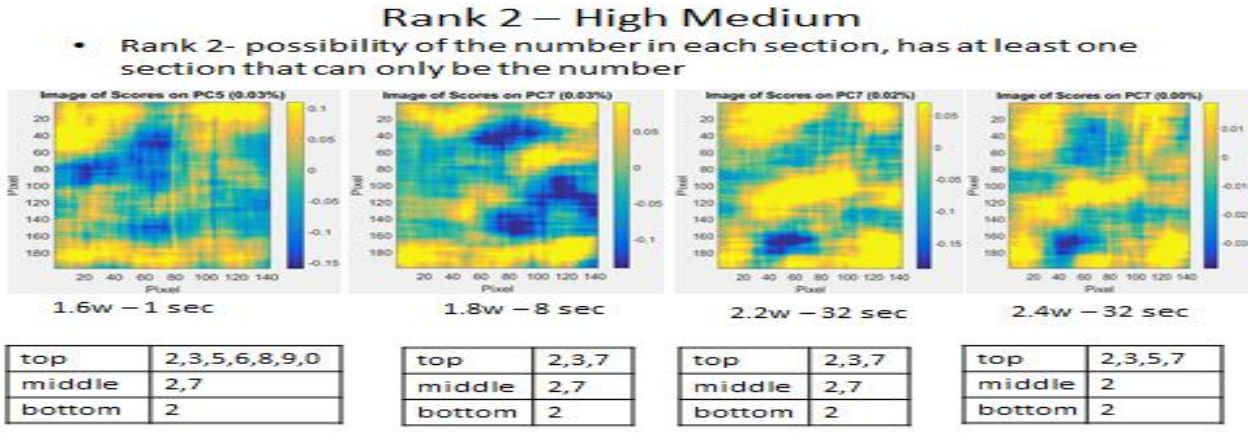

Figure 41 High Medium Rank

This resource was prepared by the author(s) using Federal funds provided by the U.S. Department of Justice. Opinions or points of view expressed are those of the author(s) and do not necessarily reflect the official position or policies of the U.S. Department of Justice

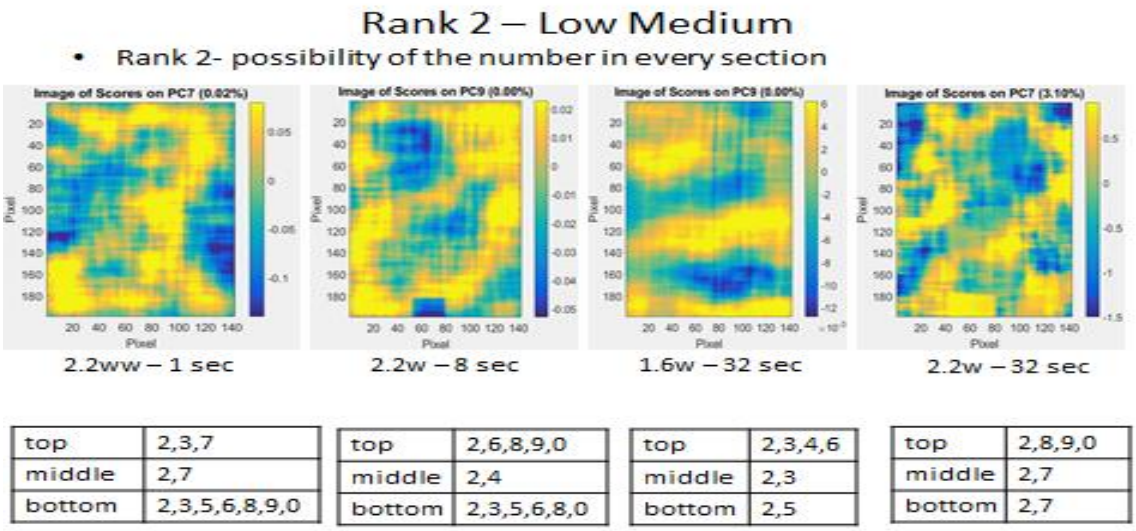

Figure 42 Low Medium Rank

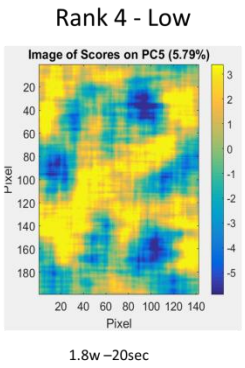

Figure 43 Low Rank

Using this ranking methodology and color coding as follows:

rank of 1 (green)

rank of 2 (yellow)

rank of 3 (orange-pink)

rank of 4 (red)

Best	
Very Good	
Good	
Bad	

With this methodology, a search for the LIT parameters which give the best serial number recovery can be accomplished in a systematic way. The results for parameter variation scheme of Table 3 are presented below in Table 4 for the black BBQ paint experiments.

This resource was prepared by the author(s) using Federal funds provided by the U.S. Department of Justice. Opinions or points of view expressed are those of the author(s) and do not necessarily reflect the official position or policies of the U.S. Department of Justice

Table 4. Data table for systematic investigation of the effect of each parameter on the quality of the serial number recovery. The values given in the table below are the maximum temperature fluctuations and the colors relate to the rank given to the quality of the recovered serial number.

Paint type	BBQ				
Base Temp.	peltier	60°C	75°C	85°C	95°C
Laser Power - after top hat					
1.6 watts - 01 sec	0.0751	0.1051	0.1137	0.25	0.5277
1.6 watts - 08 sec	0.1837	0.2837	0.1471	0.274	0.7203
1.6 watts - 20 sec	0.3121	0.382	0.4414	0.43	0.9441
1.6 watts - 32 sec	0.397	0.5094	0.5109	0.73	1.2038
1.8 watts - 01 sec	0.0842	0.1021	0.0195	0.196	0.5421
1.8 watts - 08 sec	0.5831	0.312	0.2836	0.312	0.8153
1.8 watts - 20 sec	0.3364	0.4736	0.5332	0.536	0.9783
1.8 watts - 32 sec	0.4408	0.611	0.6406	0.961	1.264
2.2 watts - 01 sec	0.3702	0.2213	0.4214	0.197	0.5679
2.2 watts - 08 sec	0.7568	0.6942	0.7724	0.645	0.3598
2.2 watts - 20 sec	0.5633	0.735	1.0277	0.541	0.7937
2.2 watts - 32 sec	1.2397	1.064	1.1946	1.097	1.2835
2.4 watts - 01 sec	0.4121	0.1642	0.453	0.349	0.361
2.4 watts - 08 sec	0.6122	0.7147	0.7562	0.747	0.4251
2.4 watts - 20 sec	1.1941	0.916	1.1346	0.892	0.5874
2.4 watts - 32 sec	1.3818	1.1176	1.2243	1.16	0.6327

A close look at the trends in the table reveal the following:

1. It appears that laser powers between 1.8 and 2.4 watts give the best recovery.
2. 75ºC appears to be the optimal temperature for performing the recovery. Both 60 and 85ºC initial temperatures appear to be good choices as well.
3. There was no overwhelming effect on pulse-length at least for the pulse-lengths tested although a more defaced sample may require different pulse lengths than one that is less defaced.

Systematic variation of these same parameters with the India ink gave very similar results, but the laser dye coating proved difficult to apply at a high enough dye concentration and the fluorescence of the dye provided an alternative mechanism for the energy to be released rather than just heating the sample. Note that this technique still requires a human component, a judgement based on whether the image contains the essential parts of the number or not.

The similarity merit measures are a more automatic way to determine the quality of the serial number recovery that is they require minimal inclusion of human judgement. Use of the

similarity merits, requires comparison to a library containing images of all the digits. This library must be available for comparison in the same format as the score images determined from the experiment. Creating the library or libraries of numbers does likely require a bit of judgement as to which number images should be included in the library. Two libraries of images of all of the digits 0-9 were created. One library was created by taking a thermal image for each digit from serial number that had not been defaced. This thermal image was then modified by filling in areas on each of the numbers that were blurred or missing a small part of the digit. This was accomplished by hand, and these thermal images were the basis of the first library, Library 1. To construct the 2nd library, each of the digits in the first library were broadened to approximate the broadening in the number expected in the plastic deformation zone. Library 1 and Library 2 are presented in Figure 44 and Figure 45.

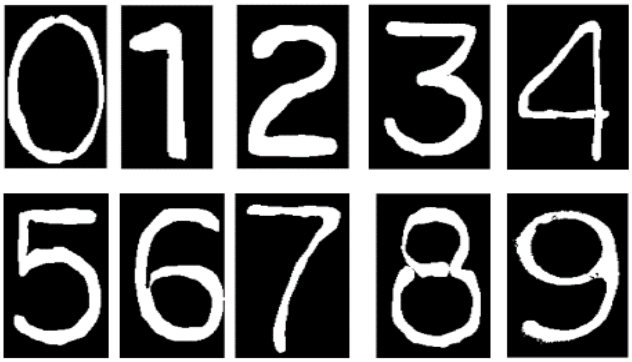

Figure 44 Library 1 of number digits 0-9.

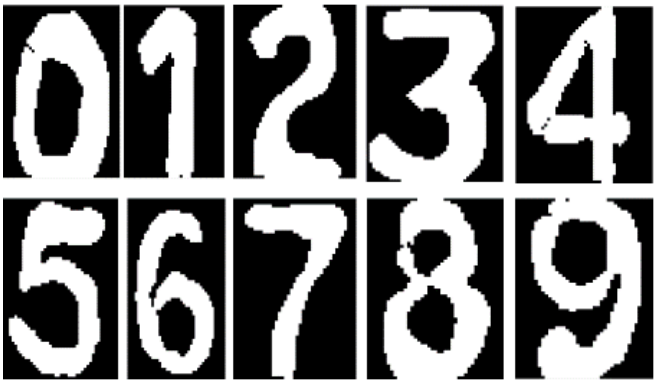

Figure 45 Library 2 of number digits 0-9. This is a modification of Library 1 to account for the expected broadening in the numbers in the plastic deformation region.

If one tries to use just the PC vectors from the PCA analysis, some problems are encountered in computing the similarity merits due to differences in size between the defaced number PC vectors and the PC vectors of the library numbers. However if PCA is applied to the phase images from the LIT experiment, and then Zernike moment (ZM) vectors are calculated for each PC score image and truncated at a predetermined number of basis polynomials, then the ZM vectors all have the same size and can be used to calculate the similarity measures. The number of polynomials to keep must be predetermined. For our experiments a plot of the change

in the calculated moment as a function of the number of polynomials included in the ZM calculations is shown in Figure 46.

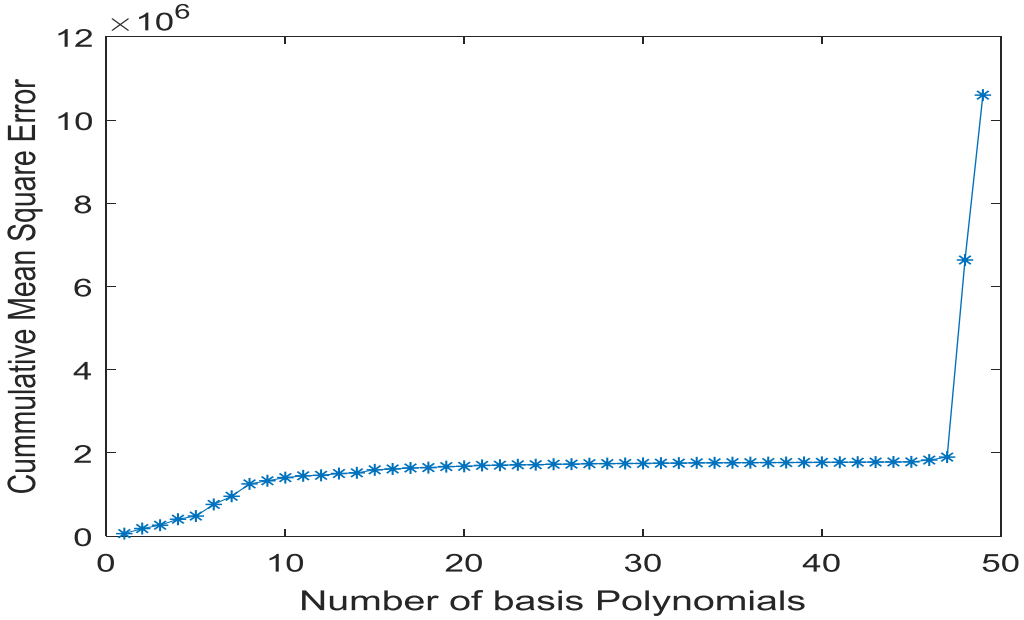

Figure 46 Cumulative sum of change in Zernike moment as a function of n, the number of Zernike polynomials included.

In the figure it is apparent that for values of n from about 0-25 the change in the mean square error (MSE) is rather large, but from 25-45 the change is much smaller and then gets large again around n=47. This can be interpreted as the polynomials out to about n=45 are associated with the image of the number, but beyond n = 45 or so, these polynomials are associated with the noise. This can be seen in the Figure 47. The first images is the original score image, and the next three images are images reconstructed images from truncating the Zernike polynomials after up to n= 20, 45, and 50 respectively. Note that with n =20, the reconstruction image contains more blur and distortion than the original score image. This indicates there was some information missing when only 20 of the Zernike polynomials were used. When n = 45, the reconstructed image is a much better match to the original score image as presumably the higher order polynomials contained information that was needed to reduce the blur and distortion. However, when the number of polynomials included is above the second sharp rise at n=48 in the cumulative sum plot, then the resulting reconstructed image becomes more severely distorted than even the reconstructed image when n=20. The Zernike polynomials with n>47 then must be largely associated with noise and leaving them out results in a much better image. Choosing a particular value for the number of polynomials to use as the basis for the Zernicke moment analysis (ZMA) allows for ease of construction of the various similarity merits. Construction of these same merits without the intermediate step of the ZMA is somewhat unmanageable due to the varying size of the score vectors that result from PCA. With ZMA truncated always at n=45, the size of the vectors is always the same allowing their similarity merits to be much more easily calculated. The overall method, using both PCA & ZMA, is the similarity merit method (SMM).

This resource was prepared by the author(s) using Federal funds provided by the U.S. Department of Justice. Opinions or points of view expressed are those of the author(s) and do not necessarily reflect the official position or policies of the U.S. Department of Justice

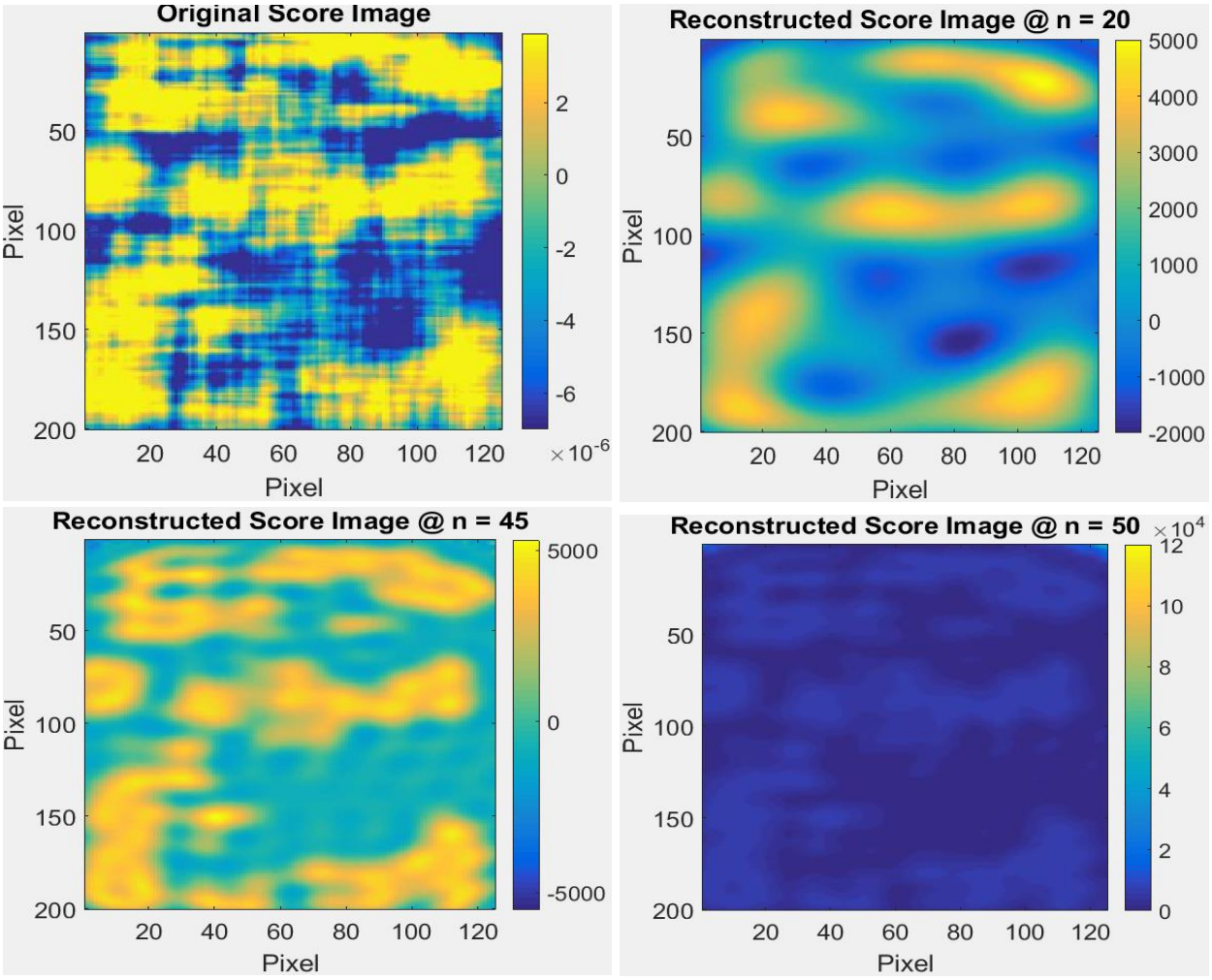

Figure 47 An original score image of a defaced number 2 along with images reconstructed from the Zernike Moment Analysis when truncating after n = 20, 45, and 50 vectors.

So the procedure that was followed to generate the similarity merits for an image, either a phase image or a magnitude image, in comparison with a set of library numbers is given here. This will be called the similarity merit method (SMM). As discussed, use of both PCA and ZMA treatments in a stepwise fashion as this allows the similarity merits to be more easily constructed.

1. Perform the LIT experiment and compute the magnitude and phase images for the area thought to contain a defaced serial number. (The phase image was generally used for the subsequent steps).
2. Perform PCA on the phase image and calculate the score images from folded score vectors.
3. Compute the Zernike Moment vectors for each of the score images determined from PCA, PC1-PC16.
4. Use the Zernike vectors to calculate the similarity merit values for each PC score image, PC1-PC16 as compared with each digit in the library. Based on the merit values for each PC image calculate a rank for each digit based on how similar it is to a number in the image library, or normalize the merit value.

5. If multiple similarity merit measurements are used, average or sum the values of the similarity measures to determine the identity of the defaced serial number.

This procedure is much less susceptible to user bias than the comparison method previously described. The former comparison method required the user to assign a rank based on whether none or some of the parts of the number were present.

The SMM was first tested with a well-defined sample set consisting of the bold Arial font from MS Word. The numbers were typed out and then each number was enlarged and converted to a .bmp format. These images were imported into Matlab and converted to Matlab images. The Matlab images of the Arial fonts were essentially the starting point or the "well-defined phase images" in ZMM procedure given above. These images are given in Figure 48.

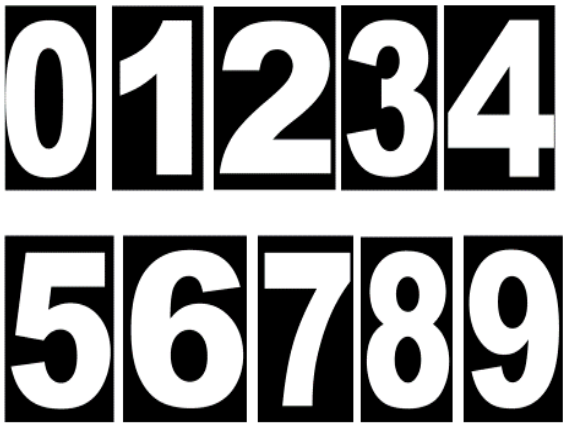

Figure 48 Set of well-defined computer generated number images used to test the ZMM method.

The results of comparing the computer generated test sample with the Library 2 defined in Figure 45 are presented here in Table 5. Four figures of merit were used for this comparison including Euclidean distance, correlation coefficient, Cos θ and Determinant.

Table 5. Average of normalized ranks of merit values comparing each number in the computer generated dataset to those in Library 2.

			Computer Generated to Manual Dataset 2							
	0	1	2	3	4	5	6	7	8	9
0	1	0.35	0.4375	0.375	0.7375	0.4875	0.525	0.35	0.5375	0.5
1	0.275	0.75	0.275	0.3375	0.725	0.35	0.25	0.625	0.475	0.375
2	0.3	0.6875	0.725	0.7	0.4625	0.8375	0.4375	0.7375	0.4375	0.4375
3	0.4625	0.625	0.8625	0.8625	0.225	0.65	0.6125	0.7	0.65	0.7
4	0.5375	0.4375	0.1875	0.2625	0.85	0.1875	0.175	0.3	0.1875	0.25
5	0.7125	0.575	0.6375	0.6	0.4375	0.7875	0.7625	0.5625	0.6875	0.7375
6	0.55	0.5375	0.4875	0.4375	0.6625	0.5125	0.8375	0.3875	0.5375	0.575
7	0.1	0.75	0.525	0.625	0.325	0.325	0.25	0.775	0.2875	0.1625
8	0.8625	0.4625	0.7875	0.75	0.6125	0.75	0.95	0.5875	0.9125	0.95
9	0.7	0.325	0.575	0.55	0.4625	0.6125	0.7	0.475	0.7875	0.8125

Note that the highest value of the similarity merit are along the diagonal in all cases except for the 2 and the 5. In the case of the 2, the highest value was a match with the Library number 3, and in the case of the 5 the best match was with the Library number 2. Visually comparing the computer generated 3 with the library 3, there is a significant difference in the top section. The computer generated 3 is flat whereas the other is rounded. The computer generated 2 and the Library 2 are similar, but the features on the computer generated 2 are much sharper the lines are much thicker. Inclusion of more similarity merit methodologies may also improve these matching. The combination of lock-in thermography with SMM is called the LIT-MIA method.

A test of the utility of the lock-in thermography-multivariate analysis, LIT-MIA method for defaced serial number recovery was to use it with the data collected from the defaced numbers on the graded test sample for the systematic variance of several experimental parameters. The SMM method was applied to the phase images collected for the different conditions for the second number 2 on the graded sample. Here only the PC of the best correlated image was used to calculate the similarity merit. The other PCs were not included. The results are given in Table 6. The similarity merit figures reported in the table were calculated by assigning a rank within each similarity merit between 1 and 10, where ten is assigned to the library number that has the highest value for each of the ten similarity merits. The one with the next highest was assigned a nine and so on. These were then summed and averaged, (normalized) across all ten merits used, to produce the values in the table. Thus if the true identity of the number was identified by all methods, the value in the table would be a 1. The ten similarity measures used to compare each number in the library to the score image of the recovered number were Euclidean distance, correlation coefficient, Cos θ, Determinant, unconstrained Procrustes analysis, constrained Procrustes analysis, Mahalanobis distance, pooled Mahalanobis distance, and Bartlett stats.

Table 6. Values of the Similarity Merits based on an average of the assigned rank.
A value of 1 corresponds to a high rank for all similarity merits used for comparison. Here the similarity merits were determined only from the value corresponding to the PC# which had the highest correlation.

		Cycle Time (Secs)			
	1.6W	1	8	20	32
Base Temp.	60	0.9571	0.9857	0.9857	0.925
	75	0.9714	0.9286	0.9429	0.7857
	85	0.95	0.9	0.95	0.925
	95	0.875	0.975	0.875	0.9

		Cycle Time (secs)			
	1.8W	1	8	20	32
Base Temp.	60	0.9571	0.9857	0.8571	0.9714
	75	0.875	0.95	0.925	0.7
	85	0.975	0.9	0.975	0.925
	95	0.95	0.95	0.95	0.95

		Cycle Time (Secs)			
	2.2W	1	8	20	32
Base Temp.	60				
	75	0.9	0.875	0.925	0.75
	85	0.85	0.875	0.925	0.975
	95	0.95	0.925	0.925	0.975

		Cycle Time (Secs)			
	2.4W	1	8	20	32
Base Temp.	60				
	75	0.95	0.9	0.95	0.975
	85	0.9429	0.9857	0.9	0.9857
	95	0.975	0.95	0.975	0.925

Note that many values in the table are greater than 0.95 indicating that the phase image of the defaced 2 matched well with the library value of the number 2. However, the SMM value used only the score image of the PC with the best correlation, and required a judgement call regarding which score image was the best.

Other questions to answer about the graded sample analysis are: is the best match for the second defaced number 2, the number 2 from the library, and **can we use all of the score image vectors** PC1-PC16 in the SMM calculation to determine the best library match for the defaced number? If this is possible then the task of recovering the defaced number becomes essentially autonomous. This calculation was performed for the LIT phase image taken at 85^{o}C and for a 1 second pulse rate for the second number 2 in the graded test sample. The information is given in Table 7. Note that the similarity merit values comparing the score image to the library number 2 are highest for ten of the score images, and only the images corresponding to PC1, PC2, PC7, PC8, PC13, and PC16 did not find the library 2 to give the highest merit value.

Table 7. Table of the similarity merit values for defaced number 2 as a function of for all score images compared with number value (0-9)

SCORE IMAGES (85 deg, 1 Second)

1	2	3	4	5	6	7	8	9	10	11	12	13	14	15	16
0.72855	0.56425	0.6571	0.59285	0.70715	0.7714	0.61425	0.71425	0.59285	0.4714	0.55	0.40715	0.7	0.5357	0.4429	0.4857
0.62145	0.4714	0.4714	0.47145	0.62145	0.55715	0.72855	0.7214	0.67855	0.25715	0.52855	0.74285	0.4071	0.42145	0.7357	0.4857
0.4286	0.6143	0.78575	0.75715	0.83575	0.86425	0.67145	0.62855	0.7	0.9	0.8714	0.94285	0.5357	0.8357	0.77145	0.57855
0.5286	0.7143	0.5286	0.54285	0.5357	0.4857	0.5714	0.5643	0.62855	0.6143	0.55	0.62145	0.7214	0.49285	0.46425	0.62855
0.8	0.61425	0.57145	0.60715	0.57145	0.46425	0.6357	0.4357	0.35715	0.5857	0.3143	0.3857	0.52855	0.72855	0.51425	0.45715
0.54285	0.53575	0.5357	0.45	0.45	0.57855	0.42145	0.57855	0.3857	0.70715	0.4929	0.60715	0.37855	0.6	0.50715	0.62855
0.40715	0.4	0.45715	0.4857	0.50715	0.50715	0.44285	0.60715	0.49285	0.4071	0.7071	0.54285	0.5143	0.32855	0.5786	0.4071
0.5357	0.51425	0.5571	0.4286	0.5143	0.5	0.59285	0.44285	0.6214	0.5857	0.5357	0.55	0.6357	0.60715	0.56425	0.7071
0.5286	0.5929	0.57145	0.72855	0.5	0.47855	0.4643	0.48575	0.66425	0.63575	0.6214	0.4	0.6857	0.4857	0.5786	0.61425
0.37855	0.4786	0.3643	0.43575	0.25715	0.29285	0.35715	0.3214	0.3786	0.3357	0.3286	0.3	0.39285	0.46425	0.34285	0.50715

Similar SMM calculations were accomplished for the LIT phase images corresponding to the 6 and the 5 defaced serial numbers as well as the number 2 with additional similarity merits, a total of seven merits. The score images from the LIT analysis and corresponding PCA are shown in Figure 49.

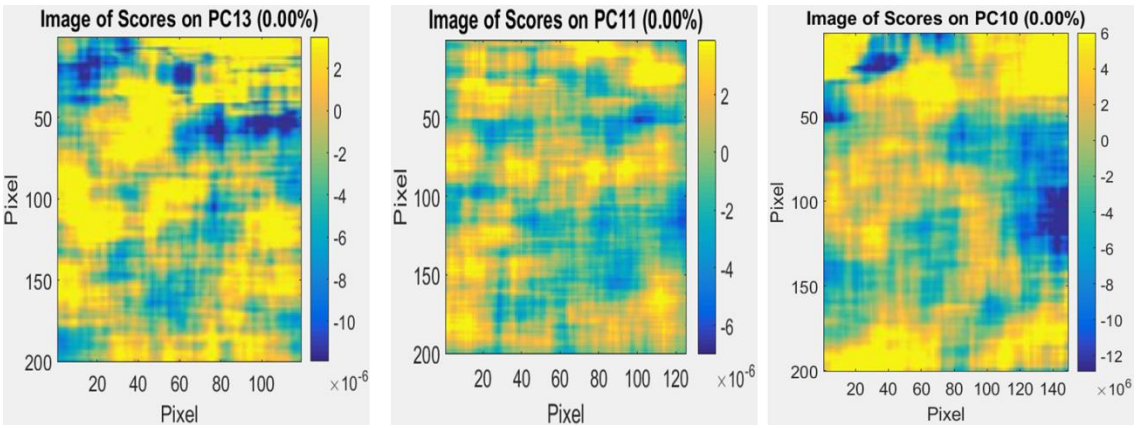

Figure 49 PCA determined score images of defaced 6, 2, and 5 from graded test sample.

The SMM method was applied to the score images with the similarity merits from 10 similarity similarity measures used in comparing digits 0-9 from number Library 2 to the score images corresponding to PC1-PC16. A summation of these merits and their ranks, both normalized, are presented in **Error! Reference source not found.** for the defaced 6,

Table 9 for the defaced 2, and Table 10 for the defaced 5. The sum of the similarity merit values for each number in the library are also included in the tables.

	SUM OF MERITS FOR SCORE IMAGES																
	1	2	3	4	5	6	7	8	9	10	11	12	13	14	15	16	SUM
0	2.42	2.53	2.38	2.39	2.39	2.47	2.62	2.66	2.34	2.45	2.18	2.027	2.07	2.04	1.92	2.39	37.3
1	1.47	1.92	1.52	1.70	2.05	1.41	2.28	1.80	1.51	1.74	1.58	1.28	0.311	1.56	1.44	2.49	26.1
2	2.32	2.98	2.28	2.13	1.91	2.52	2.68	2.53	2.30	2.20	2.26	2.41	1.98	1.99	2.22	2.13	36.9
3	2.06	2.86	2.00	1.79	2.04	2.19	2.34	2.03	2.07	2.03	1.96	2.02	1.44	1.67	2.17	2.04	32.8
4	1.60	2.34	1.76	1.75	2.45	1.65	2.37	1.50	1.71	1.91	1.55	1.44	1.42	1.55	1.58	2.38	29.0
5	2.20	3.94	2.28	2.29	3.26	2.51	2.48	2.24	2.27	2.04	2.11	2.37	1.62	2.02	2.42	2.89	39.0
6	2.87	3.48	3.26	2.85	2.41	3.19	2.47	2.97	3.02	2.67	2.61	2.88	2.60	2.45	2.58	2.16	44.5
7	2.36	2.80	2.36	1.39	2.39	1.61	2.14	2.54	2.34	1.70	2.34	2.26	0.42	2.33	2.30	2.46	33.8
8	1.90	2.97	2.09	1.72	2.04	2.09	2.27	1.81	1.84	1.81	1.86	2.09	0.95	1.62	1.96	2.14	31.1
9	2.25	2.45	2.37	2.30	1.99	2.38	2.44	2.39	2.29	2.20	2.25	2.28	1.97	1.94	2.38	1.90	35.8

Table 8. Sum of Similarity Merits for all 16 score images of a 6 compared with the library of clean digits.

Table 9. Sum of Similarity Merits for all 16 score images of a 2 compared with the library of clean digits.

	SUM OF MERITS FOR SCORE IMAGES																
	1	2	3	4	5	6	7	8	9	10	11	12	13	14	15	16	SUM
0	3.58	2.58	3.54	2.79	2.89	2.78	2.43	2.71	3.49	2.34	2.88	3.02	2.62	2.69	2.39	1.97	44.7
1	1.65	2.70	1.56	1.34	1.50	1.46	1.40	1.40	1.53	1.39	1.52	1.49	1.42	1.38	1.54	2.19	25.5
2	3.82	2.29	3.43	3.41	3.59	3.17	3.11	3.28	4.21	2.82	3.17	3.53	3.12	2.82	2.61	2.04	50.5
3	3.95	2.26	3.30	2.96	3.15	2.73	2.60	2.77	3.81	2.39	2.69	2.90	2.80	2.63	2.32	2.19	45.5
4	2.65	2.49	2.37	2.12	2.11	1.97	1.70	2.00	2.33	1.73	1.79	2.17	1.92	1.76	1.64	1.94	32.7
5	4.89	3.16	3.46	3.02	3.11	2.92	2.70	2.79	3.61	2.53	2.96	3.13	2.87	2.76	2.41	3.17	49.3
6	3.62	2.11	3.40	3.14	3.34	2.94	2.74	3.09	3.87	2.59	2.81	3.25	3.03	2.83	2.55	2.32	47.7
7	2.13	3.46	2.34	1.90	2.04	1.85	1.71	1.86	2.22	1.72	1.89	1.88	1.79	1.79	1.52	2.03	32.1
8	3.58	2.53	3.14	2.85	3.05	2.88	2.51	2.72	3.75	2.38	2.74	2.98	2.74	2.68	2.37	2.30	45.3
9	3.84	2.42	3.32	2.81	2.72	2.61	2.31	2.62	3.46	2.16	2.55	2.96	2.46	2.42	2.24	2.48	43.4

Table 10. Sum of Similarity Merits for all 16 score images of a 5 compared with the library of clean digits.

	SUM OF MERITS FOR SCORE IMAGES																
	1	2	3	4	5	6	7	8	9	10	11	12	13	14	15	16	SUM
0	2.23	2.10	2.51	1.97	2.69	2.77	2.62	2.36	1.93	2.30	2.56	2.46	2.49	2.33	2.54	0	35.8
1	2.27	1.95	1.61	2.17	1.92	1.96	1.99	2.34	1.99	1.50	1.64	2.38	1.72	2.09	1.72	2.05	31.3
2	2.24	2.30	2.26	2.17	2.62	2.60	2.40	2.41	1.96	2.30	2.20	2.22	2.40	2.64	2.82	0	35.5
3	2.26	2.38	2.13	2.03	2.38	2.39	2.15	2.38	2.07	2.14	1.97	2.21	2.19	2.59	2.17	0	33.5
4	2.19	2.71	1.81	2.18	1.86	1.91	1.99	2.38	2.02	1.68	1.75	2.33	1.52	2.16	1.57	2.10	32.1
5	3.26	3.328	2.33	3.00	2.65	2.75	2.46	2.22	3.06	2.23	2.36	3.21	2.22	3.42	2.90	0	41.4
6	2.37	2.47	3.23	2.28	2.92	2.74	3.16	2.35	2.12	2.61	3.18	2.39	3.30	2.37	3.29	0	40.8
7	2.28	2.15	1.25	2.31	1.33	1.38	1.37	2.17	2.20	2.40	1.29	2.34	1.48	1.71	1.58	3.29	30.6
8	2.24	2.28	1.92	2.08	2.05	2.08	1.91	2.34	2.11	2.04	1.79	2.24	1.81	2.42	1.90	0	31.3
9	2.27	2.34	2.68	2.09	3.04	2.72	2.66	2.24	2.96	2.42	2.46	2.23	2.28	2.48	2.79	0	37.7

Thus use of the LIT method to collect the phase images followed by PCA, ZMA, and SMM treatments to determine the similarity merits for all the score images allowed calculation of the sum of the merits. This sum correctly associated the defaced serial number with the library number. In the graded test sample, the 6 was very near the surface and partly showing, the 2 was defaced by machining to a deeper depth and the 5 was machined down even more than the 2. Looking at the difference between the merit sum of the correct value and the merit sum of the closest incorrect value, the difference is 5.5 (44.5-39.0) for the 6, 1.2 for the 2 (50.5-49.3), and 0.6 (41.4.40.8) for the 5 suggesting that when the numbers are defaced to a greater depth, a uniquely correct identification may be difficult.

Since the method appeared to work well with flat test samples, the next step was to use the method on a rounded sample, the gun barrel obtained from the Bannock County Sheriff's Office. The numbering and lettering on the barrel are shown in Figure 50. Unfortunately, the gun provided by the Sheriff had no serial number.

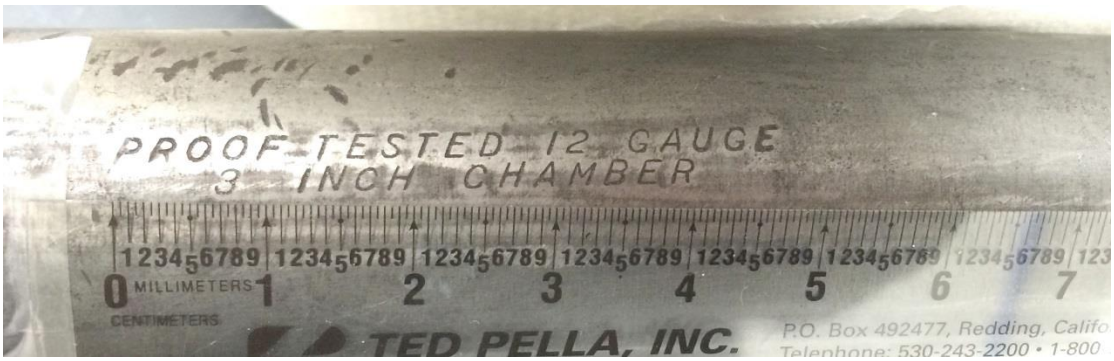

Figure 50 Numbering and lettering on the gun barrel.

The numbers 1 and 2 from the label "12 GAUGE" were defaced with a file and subsequently polished with 200 and 600 grit sand paper as shown in Figure 51. The 1 and the 2 appear completely removed in this picture of the defaced gun barrel.

Figure 51 Picture of the gun barrel after defacing the 1 and 2 from the label "12 gauge".

The defaced area was then painted with the black India ink as outlined previously, and then placed into the thermal imaging experimental apparatus as shown below in Figure 52. Heating tape was wrapped around the parts of the barrel that extended beyond the temperature-controlled hot plate to help maintain a constant initial temperature on the sample and chopped laser light was used for the pulsed heating.

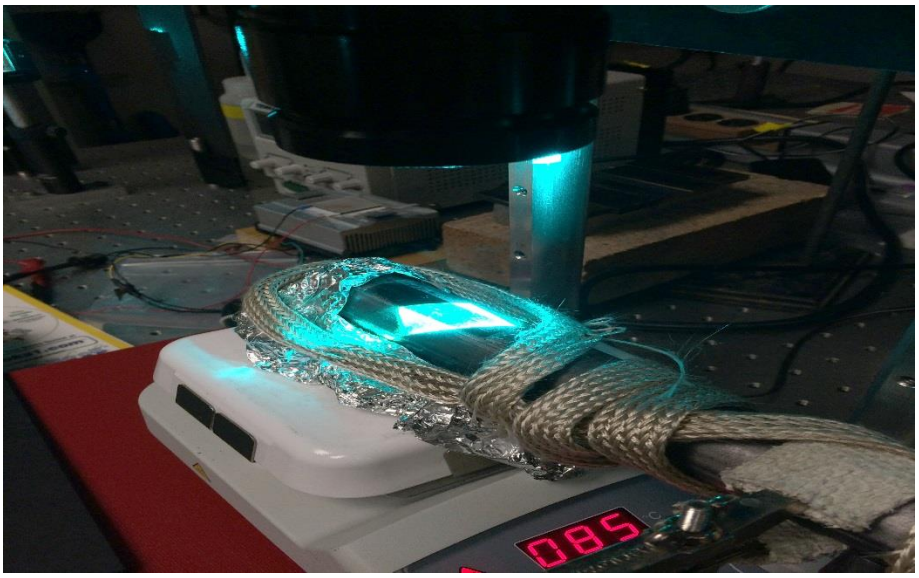

Figure 52 Defaced gun barrel mounted on the constant temperature hot plate in the thermal imaging experiment.

The barrel was subjected to the LIT method and magnitude and phase images were created from the collected image data. These images were subjected to PCA, ZMA, and SMM treatment and the results are given in Figure 53 and Figure 54 as well as Table 11 and Table 12.

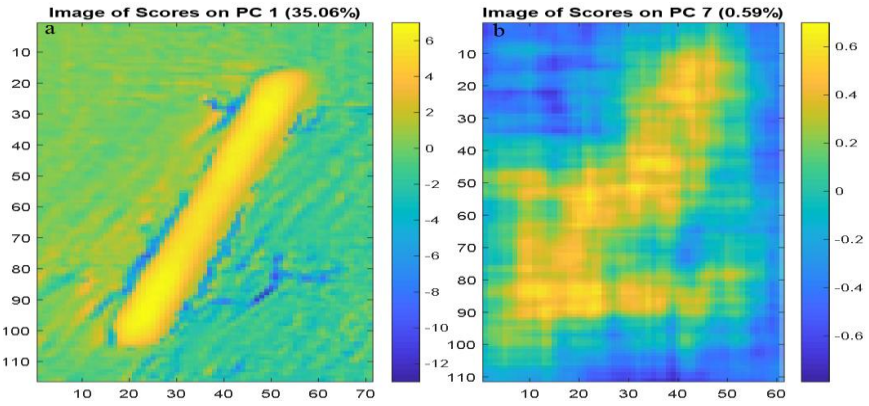

Figure 53 Score Images of a) Clean 1 before defacing and b) Recovered 1 after defacing.

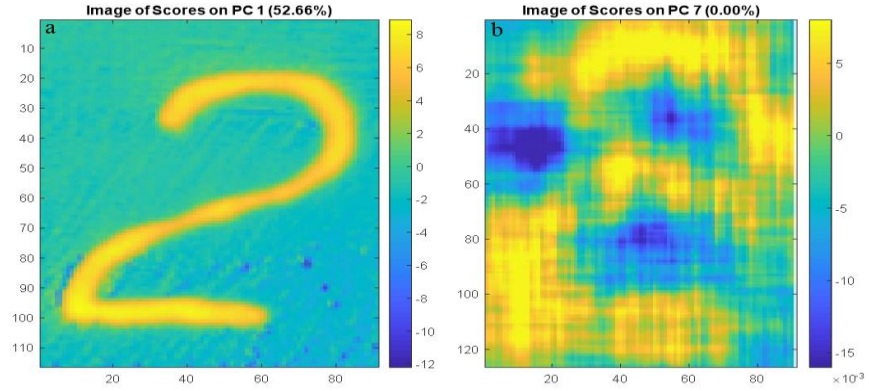

Figure 54 Score Images, both PC 7, of a) Clean 2 before defacing and b) Recovered 2 after defacing.

Table 11. Sum of Similarity Merits for all 16 score images of a 1 compared with the library of clean digits.

	SUM																
	1	2	3	4	5	6	7	8	9	10	11	12	13	14	15	16	SUM
0	7.46	10.1	9.01	9.51	7.75	8.36	9.13	9.21	10.0	7.32	9.68	10.1	8.53	9.40	7.63	9.42	142.7
1	9.82	11.1	14.5	10.0	12.3	10.9	15.2	13.4	11.2	10.9	13.3	10.4	12.4	13.0	12.1	13.1	194.4
2	10.6	10.9	9.5	10.6	12.1	11.1	9.43	10.0	11.6	11.6	10.1	11.3	11.8	9.65	13.5	8.79	173.0
3	11.6	10.5	11.8	10.9	11.3	10.8	11.7	9.68	10.9	11.8	10.2	10.4	9.79	10.8	10.2	10.6	173.4
4	14.1	12.0	12.6	12.4	15.8	13.6	14.0	13.0	10.5	12.7	12.0	11.8	13.9	13.0	14.1	12.6	209.1
5	11.4	10.9	8.59	12.9	10.8	11.2	10.2	9.76	11.4	10.8	9.64	11.0	10.9	9.64	10.7	8.92	169.3
6	10.3	11.7	9.80	12.0	9.81	11.4	10.1	9.59	11.4	12.5	10.8	12.1	10.2	10.5	9.64	9.85	172.3
7	10.4	10.8	11.5	9.02	11.3	11.3	11.0	12.8	9.30	9.67	11.0	9.55	12.7	11.7	9.73	12.6	175.0
8	10.9	10.8	9.69	10.3	10.1	12.8	10.2	9.08	14.1	10.9	10.8	13.5	10.9	10.6	10.3	11.0	176.6
9	10.4	9.75	10.0	11.6	9.93	9.68	9.86	10.3	11.7	10.2	9.91	9.92	8.75	11.3	9.07	9.43	162.1

Table 12. Sum of Similarity Merits for all 16 score images of a 2 compared with the library of clean digits.

	SUM																
	1	2	3	4	5	6	7	8	9	10	11	12	13	14	15	16	SUM
0	11.15	11.09	12.42	10.94	13.16	9.90	9.83	12.22	11.20	12.82	11.26	13.33	11.08	12.22	12.22	10.69	185.54
1	8.85	7.94	8.06	8.08	7.83	7.04	8.87	8.30	8.43	6.68	7.78	8.03	7.53	12.31	7.18	7.78	130.72
2	9.98	11.68	14.62	13.14	13.46	13.26	13.06	13.96	12.81	13.99	12.77	14.15	16.50	10.10	14.38	14.99	212.86
3	11.04	11.58	11.74	10.90	12.89	11.38	11.94	9.86	10.96	11.18	10.62	11.25	11.58	11.32	10.90	11.45	180.57
4	10.38	10.95	9.30	8.12	8.84	9.52	8.41	8.39	9.15	8.67	8.17	9.29	9.86	10.95	8.59	9.68	148.26
5	11.57	10.81	9.60	11.77	13.25	11.66	9.64	10.91	10.55	13.40	10.59	11.22	11.74	11.84	10.36	11.80	180.69
6	9.25	11.00	11.72	11.19	11.13	12.91	11.63	11.53	9.62	12.12	12.30	11.20	12.49	11.63	10.43	10.60	180.74
7	9.79	11.63	9.00	8.64	9.72	9.27	9.04	8.26	10.14	8.59	8.80	8.56	8.31	10.66	9.57	8.90	148.89
8	10.08	10.02	10.45	11.14	10.45	10.84	11.36	10.39	10.63	11.44	10.50	10.90	12.32	11.35	11.98	13.44	177.29
9	9.91	8.35	9.23	9.94	8.68	9.69	8.55	8.78	9.31	10.08	9.40	10.65	11.05	9.24	8.70	9.69	151.27

From the resulting images, both the defaced numbers were reconstructed and could be identified in the score images. Using the similarity measures to independently confirm this, in the case of the defaced number 1, the highest merit sum predicted a 4 rather than a 1. The 1 had the second highest sum. For the defaced number 2 on the gun barrel, the highest merit sum predicted that the defaced number was a 2, with the next highest sum predicting a 0. The miss prediction of the 1 is likely partly due to the number on the barrel being an italic number 1, which is slanted, and

the number 1 in the library is not. It appears that the LIT method coupled with the Multivariate Image Analysis has great potential for correctly recovering defaced serial numbers, where the serial numbers were stamped into the metal. An even more pertinent test was to recover a serial number from a sample that has been defaced by someone with criminal intent.

While the gun barrel studies were being completed, the Power County Sheriff's Office made contact about recovering the VIN number and the motor number from a Yamaha motorcycle. The motorcycle was brought into the lab and LIT-MIA technique was applied to the defaced areas of VIN and motor identification numbers to attempt to recover the defaced serial numbers. The motorcycle and defaced serial numbers are presented in Figure 55 and Figure 56.

Figure 55 Yamaha motorcycle with defaced VIN and motor identification number.

Figure 56 Defaced VIN number and defaced motor ID number from Yamaha motorcycle.

From Figure 56, it is seen that while the VIN numbers on the fork were completely removed, those on the motor were only partially removed with some of the numbers left visible. The camera was resituated at the edge of the table and the beam path of the laser heating source was altered as well to use the process, as developed up to this point, to try to recover the numbers removed. Figure 57 shows the score images of the recovered numbers.

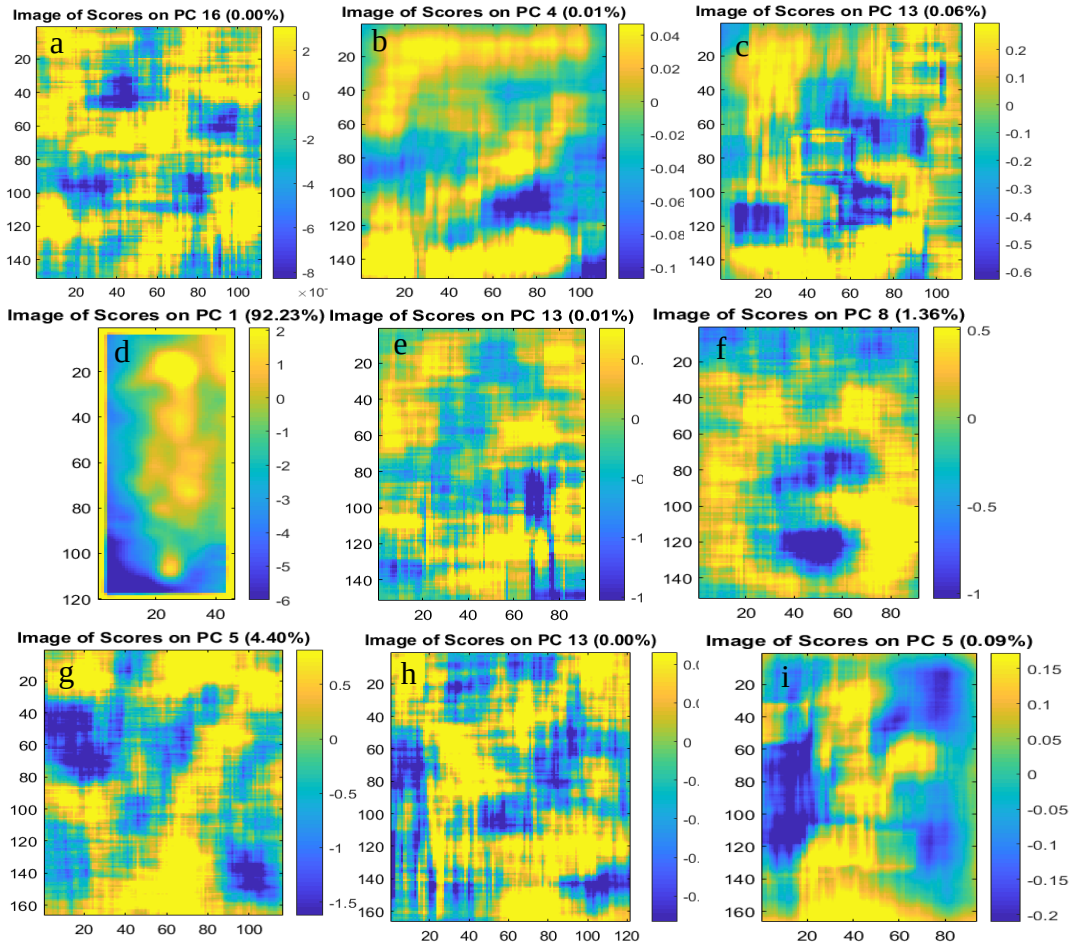

Figure 57 Score Images of Recovered VIN Numbers from Motorcycle a)Five b)Two c) Five d) One e) Zero f) Zero g) Seven h)Four and i) One

From the score images, the removed serial numbers were reconstructed though not easily discerned, highlighting once again the importance of correctly identifying the numbers independent of human bias as can be done using similarity measures. The results of the similarity merit measurements are given below, but first additional data was taken on another type of engraved sample.

If the LIT coupled with Multivariate Analysis technique can be used to recover serial numbers that were stamped into the metal, can the technique be used to recover serial numbers that were laser engraved? A laser engraved Aesculap surgical needle holder (Model BM034R) was obtained. Some of the laser etched characters were removed and the process applied to recover them. Figure 58 shows the unaltered holder and Figure 59 shows the defaced characters painted with India ink.

Figure 58 Laser Engraved Aesculap needle holder.

Figure 59 Defaced and painted needle holder.

Figure 60 shows the results from the LIT and multivariate image analysis of the forceps.

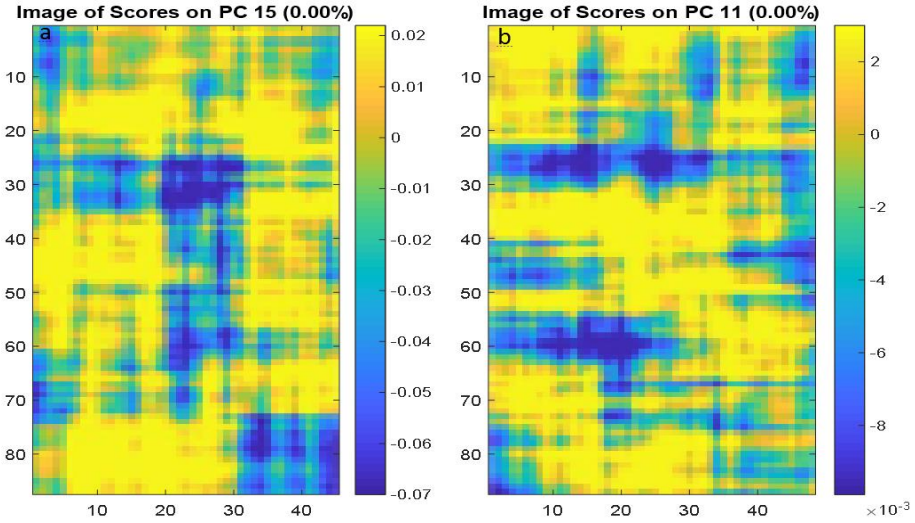

Figure 60 Score images of Laser Engraved Numbers a) Zero and b) Three

Sum of Ranking Differences and Fusion Rules

Rather than simply adding the similarity merits as was done previously, another method of combining them was tested to optimize the use of several similarity measures. This involved obtaining a consensus among them and thus minimizing the possible effects of some incorrectly ranked values. To do this, the similarity merits for each score image were compared to the digital number images across four libraries (the two manually defined libraries and two computer generated number libraries). These merits for all 16 score images were then combined into a larger matrix. A variety of fusion rules including the L2 norm, sum, median and standard deviation were used to analyze both the raw merits as well as their ranks. Also the sum of ranking difference (SRD) was used as a fusion rule. SRD is carried out by first determining the maximum value of a particular similarity measure across all the numbers compared, thus creating a target value for each similarity merit in a target vector. The values in this target vector are then ranked low to high with their original positions (row index) noted. The similarity measures are then reordered with each column (similarity measures for a particular number) also arranged low to high and ranked. The absolute value of the difference between the target vector ranking of each similarity measure and its ranking within the column of each number is then computed and summed for each column (number) to form the column-wise vector of the final SRD ranks for each number. The smallest SRD value denotes the smallest absolute difference in the rank of the target vector and the number in question, and thus indicates that to be the best fit for the defaced

This resource was prepared by the author(s) using Federal funds provided by the U.S. Department of Justice. Opinions or points of view expressed are those of the author(s) and do not necessarily reflect the official position or policies of the U.S. Department of Justice

number being compared to it. The results of these fusion rules of the similarity merits for the numbers of one library compared to the other three libraries, as well as the degraded samples: graded defaced samples, the gun barrel, the laser engraved forceps, and the motorcycle fork compared to the four libraries, are all given in Table 13 to 21.

Table 13 Sum of Fusion Rules for each number in the computer generated library compared to the other libraries.

	0	1	2	3	4	5	6	7	8	9
0	18	67	56	54	65	31	30	67	48	46
1	60	19	37	53	29	43	66	37	64	74
2	61	59	19	35	64	28	63	31	53	69
3	50	64	34	18	53	37	54	58	49	65
4	48	56	37	43	26	40	67	40	64	61
5	56	63	33	48	66	20	29	59	54	54
6	45	64	47	59	68	28	19	62	42	48
7	62	33	28	44	51	45	74	19	64	62
8	43	66	52	51	61	30	40	69	18	52
9	40	63	55	60	67	29	38	68	44	18

Table 13 shows the comparison of the computer generated library with both libraries 1 and 2 as well as another computer generated library. It can be seen that the lowest values lie along the diagonal, correctly matching each number in the test library with its corresponding within the other libraries. This method of using fusion rules to combine the similarity merits performed better than the previous method tested of summing up the merits directly as all the numbers were correctly identified with no exceptions.

Table 14 Fusion Rules Results for Defaced Number 6 from the Graded Sample

	SIX										
FUSION RULES		0	1	2	3	4	5	6	7	8	9
	L2Rank	3	7	10	8	4	9	1	5	6	2
	L2RawRank	5	7	9	2	3	8	1	10	4	6
	medRank	5	9	10	8	6	7	2	4	3	1
	medRawRank	3	2	9	4	7	8	1	10	6	5
	srdRawRank	2	3	8	6	10	9	1	4	5	7
	stdRank	8	10	2	1	7	5	4	9	3	6
	stdRawRank	8	10	5	1	2	6	4	9	3	7
	sumRank	3	8	10	6	4	9	1	7	5	2
	sumRawRank	3	4	10	2	7	9	1	8	6	5
	SUM	40	60	73	38	50	70	16	66	41	41

Table 15 Fusion Rules Results for Defaced Number 2 from the Graded Sample

	TWO										
FUSION RULES		0	1	2	3	4	5	6	7	8	9
	L2Rank	8	3	1	4	7	2	9	5	6	10
	L2RawRank	5	1	3	9	8	4	10	2	6	7
	medRank	5	1	2	6	7	3	9	4	8	10
	medRawRank	8	1	3	6	9	5	10	2	4	7
	srdRawRank	9	8	1	6	7	2	3	5	4	10
	stdRank	8	10	4	1	7	5	2	9	3	6
	stdRawRank	2	1	5	10	9	4	8	3	7	6
	sumRank	7	3	1	5	8	2	10	4	6	9
	sumRawRank	7	3	2	8	9	5	10	1	4	6
	SUM	59	31	22	55	71	32	71	35	48	71

Table 16 Fusion Rules Results for Defaced Number 5 from the Graded Sample

	FIVE										
FUSION RULES		0	1	2	3	4	5	6	7	8	9
	L2Rank	9	3	1	6	5	2	10	4	7	8
	L2RawRank	1	2	3	4	5	6	7	8	9	10
	medRank	6	1	2	7	3	4	10	5	8	9
	medRawRank	3	10	8	7	6	5	1	9	4	2
	srdRawRank	10	4	6	3	5	1	9	2	7	8
	stdRank	8	10	7	2	6	3	5	9	1	4
	stdRawRank	8	10	7	3	1	5	6	9	2	4
	sumRank	9	3	1	6	5	2	10	4	7	8
	sumRawRank	6	2	3	5	7	4	10	1	8	9
	SUM	60	45	38	43	43	32	68	51	53	62

Table 17 Fusion Rules Results for Defaced Number 1 from the Gun Barrel

	BARREL ONE										
FUSION RULES		0	1	2	3	4	5	6	7	8	9
	L2Rank	3	5	10	8	4	9	2	7	6	1
	L2RawRank	3	5	10	8	4	9	2	7	6	1
	medRank	6	2	1	3	7	4	9	5	8	10
	medRawRank	8	3	2	6	5	4	9	1	7	10
	srdRawRank	7	2	4	6	3	5	10	1	8	9
	stdRank	3	1	5	10	4	6	7	2	9	8
	stdRawRank	3	1	5	10	4	8	6	2	9	7
	sumRank	8	4	1	5	6	2	9	3	7	10
	sumRawRank	3	7	10	6	5	9	2	8	4	1
	SUM	44	30	48	62	42	56	56	36	64	57

Table 18 Fusion Rules Results for Defaced Number 2 from the Gun Barrel

	BARREL TWO										
FUSION RULES		0	1	2	3	4	5	6	7	8	9
	L2Rank	8	3	1	5	6	2	10	4	7	9
	L2RawRank	9	2	3	6	5	4	10	1	7	8
	medRank	6	2	1	7	3	4	10	5	8	9
	medRawRank	10	2	3	6	4	5	9	1	7	8
	srdRawRank	10	2	4	6	3	5	9	1	7	8
	stdRank	8	9	4	2	7	3	6	10	1	5
	stdRawRank	8	9	4	1	7	3	6	10	2	5
	sumRank	8	3	1	6	5	2	10	4	7	9
	sumRawRank	9	2	3	6	5	4	10	1	7	8
	SUM	76	34	24	45	45	32	80	37	53	69

Table 19 Fusion Rules Results for Defaced Number 0 from the Laser Engraved Forceps

	FORCEPS ZERO										
FUSION RULES		0	1	2	3	4	5	6	7	8	9
	L2Rank	3	8	10	7	4	9	2	6	5	1
	L2RawRank	2	9	8	4	6	7	1	10	5	3
	medRank	4	10	9	8	7	6	2	5	3	1
	medRawRank	2	8	9	5	7	6	1	10	4	3
	srdRawRank	2	9	7	5	8	6	1	10	4	3
	stdRank	3	1	6	10	4	8	7	2	9	5

	stdRawRank	3	1	5	9	4	8	7	2	10	6
	sumRank	3	8	10	4	6	9	1	7	5	2
	sumRawRank	1	9	8	4	6	7	2	10	5	3
	SUM	23	63	72	56	52	66	24	62	50	27

Table 20 Fusion Rules Results for Defaced Number 3 from the Laser Engraved Forceps

	FORCEPS THREE										
FUSION RULES		0	1	2	3	4	5	6	7	8	9
	L2Rank	8	6	1	3	7	2	10	5	4	9
	L2RawRank	3	9	8	5	6	7	1	10	4	2
	medRank	6	2	1	3	7	4	9	5	8	10
	medRawRank	2	8	9	5	6	7	1	10	4	3
	srdRawRank	2	9	7	5	8	6	1	10	4	3
	stdRank	8	10	4	1	7	3	5	9	2	6
	stdRawRank	8	10	5	1	7	3	6	9	2	4
	sumRank	8	4	1	5	7	2	10	3	6	9
	sumRawRank	2	8	9	5	6	7	1	10	4	3
	SUM	47	66	45	33	61	41	44	71	38	49

From the results shown in Table 14 through 21, the use of fusion rules to combine the similarity merits proved useful in eliminating ambiguities and all the defaced numbers were correctly identified from the libraries.

Table 21 Sum of Fusion Rules for each defaced number on Motorcycle Fork

	LIBRARY NUMBERS										
DEFACED NUMBERS		0	1	2	3	4	5	6	7	8	9
	FIVE	52	66	37	37	50	33	53	59	56	52
	TWO	64	79	18	52	37	29	74	24	54	64
	FIVE	53	63	38	40	50	33	53	58	54	53
	ONE	75	14	33	61	45	49	75	21	57	65
	ZERO	32	50	47	57	55	45	54	48	52	55
	ZERO	20	49	75	61	34	73	25	62	60	36
	SEVEN	47	44	58	54	50	63	42	29	59	49
	FOUR	57	52	48	47	42	43	53	58	44	51
	ONE	49	30	41	57	44	52	62	33	63	64

From Table 21, the numbers recovered from the motorcycle in score images shown previously were matched to their corresponding digits in the libraries by utilizing the fusion rules to combine the similarity merits obtained from the comparison of each number to all in the

libraries. Based on these results, the fusion rules provide a more robust method of combining the similarity merits, helping to remove possible biases and minimize contradictions.

Thermal Imaging from Other Perspectives

The studies that have been presented thus far are treatment of the data from the "front" view point of view of the two dimensional x, y pixel array and the third dimension in the z direction is time. However one could also rather treat the data from an xz or a yz perspective, that is from the xz perspective, monitoring how a particular pixel column vs time changes as a function of its row position, or from the yz perspective, monitoring how a particular pixel row versus time evolves as a function of its column position. These refer to the top view and a side view respectively. Thus the set of thermal images collected as a function of time could be treated from a front view, top view, or side view perspective, and the top and side view perspectives may provide direct information on the change in the thermal conductivity as a function of the surface condition since the plot is now pixel position vs time (which relates to the temp). Here one of the direct variables is time rather than just the x,y pixels. The idea is shown below in Figure 61.

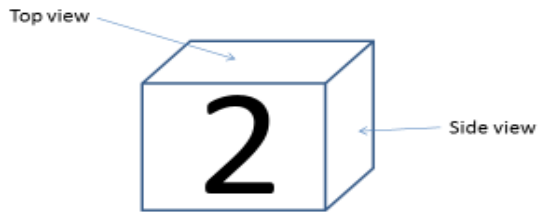

Figure 61 Picture describing the tope views and side view perspectives for a number 2.

Here the side-view and top-view process is applied to the PCA-processed data collected from the LIT experiments. For comparison, in the following figures, Figures 62-Figure 67, the PCA processed score images for PC1 through PC15 side view and top view are given for an undefaced number "2", the defaced number 2 which was machined off as described previously, and a section of the metal sample which did not contain any numbers. One can compare the score images from the undefaced, defaced, and no-number section to identify score plots which may vary similarly for the undefaced and defaced numbers, but differ greatly from the clean areas.

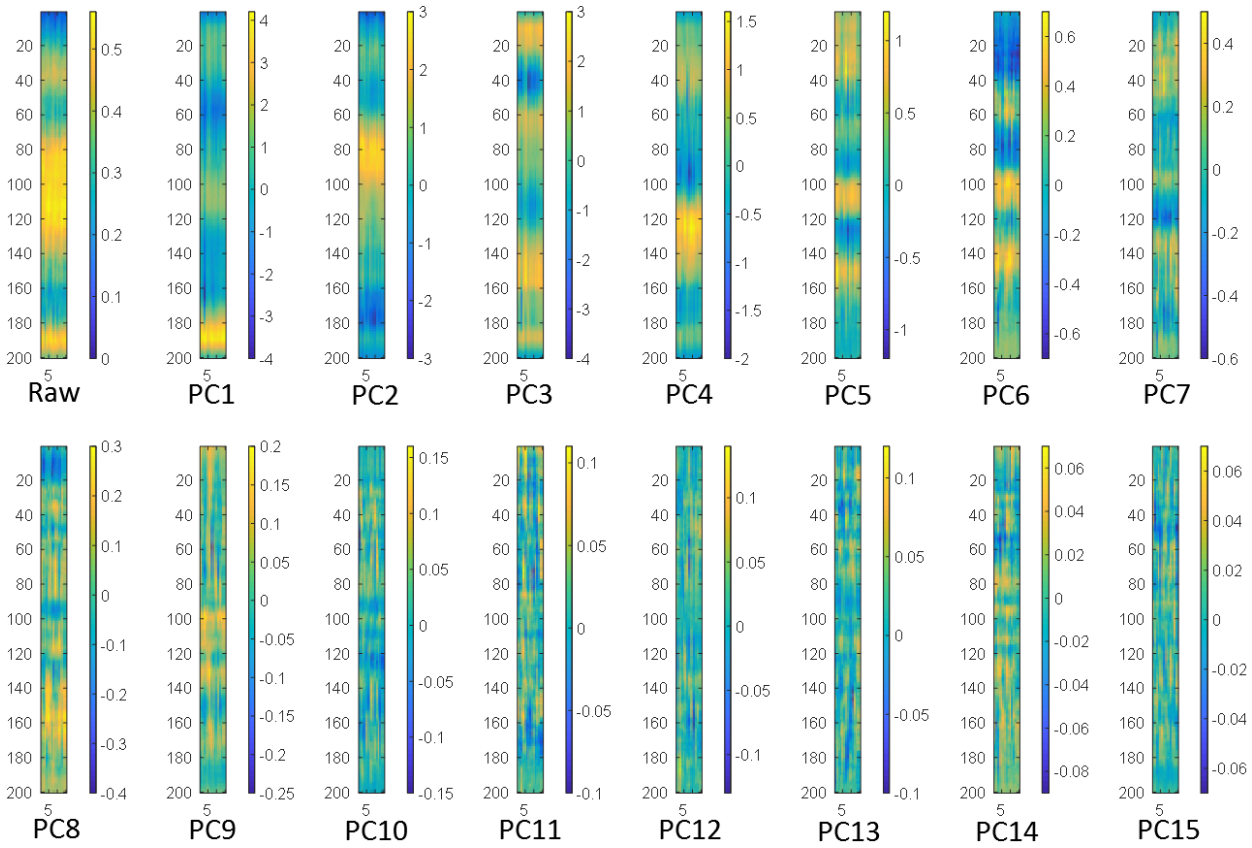

Figure 62 Side View of a undefaced number 2. (All axes represent pixel positions)

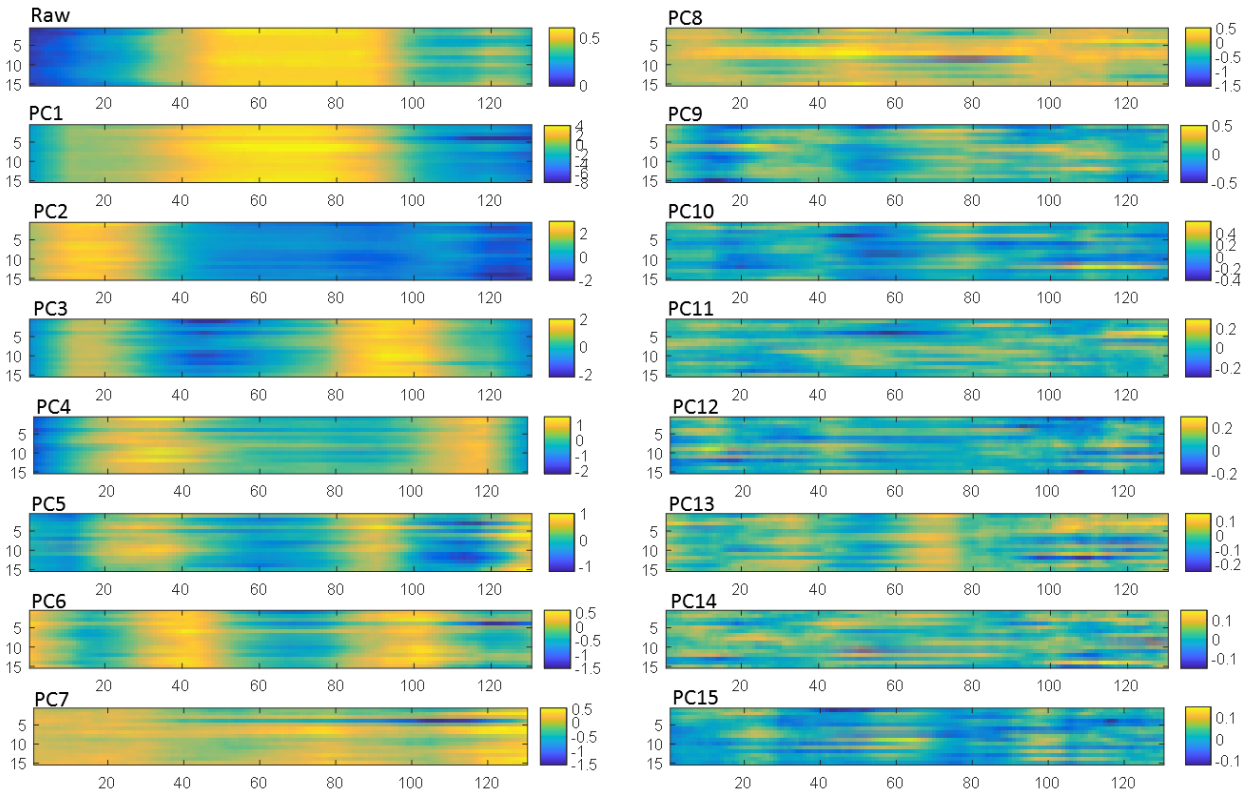

Figure 63 Top View of a undefaced number 2.

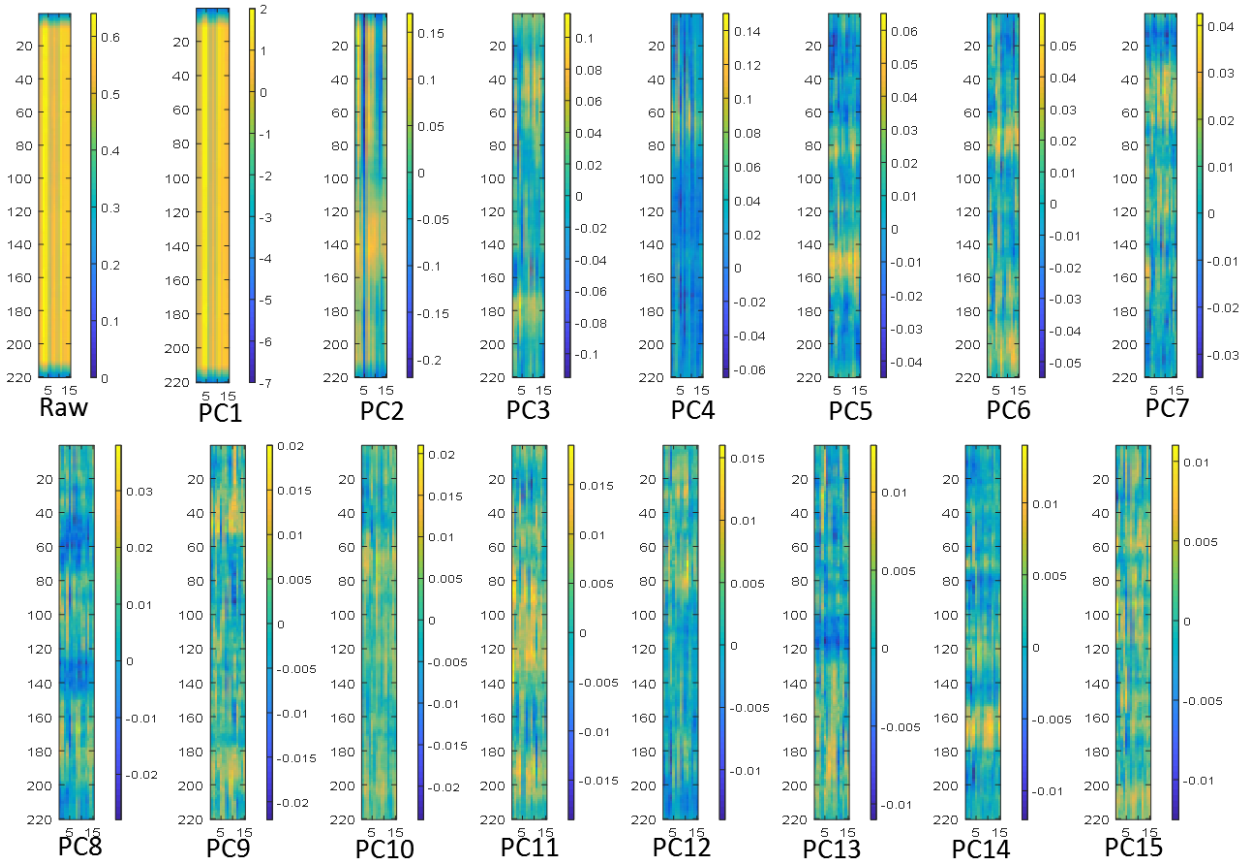

Figure 64 Side View of a defaced number 2.

This resource was prepared by the author(s) using Federal funds provided by the U.S. Department of Justice. Opinions or points of view expressed are those of the author(s) and do not necessarily reflect the official position or policies of the U.S. Department of Justice

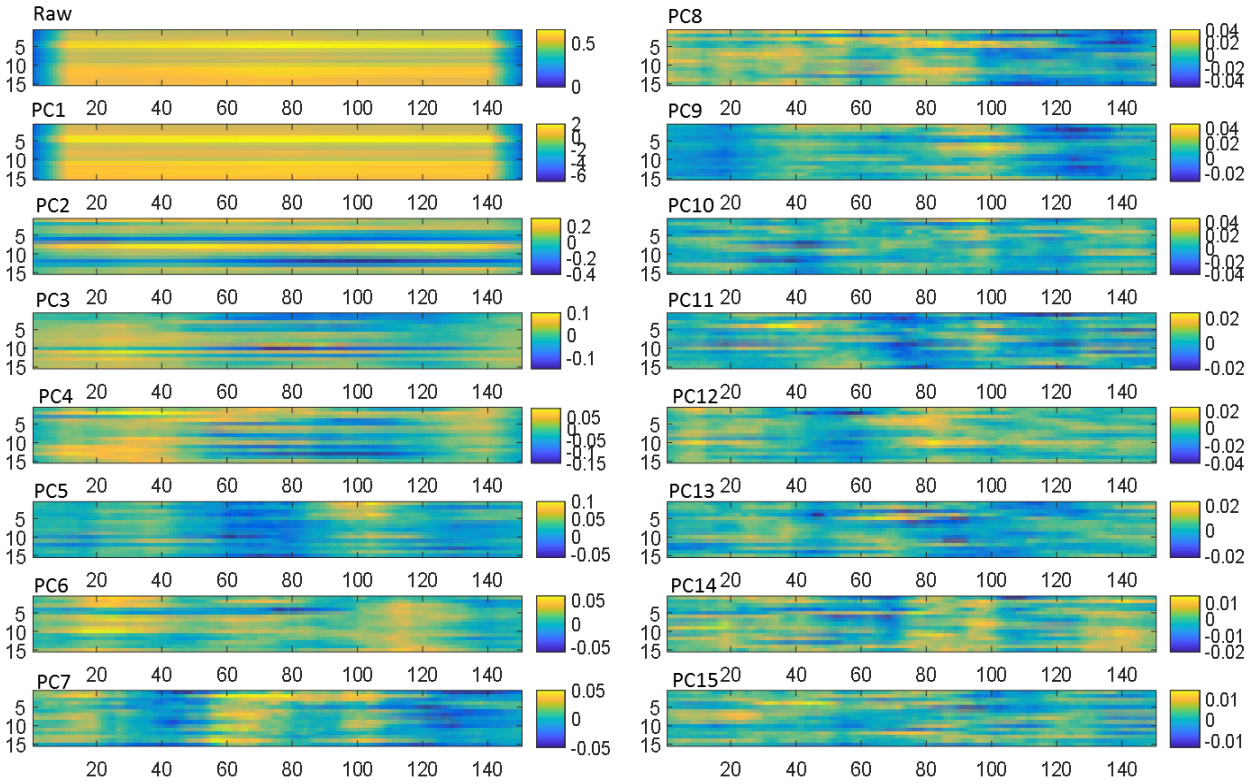

Figure 65 Top View of a defaced number 2.

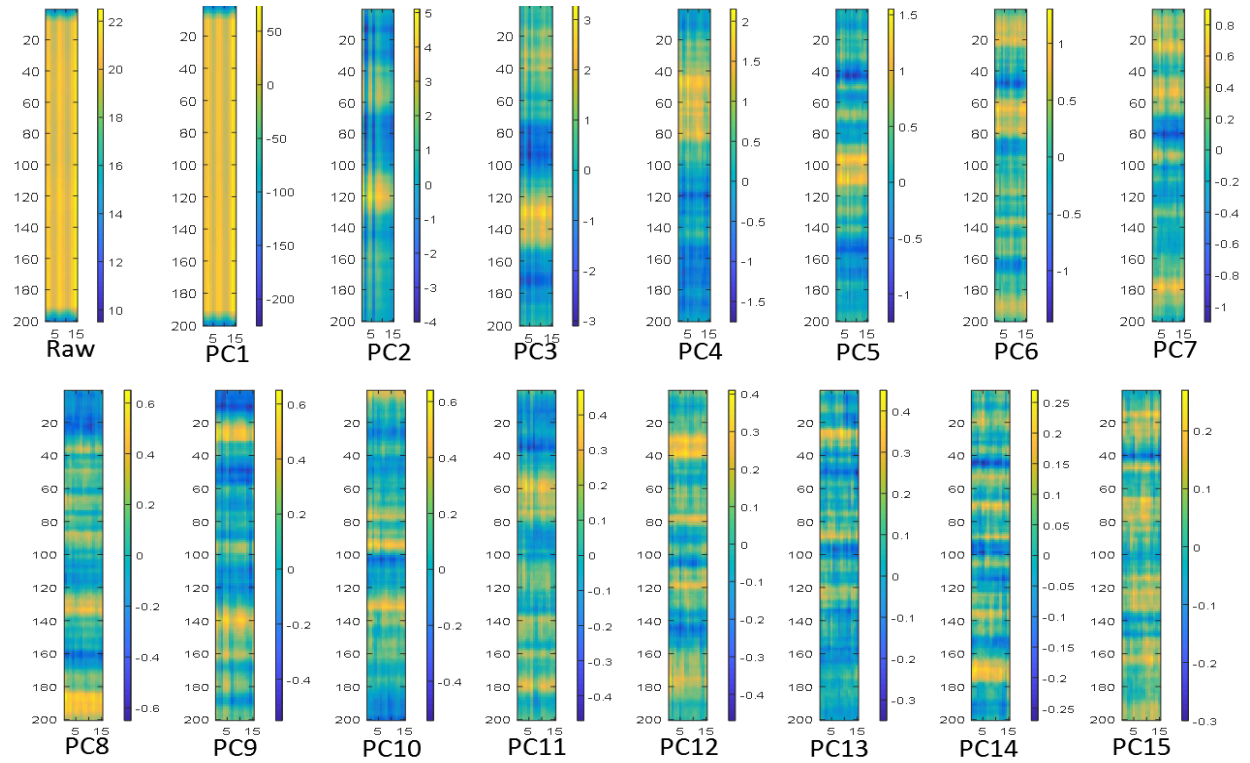

Figure 66 Side View of a section of the sample without any number present.

This resource was prepared by the author(s) using Federal funds provided by the U.S. Department of Justice. Opinions or points of view expressed are those of the author(s) and do not necessarily reflect the official position or policies of the U.S. Department of Justice

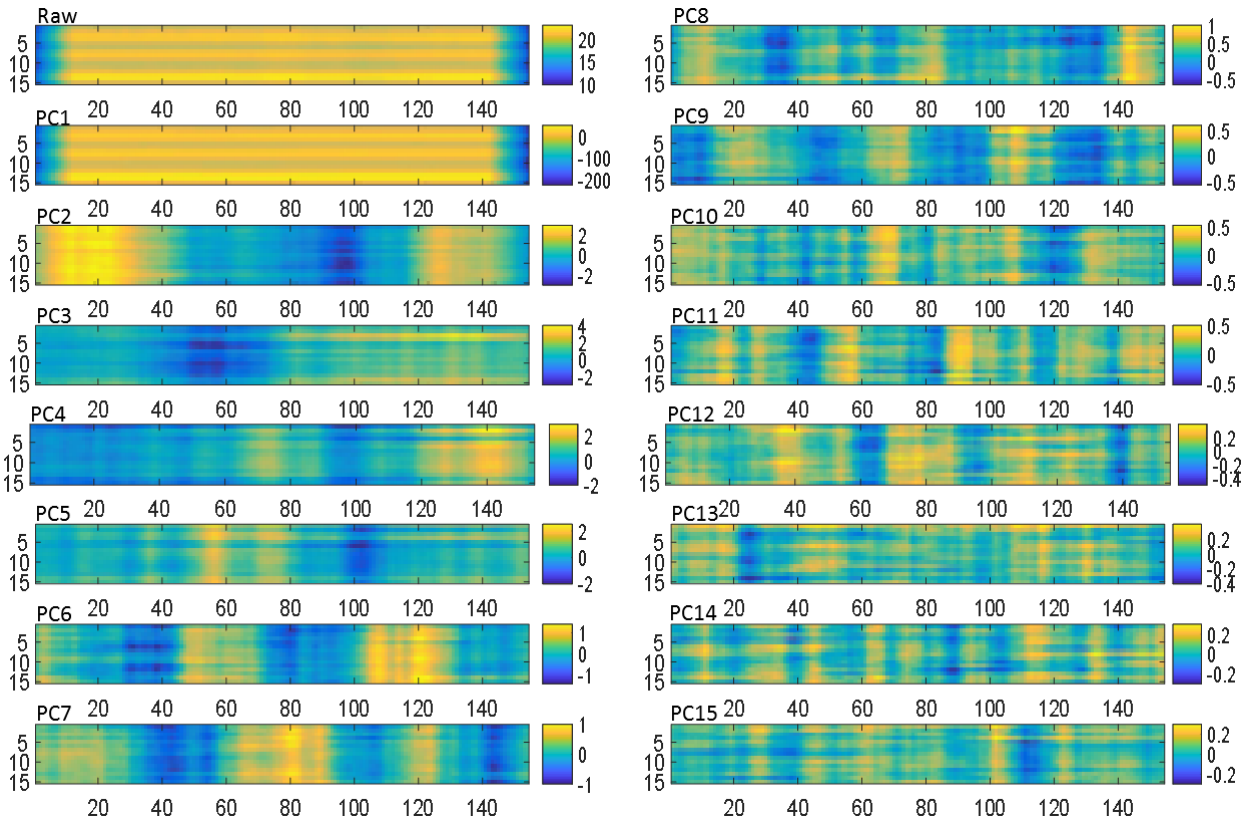

Figure 67 Top View of a section of the sample without any number present.

If there is a significant similarity in a particular score image(s) between the undefaced number, and the defaced number, but no similarity in this score image for the no-number area, then this could be used in the identification of the defaced serial number. For example, in scanning through the below images, as can be seen in Figure 68, one finds that the PC6 side view score images for the undefaced number and the defaced number have banding which are not very similar with each other and also are much different than the PC 6 score image from the no-number area. Looking now at the PC 7 score images, these side view score images for the un-defaced number and the defaced number have more similar looking banding (though it is not the same), and both of these score images differ from the PC7 score image for the no-number area.

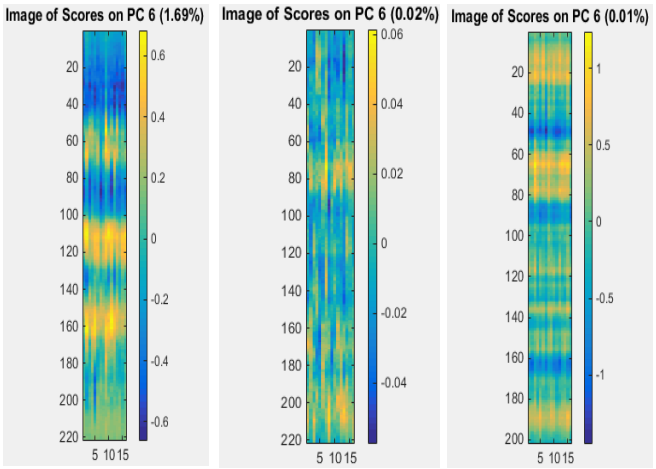

undefaced defaced no-number

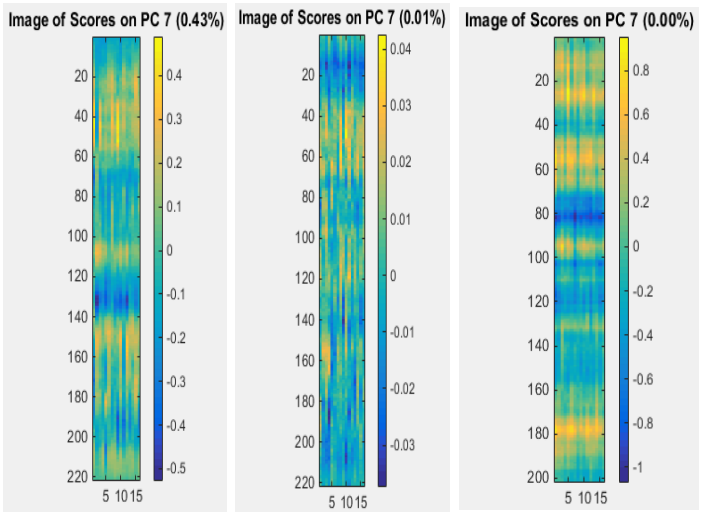

undefaced defaced no-number

Figure 68 Side views of score images for PC6 and PC7. Going from left to right are listed the undefaced, defaced, and no-number images.

If one compares the top view PC score images for the same PC numbered images, one finds that there is very limited similarity in these images as can be seen in Figure 69 below.

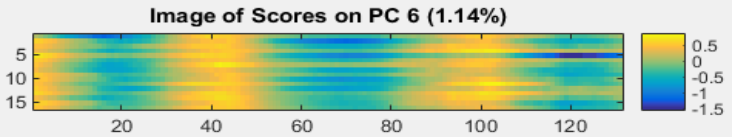

undefaced

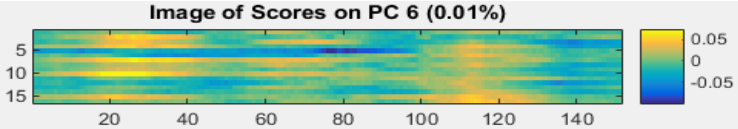

defaced

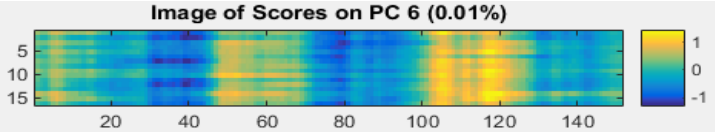

no-number

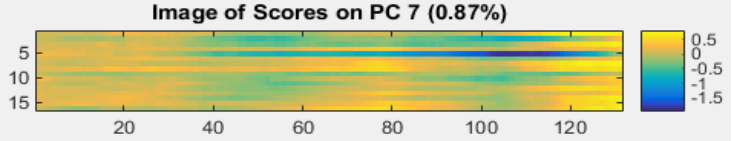

undefaced

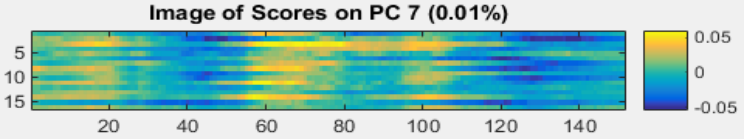

defaced

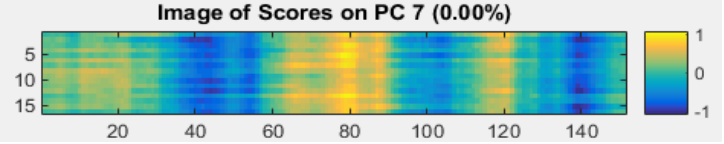

no-number

Figure 69 Top views of score images for PC6 and PC7. Going from top to bottom are listed the undefaced, defaced, and no-number images.

Based on this study of the score images, it appears that, although there is some information about the defaced numbers being provided by processing of the images collected from the side view and top view images, currently it cannot be used to make an independent determination of the identity of the number which is being recovered.

IV. CONCLUSIONS

The overall goal of the study was to determine if infrared thermography techniques coupled with multivariate analysis methods could be used as a non-destructive method to recover defaced serial numbers from materials that are typically involved in criminal activities. The non-destructive nature of the technique would be especially useful if evidence needed reexamination at some later time. More specifically do any of the methods of Transient Infrared Thermography

(TIT), Pulsed Infrared Thermography (PIT), and Lock-in Thermography coupled with Multivariate Image Analysis (MIA) provide a quick and cost effective means for recovery of defaced serial numbers that were stamped or laser engraved into a metal surface such as a part on a firearm, a VIN number, or a motor identification number. These investigations revealed that LIT coupled with MIA appears to be a promising technique for this purpose.

The studies indicate an LIT instrument constructed from an ~2 Watt pulsed laser heating source operating at a frequency between 0.025 Hz and 10 Hz incident on a heated, polished, and painted sample, imaged with a FLIR SC6700 model infrared camera provided the capacity needed to construct phase images of the defaced samples. These phase images were processed with Principal Component Analysis to generate score images that were then subjected to Zernike Moment Analysis. The Zernike Analysis provided a way that the phase images of the defaced numbers could be compared with libraries of numbers for identification purposes using several similarity merit measures. When applied to (stamped) defaced numbers on steel test samples, shotgun barrels, an aluminum motor, and a VIN number from a motorcycle, each number was found to be recoverable. Also, based on our tests of a set of steel forceps, the method also shows good promise for recovery of defaced serial numbers from laser engraved materials.

Using this technique, in the case of the gun barrel, the defaced number 2 was correctly identified by the LIT-Multivariate Image Analysis (LIT-MIA) method with a zero identified as the second most likely choice. A false identification did occur for the defaced number 1 on the barrel, but false identification of the italics number 1 could be due to the fact that non-italics libraries were used. The number 1 was the next highest choice as identified by the similarity merit values. If however, a set of fusion rules was defined which, rather than simply adding the similarity merits as was done previously, combined them to optimize the use of several similarity measures by obtaining a consensus among them and thus minimizing the possible effects of some incorrectly ranked values, then the number 1 was correctly identified as being the best match. This involved determining the similarity merits for each score image in comparison to the digital number images across four libraries.

A particularly interesting test sample for this LIT-MIA-fusion rules technique was a motorcycle with a defaced VIN number on the steel neck of the frame and a partially defaced number on the aluminum motor. This was obtained from Chief Deputy Max Sprague of the Power County Sheriff's Office. The VIN number recovered by this method matched the VIN of a motorcycle that was reported stolen in the neighboring city, Pocatello. This recovery is allowed the owner of the motorcycle to be notified. This set of fusion rules worked well for all of the LIT-MIA studies that were attempted.

The current instrumentation needed to implement the LIT-MIA method is somewhat costly. The cost stems largely from the cost of the infrared camera and the laser heating source. There are other, less costly cameras available with lower temperature resolution, and these may be able to provide enough resolution for the method to work. Part of this work used theatre lamps for the pulsed heated, and although these did not appear to work quite as well as the laser, and are not as easy to manipulate onto the sample, they may represent a lower cost alternative.

Also there are some inexpensive diode lasers now available with power similar to that used for these experiment. If the camera cost could be lowered, then this type of instrument could possibly be placed in local police stations if the analyses were performed by a trained technician. Sample preparation is important, so the technician would have to be trained in the polishing and painting of the samples and the technician would also require a working knowledge of computer mathematical and imaging software.

Future laboratory studies could include repeating some of the experiments with a lower cost camera and laser source. Experiments with the graded test sample had serial numbers defaced to different depths below the surface, and they suggest that this technique shows promise to 2mm removal of the surface metal before the defaced number becomes unrecoverable. Additional experiments should be done to determine if this depth can be extended by increased heating or improved surface preparation. The multivariate image analysis needs further investigation as well. Currently the analysis uses both Principal Component and Zernike Moment analysis techniques to generate vectors that can be more easily used in the similarity merit measures for comparison with the library numbers. This requires a significant amount of computer processing time. This process of generating the vectors for the similarity measures should be studied more for streamlining the process, and the set "fusion rules" used to combine the various similarity measures should be studied for further optimization opportunities. The similarity merit measures themselves should be scrutinized to determine if they contribute positively to the identification. Currently ten merits are being used to determine the best fit of a number in a library to the defaced number image. Libraries also should be more carefully constructed to match the characteristics of the serial numbers before they were defaced.

The LIT-MIA method should be more "field tested" on real world samples. The defaced numbers from the gun barrel and motorcycle are a good start in this direction, but more samples of this type should be evaluated with this method. These types of samples provide a better cross section of the types of samples that would be encountered, and different surface preparation methods may be necessary for these samples.

V. REFERENCES

1. H. Liu, Y. Wang, J. Liu, and H. Gong, "Effect of Modulation Frequency on Detecting Defects of Metal Places using Infrared Lock-in Thermography," Proceedings of SPIE: The International Society for Optical Engineering, **7283**, 1-7 (2009).

2. C. M. Sayers, "Detectability of Defects by Thermal Non-Destructive Testing," British Journal of Non-Destructive Testing, **26 (1),** 28-33 (1984).

3. A. Killey, and J. P. Sargent, "Analysis of Thermal Non-Destructive Testing," Journal of Physics D: Applied Physics, **22(1),** 216-224 (1989).

4. R. Kuppuswamy, "Metallographic etching of aluminium and its alloys for restoration of obliterated marks in forensic science practice and investigations," T. Kračkaj, R. Bidulsky (Eds.), Aluminium Alloys, Theory and Application, Intech, Croatia (2011), pp. 331-352

5. O. Breitenstein and M Langenkamp, Lock-in Thermography: Basics and Use for Functional Diagnostics of Electronic Components, Springer-Verlag, Berlin, pp. 15-20 (2003).

6. C. Wallbrink, S. A. Wade, and R. Jones, "The effect of size on the quantitative estimation of defect depth in steel structures using lock-in thermography", Journal of Applied Physics, **101**, 104907-1 – 104907-8 (2007).

VI. DISSEMINATION OF RESEARCH FINDINGS

1. Poster Presentation at the International Association for Spectral Imaging (IASIM14) International Meeting in Dec., 2014. The poster was presented by Prof. John Kalivas

2. Poster Presentation at the Association of Firearm and Toolmark Examiners Seminar Meeting in Dallas, Texas in May 2015.

3. Oral Presentation at the 2016 Annual Idaho Academy of Science and Engineering Meeting in Pocatello, ID, April 2016

4. Oral Presentation at The 2nd International Congress of Technology, Management and Social Sciences-16 in Toronto, Canada. The intended focus of the conference MICCVTA-16 was on frontier topics in Computer Vision and Image Processing

5. Oral Presentation to Rachel Cutler, F-ABC, Laboratory Manager, Idaho State Police Forensic Services, Pocatello, ID, Dec. 2016

7. Oral Presentation to Matthew Gamette, Laboratory System Director, Idaho State Police Forensic Services, Pocatello, ID, Jan. 2017

8. Oral Presentation at the Association of Firearm and Toolmark Examiners Conference in Denver, Colorado in May 2017

Appendix 1 Similarity Merits

i. Correlation Coefficient:

$$CC = \frac{S_{12}}{S_1 S_2}$$

Where,

S_1 and S_2 = the standard deviations of variables (vectors) 1 and 2 respectively

S_{12} = covariance of variables

ii. Euclidean Distance:

$$\text{1-ED} = 1 - \sqrt{(\boldsymbol{x_1} - \boldsymbol{x_2})(\boldsymbol{x_1} - \boldsymbol{x_2})^T}$$

Where,

$\mathbf{x}_1$ and $\mathbf{x}_2$ = vectors representing Zernike moments for a pristine number from the library and a score image from the recovered numbers respectively.

iii. Angle between vectors:

$$\cos\theta = \frac{|x_1^T x_2|}{\|x_1\|\|x_2\|}$$

iv. Determinant:

$$Det = 1 - \left| \begin{pmatrix} \boldsymbol{x_1^T} \\ \boldsymbol{x_2^T} \end{pmatrix} (\boldsymbol{x_1} \quad \boldsymbol{x_2}) \right| = (\|\boldsymbol{x_1}\|\|\boldsymbol{x_2}\| sin\theta_1)^2$$

v. Procrustes Analysis:

$$\boldsymbol{x_1} = \boldsymbol{x_2 F_{21}}$$

$$\boldsymbol{F_{21}} = (\boldsymbol{x_2 x_2^T})^+ (\boldsymbol{x_2 x_1^T})$$

$$\boldsymbol{F_{22}} = (\boldsymbol{x_2 x_2^T})^+ (\boldsymbol{x_2 x_2^T})$$

This resource was prepared by the author(s) using Federal funds provided by the U.S. Department of Justice. Opinions or points of view expressed are those of the author(s) and do not necessarily reflect the official position or policies of the U.S. Department of Justice

$$\boldsymbol{F} = \|\boldsymbol{F_{21}} - \boldsymbol{F_{22}}\|_{\boldsymbol{F}}$$

Where,

F = a transformation matrix necessary to make $\mathbf{x}_2$ most similar to $\mathbf{x}_1$

$(\boldsymbol{x}_2\boldsymbol{x}_2^T)^+$ = pseudoinverse of $\boldsymbol{x}_2\boldsymbol{x}_1^T$

$\|\boldsymbol{F}_{21} - \boldsymbol{F}_{22}\|_F$ = the Frobenius norm for the matrix difference between the two transformation matrices $\boldsymbol{F}_{21}$ and $\boldsymbol{F}_{22}$

vi. Constrained Procrustes Analysis

$$\boldsymbol{x}_2{}^T\boldsymbol{x}_1 = \boldsymbol{U}_{21}\sum_{21}\boldsymbol{V}_{21}{}^T$$

$$\rho_{21} = \frac{tr(\sum_{21})}{tr(\boldsymbol{x}_2\boldsymbol{x}_2{}^T)}$$

$$\boldsymbol{H}_{21} = \boldsymbol{U}_{21}\boldsymbol{V}_{21}^T$$

$$\rho = \|\rho_{21} - \rho_{22}\|_{Frob}$$

$$H = \|\boldsymbol{H}_{21} - \boldsymbol{H}_{22}\|_{Frob}$$

Where,

X = $\boldsymbol{x}_2{}^T\boldsymbol{x}_1$

U = eigenvectors of matrix $\mathbf{X}\mathbf{X}^T$

Σ = diagonal matrix of singular values

V = loading matrix = eigenvectors of matrix $\mathbf{X}^T\mathbf{X}$

vii. Mahalanobis Distance:

$$\boldsymbol{C}_1 = \boldsymbol{x}_1\boldsymbol{x}_1^T$$

$$MD = \sqrt{(\boldsymbol{x}_2 - \boldsymbol{x}_1)^T\boldsymbol{C}_1^+(\boldsymbol{x}_2 - \boldsymbol{x}_1)}$$

viii. Pooled Mahalanobis Distance:

$$\boldsymbol{S}_1 = \boldsymbol{x}_1\boldsymbol{x}_1^T$$

This resource was prepared by the author(s) using Federal funds provided by the U.S. Department of Justice. Opinions or points of view expressed are those of the author(s) and do not necessarily reflect the official position or policies of the U.S. Department of Justice

$$\boldsymbol{S}_2 = \boldsymbol{x}_2\boldsymbol{x}_2^T$$

$$\boldsymbol{C} = \frac{\boldsymbol{S_1}+\boldsymbol{S_2}}{\boldsymbol{2}}$$

$$PMD = \sqrt{(\boldsymbol{x}_1 - \boldsymbol{x}_2)^T\boldsymbol{C}^+(\boldsymbol{x}_1 - \boldsymbol{x}_2)}$$

ix. Bartlett Statistics:

$$\boldsymbol{S}_1 = \boldsymbol{x}_1\boldsymbol{x}_1^T$$

$$\boldsymbol{S}_2 = \boldsymbol{x}_2\boldsymbol{x}_2^T$$

$$\boldsymbol{S} = \frac{\boldsymbol{S}_1 + \boldsymbol{S}_2}{2}$$

$$\nu = \left(\frac{2n^2+3n-1}{6(n+1)}\left[\frac{-1}{m_1+m_2}\right]\right)$$

$$c = \nu[(m_1)\ln(|\boldsymbol{S}_1^+\boldsymbol{S}|) + (m_2)\ln(|\boldsymbol{S}_2^+\boldsymbol{S}|)]$$

$$\boldsymbol{BS} = \mathbf{exp}\left(\frac{-\boldsymbol{c}}{\boldsymbol{m_1}+\boldsymbol{m_2}}\right)$$

Where,

n = the number of variables

m_1 and m_2 = the number of samples in each dataset being compared. In this study, only two vectors are being compared so $m_1$and m_2 are equal to one.

This resource was prepared by the author(s) using Federal funds provided by the U.S. Department of Justice. Opinions or points of view expressed are those of the author(s) and do not necessarily reflect the official position or policies of the U.S. Department of Justice